

NM1-63

**Permit
Application**

Vol 3

Part 6 of 8

10/12/16

**APPLICATION FOR PERMIT
OWL LANDFILL SERVICES, LLC**

**VOLUME III: LANDFILL ENGINEERING CALCULATIONS
SECTION 4: HELP MODEL**

ATTACHMENT III.4.D

HELP MODEL INPUT AND OUTPUT FILES: CD-ROM

**APPLICATION FOR PERMIT
OWL LANDFILL SERVICES, LLC**

**VOLUME III: ENGINEERING DESIGN AND CALCULATIONS
SECTION 5: PIPE LOADING CALCULATIONS**

TABLE OF CONTENTS

Section No.	Title	Page
1.0	INTRODUCTION	III.5-1
1.1	Site Location	III.5-1
1.2	Description.....	III.5-1
2.0	DESIGN CRITERIA	III.5-2
3.0	PIPE STRENGTH CALCULATIONS.....	III.5-3
3.1	6-Inch SDR 13.5 HDPE Pipe.....	III.5-3
3.1.1	6-Inch Diameter SDR 13.5 HDPE Pipe Dimensions (Attachment III.5.E).....	III.5-3
3.1.2	Loads Acting on the Leachate Collection Pipe.....	III.5-3
3.1.3	Correction of Load on Pipe with Perforations (HDPE SDR 13.5)	III.5-4
3.1.4	Deflection.....	III.5-5
3.1.5	Wall Buckling	III.5-6
3.1.6	Wall Crushing	III.5-7
3.1.7	Equipment Loading.....	III.5-7
3.1.8	HDPE Pipe Loading Results.....	III.5-9
4.0	REFERENCES	III.5-9

LIST OF FIGURES

Figure No.	Title	Page
III.5.1	LANDFILL CROSS SECTIONS	III.5-10

LIST OF TABLES

Table No.	Title	Page
III.5.1	HDPE PIPE SPECIFICATIONS	III.5-2
III.5.2	PIPE LOADING PARAMETERS.....	III.5-4
III.5.3	SDR 13.5 HDPE PIPE RESULTS.....	III.5-9
III.5.4	LEACHATE PIPE STRENGTH REFERENCES	III.5-9

**APPLICATION FOR PERMIT
OWL LANDFILL SERVICES, LLC**

**VOLUME III: ENGINEERING DESIGN AND CALCULATIONS
SECTION 5: PIPE LOADING CALCULATIONS**

LIST OF ATTACHMENTS

Attachment No.	Title
III.5.A	QIAN, XUEDE; KOERNER, ROBERT M.; AND GRAY, DONALD H. 2002. <i>GEOTECHNICAL ASPECTS OF LANDFILL DESIGN AND CONSTRUCTION</i> . NEW YORK: PRENTICE HALL
III.5.B	SHARMA, HARI .D. AND SANGEETA P. LEWIS. 1994. <i>WASTE CONTAINMENT SYSTEMS, WASTE STABILIZATION AND LANDFILLS: DESIGN AND EVALUATION</i> . NEW YORK: JOHN WILEY AND SONS
III.5.C	WASHINGTON STATE DEPARTMENT OF ECOLOGY. 1987. <i>SOLID WASTE LANDFILL DESIGN MANUAL</i> . WASHINGTON: WDOE
III.5.D	POLY PIPE INDUSTRIES, INC. 2008. <i>DESIGN AND ENGINEERING GUIDE FOR POLYETHYLENE PIPING</i> . WWW.PLASTICPIPE.ORG
III.5.E	DRISCOPIPE, INC. 2008. <i>POLYETHYLENE PIPING SYSTEMS MANUAL</i>
III.5.F	CHEVRON PHILLIPS CHEMICAL COMPANY, LP. 2003. <i>PERFORMANCE PIPE ENGINEERING MANUAL</i> . BULLETIN: PP 900

**APPLICATION FOR PERMIT
OWL LANDFILL SERVICES, LLC**

**VOLUME III: ENGINEERING DESIGN AND CALCULATIONS
SECTION 5: PIPE LOADING CALCULATIONS**

1.0 INTRODUCTION

OWL Landfill Services, LLC (OWL) is proposing to permit, construct, and operate a “Surface Waste Management Facility” for oil field waste processing and disposal services. The proposed OWL Facility is subject to regulation under the New Mexico (NM) Oil and Gas Rules, specifically 19.15.36 NMAC, administered by the Oil Conservation Division (OCD). The Facility has been designed in compliance with the requirements of 19.15.36 NMAC, and will be constructed, operated, and closed in compliance with a Surface Waste Management Facility Permit issued by the OCD.

The OWL Facility is one of the first designed to the new more stringent standards that, for instance, mandate double liners and leak detection for land disposal. The new services that OWL will provide fill a necessary void in the market for technologies that exceed current OCD requirements.

1.1 Site Location

The OWL site is located approximately 22 miles northwest of Jal, adjacent to the south of NM 128 in Lea County, NM. The OWL site is comprised of a 560-acre ± tract of land located within a portion of Section 23, Township 24 South, Range 33 East, Lea County, NM (**Figure IV.1.1**). Site access will be provided on the south side of NM 128. The coordinates for the approximate center of the OWL site are Latitude 32.203105577 and Longitude - 103.543122319 (surface coordinates).

1.2 Description

The OWL Surface Waste Management Facility will comprise approximately 500 acres of the 560-acre site, and will include two main components: an oil field waste Processing Area and an oil field waste Landfill Disposal Area, as well as related infrastructure. Oil field wastes are anticipated to be delivered to the OWL Facility from oil and gas exploration and production

operations in southeastern NM and west Texas. The Permit Plans (**Attachment III.1.A**) identify the locations of the Processing Area and Landfill Disposal Area.

2.0 DESIGN CRITERIA

The leachate collection system piping for the OWL Landfill Disposal Area is designed to meet the requirements of the regulatory standards identified in the New Mexico Oil and Gas Rules (i.e., 19.15.36 NMAC). More specifically, 19.15.36.14.C.(3) NMAC requires that the leachate collection pipe be able to:

“...[withstand] structural loading and other stresses and disturbances from overlying oil field waste, cover materials, equipment operation, expansion or contraction...”

The purpose of these Pipe Loading Calculations is to confirm that high-density polyethylene (HDPE) standard dimension ratio (SDR 13.5) solid and perforated piping incorporated into the OWL Landfill design will remain intact after placement of waste fill, and retain its required characteristics after exposure to operating equipment and long term stresses (see **Figure III.5.1**). The basic design approach consists of calculating the deflection on the leachate collection pipe, which cannot exceed its allowable value, with a minimum factor of safety against failure of 1.0.

TABLE III.5.1
HDPE Pipe Specifications
OWL Landfill Services, LLC

Characteristic	6” Diameter Leachate Collection Pipes
	HDPE
Dimension Ratio	13.5
Method of Joining	Welded
Manning’s Number (n)	0.010
Outside Diameter (in)	6.625
Min. Wall Thickness (in)	0.491
Nominal Weight/ft (lb/ft)	4.13
Tensile Strength (psi)	5,000
Modulus of Elasticity (psi)	35,000
Flexural Strength (psi)	135,000

Information listed in **Table III.5.1** is provided in **Attachment III.5.E**.

3.0 PIPE STRENGTH CALCULATIONS

3.1 6-Inch SDR 13.5 HDPE Pipe

In order to determine the capability of 6-in HDPE SDR 13.5 perforated collection pipes to withstand maximum stresses from the overlying soil profile, the pipes were analyzed for adequate protection against ring deflection and wall buckling using **Attachment III.5.E**, Driscopipe, Inc., Polyethylene Piping Systems Manual.

Wall buckling occurs if the total external soil pressure exceeds the pipe-soil system's critical buckling pressure; and excessive ring deflection occurs if the vertical strain in the surrounding soil envelope is greater than the allowable ring deflection of the pipe. SDR 13.5 HDPE pipe has been found to be equivalent or better than PVC piping in landfill leachate pipe applications (i.e., greater resistance to buckling and crushing). SDR stands for standard dimension ratio which is the ratio of the outside pipe diameter to the pipe wall thickness $SDR = OD/t$. As opposed to the schedule nomenclature used for PVC piping, as the SDR gets smaller the thickness of the pipe wall is increased. A comparison of the two pipe types is made in **Table III.5.1**.

3.1.1 6-Inch Diameter SDR 13.5 HDPE Pipe Dimensions (Attachment III.5.D)

- Pipe nominal diameter: 6-in
- Pipe Outside Diameter (OD): 6.625-in
- Pipe Wall Thickness (t): 0.491 in
- Pipe Inner Diameter (ID): 5.58 in
- SDR : 13.5
- Perforation Hole (/FT): 9 perforation holes
- Perforated Hole Diameter (IN): 0.5 in

3.1.2 Loads Acting on the Leachate Collection Pipe

To calculate the total vertical load on the pipes, P_T , the pressure from each overlying layer was calculated and summed. The greatest waste depth occurs in Unit 5 on cross section A-A' (**Figure III.5.1**). There will be 56 layers:

- 3-ft thick final cover
 - 24-inch thick soil erosion layer
 - 6-inch thick protection layer
- 1-ft thick intermediate cover

- Forty-nine 5-ft thick layers of waste for 245 ft of total waste
- 2 ft of protective soil layer

Based on the known thickness of each layer and assigned unit weights, the pressure that will be exerted by each layer was calculated. The results for P_T are presented in **Table III.5.2**.

TABLE III.5.2
Pipe Loading Parameters
OWL Landfill Services, LLC

Layer	Thickness (feet)	Unit Weight (pcf)	Actual Load (psf)
Final Cover Soil	3	120.5	361.5
Intermediate Cover Soils	1	120.5	120.5
Waste	245	74	18,130
Protective Soil Layer	2	120.5	241
Drainage Rock above Pipe	1	130	130
Design Load (P_T)		TOTAL:	18,983 psf (131.8 psi)

Note: Evaporation pond liquid load on piping = 11.16 psf

3.1.3 Correction of Load on Pipe with Perforations (HDPE SDR 13.5)

Perforating pipes reduces the effective length of pipe available to carry loads and resist deflection. The effect of perforations can be taken into account by using an increased load per nominal unit length of the pipe. The increased vertical load per unit length of pipe is calculated as follows:

Static Vertical Load per Unit Length of Pipe (W_C):

$$W_C = (P_T)(D_o) / (1 - ((n)(d)/12)) \quad (\text{Attachment III.5.A, p. 306})$$

Where:

- P_T = Design load (psi)
- D_o = Outside Diameter of the Pipe (in)
- n = number of perforated holes per foot of pipe
- d = diameter of perforated hole on the pipe (in)

$$W_C = [(131.8 \text{ psi})(6.625)] / [1 - ((9)(0.5 \text{ in}) / 12)]$$

$$W_C = [(131.8 \text{ psi})(6.625)]/0.625$$

$$W_C = 1,397 \text{ lbs/in} = 16,789 \text{ lbs/ft}$$

The design value in psi is found by dividing the design load in lbs/in by the diameter of pipe.

$$P_D = 1,397/6 = 232.8 \text{ psi.}$$

3.1.4 Deflection

The ring deflection of the pipe can be calculated from the following Modified Iowa formula:

$$\Delta X = \left(\frac{(D_L)(K)(W_c)(r^3)}{(E)(I) + 0.061(E')(r^3)} \right)$$

Where:

ΔX = Ring deflection (in)

D_L = Deflection lagging factor = 1.5 , compensating for the lag or time dependent behavior of the soil/pipe systems (dimensionless) (**Attachment III.5.A, Page 307**)

K = Bedding factor = 0.083 (**Attachment III.5.A, Page 306**)

W_C = Vertical load per unit length of pipe, lb/in = 1,397 lb/in

r = mean radius of the pipe (OD - t) = ((6.625 in - 0.491 in)/2) = 3.07 in

E = Modulus of elasticity = 35,000 psi (**Attachment III.5.E, Page 43**)

I = Moment of Inertia = $t^3/12$ (in⁴/in) = ((0.491)³/12) = 0.0098

E' = Soil modulus = 3,000 psi (**Attachment III.5.A, Page 307**)

Ultimate degree of compaction and E' will increase as waste is placed over the leachate trench resulting in at least 3,000 psi for the modulus of passive soil resistance.

$$\Delta X = \left(\frac{(1.5)(0.083)(1,397)(3^3)}{(35,000)(0.0098) + (0.061)(3,000)(3^3)} \right)$$

$$\Delta X = \left(\frac{4,696}{343 + 4,941} \right) = 0.89 \text{ in}$$

The ring deflection is then used to determine the ring bending strain using the equation:

$$\varepsilon = f_D \left(\frac{\Delta x}{D_M} \right) \left(\frac{2C}{D_M} \right)$$

Where:

- ε = Wall strain
- f_D = deformation shape factor = 6.0 (**Attachment III.5.F, page 112**)
- Δx = Deflection From previous calculation = 0.89 in
- D_M = Mean Diameter, in
- C = Distance from outer fiber to wall centroid, in

$C = 0.5(1.06t)$, where t = wall thickness

$$C = 0.5 \times 1.06 \times 0.491 = 0.260 \text{ in}$$

$$\varepsilon = (6.0) \left(\frac{0.89}{6} \right) \left(\frac{2(0.260)}{6} \right) = 0.077 = 7.7\%$$

The wall strain of 7.7% is less than 8%, which has an acceptable factor of safety of $8\%/7.7\% = 1.04$ (**Attachment III.5.F, page 112**).

3.1.5 Wall Buckling

Wall buckling may govern design of flexible pipes under conditions of loose soil burial, if the external load exceeds the compressive strength of the pipe material. To determine a factor of safety for wall buckling the pipe critical-collapse differential pressure P_c must be calculated using the following formula (**Attachment III.5.E, p. 43**):

$$P_c = \frac{2.32(E)}{SDR^3} \text{ where } E \text{ is the modulus of elasticity, approximately } 35,000 \text{ psi}$$

$$P_c = \frac{2.32(35,000)}{13.5^3} = 33 \text{ psi}$$

The critical-collapse pressure can then be used to determine the critical buckling pressure from the following relation (**Attachment III.5.E, p. 43**):

$$P_{cb} = 0.8\sqrt{(E')(P_c)}$$

Where:

- P_{cb} = Critical buckling pressure
- E' = Long term degree of compaction of bedding = 3,000 psi (**Attachment III.5.A, p. 307**)

$$P_{cb} = 0.8\sqrt{(3,000)(33)} = 251.7 \text{ psi}$$

The factor of safety is then determined:

$$FS = \frac{P_{cb}}{P_D} = \frac{251.7}{232.8} = 1.08$$

3.1.6 Wall Crushing

To determine a factor of safety for wall crushing the following equations were used (**Attachment III.5.E, p. 42**):

$$S_A = \frac{(SDR - 1)}{2} \times P_D$$

Where:

- S_A = Actual compressive stress, psi
- P_D = Total external pressure on the top of the pipe, psi
- P_D = $W_c/D = 1,397/6 = 232.8$ psi

For a SDR of 13.5 the actual compressive stress is:

$$S_A = \frac{(13.5 - 1)}{2} \times 232.8 = 1,455 \text{ psi}$$

The factor of safety can then be found using the compressive yield strength of HDPE pipe of 1,500 psi (**Attachment III.5.E**):

$$FS = \frac{1,500 \text{ psi}}{1,455 \text{ psi}} = 1.03$$

3.1.7 Equipment Loading

Worst-case conditions would include a piece of equipment operating over the leachate collection pipe after 2 ft of protective soil layer has been placed. A loaded CAT 627 Scraper was used conservatively as the piece of equipment operating on top of the leachate collection pipe. The CAT 627 Scraper has the following specifications (Reference Caterpillar Performance Handbook, Edition 29):

- Tractor Weight = 48,061 lbs
- Scraper Weight = 33,399 lbs
- Soil Load (20 cy) = 48,000 lbs
- Total weight = 129,460 lbs

- Max weight per tire = 33,012 lbs (assumes 49% of the total weight acts on the rear tires and 51% of the weight acts on the front tires).
- Tire width = approximately 18 in = 1.5 ft
- Tire contact length = approximately 4 in = 0.33 ft
- Tire contact area = (18 in)(4 in) = 72 in² = 0.50 ft²

Superimposed loads distributed over an area during equipment operations are determined from the following equation (ASCE, 1982):

$$W_{SD} = (C_S)(p)(F)(B_C)$$

Where:

- W_{SD} = Load on pipe (lbs/ft)
- p = Intensity of distributed load (lbs/ft²)
- F = Impact factor
- B_C = Outside diameter of pipe (ft)
- C_S = Load coefficient

The load coefficient is a function of $D/2H$ and $M/2H$, in which H is the height from the top of the pipe to the ground surface (2 ft) and D and M are the width and length, respectively, or the area over which the distributed load acts. Table 4C.3, **Attachment III.5.C, p. 4C-16**, lists values of the load coefficients for loads centered over the pipe.

Determining the required parameters:

- $H = 3$ ft
- $D = 1.5$ ft
- $M = 0.33$ ft
- $F = 1.0$ (Table 4C.4, **Attachment III.5.C, p. 4C-17**)
- $B_C = 6.625$ in = 0.55 ft
- $D/2H = 1.5$ ft/(2(3 ft)) = 0.250
- $M/2H = 0.33$ ft/(2(3 ft)) = 0.055
- $p = 33,012$ lbs/(1.5 ft)(0.33 ft) = 66,691 lbs/ft²
- $C_S \sim 0.053$ per Table 4C.3, **Attachment III.5.C, p. 4C-16**

Therefore:

$$W_{SD} = (0.053)(66,691 \text{ lbs/ft}^2)(1.0)(0.55 \text{ ft})$$

$$W_{SD} = 1,944.0 \text{ lbs/ft} = 162.0 \text{ lbs/in}$$

The superimposed load due to equipment loading is less than static loading conditions (W_C) calculated in Chapter 3.1.3 as 1,029.5 lbs/in; therefore the static loading conditions govern.

3.1.8 HDPE Pipe Loading Results

Calculations for ring deflection, wall crushing, wall buckling, due to dead and live loading stresses for the existing and proposed 6-in laterals were completed and the following table summarizes the results.

TABLE III.5.3
SDR 13.5 HDPE Pipe Results
OWL Landfill Services, LLC

Design Criteria	Critical Value	Actual Value	Factor of Safety
Dead Load Only			
Ring Deflection	8.0 %	7.7%	1.03
Wall Buckling	251.7 psi	232.8 psi	1.08
Wall Crushing	1,500 psi	1,455 psi	1.03

As shown, for each limiting design criterion, the factor of safety is greater than design criteria, thus the performance standard for the HDPE pipes is more than adequate.

4.0 REFERENCES

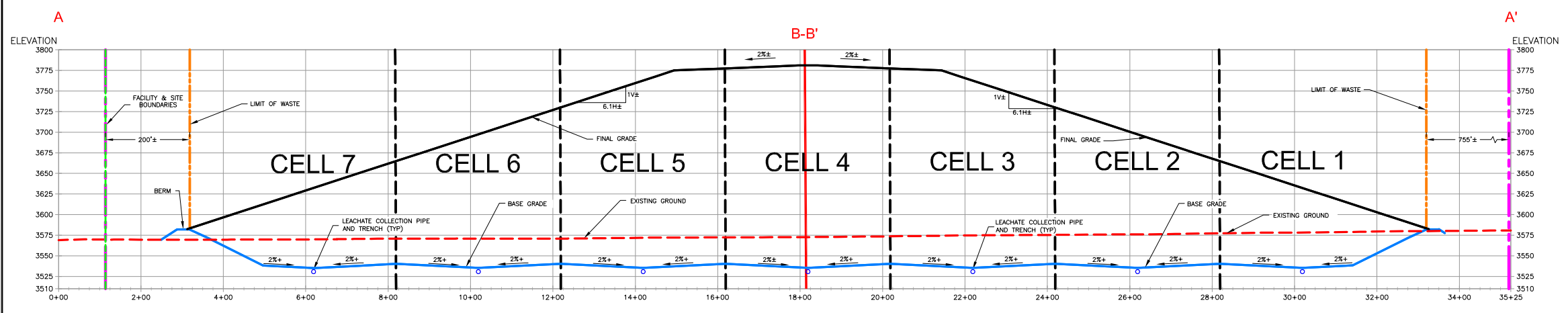
Leachate pipe strength calculations were completed using guidelines provided on **Table III.5.4**.

TABLE III.5.4
Leachate Pipe Strength References
OWL Landfill Services, LLC

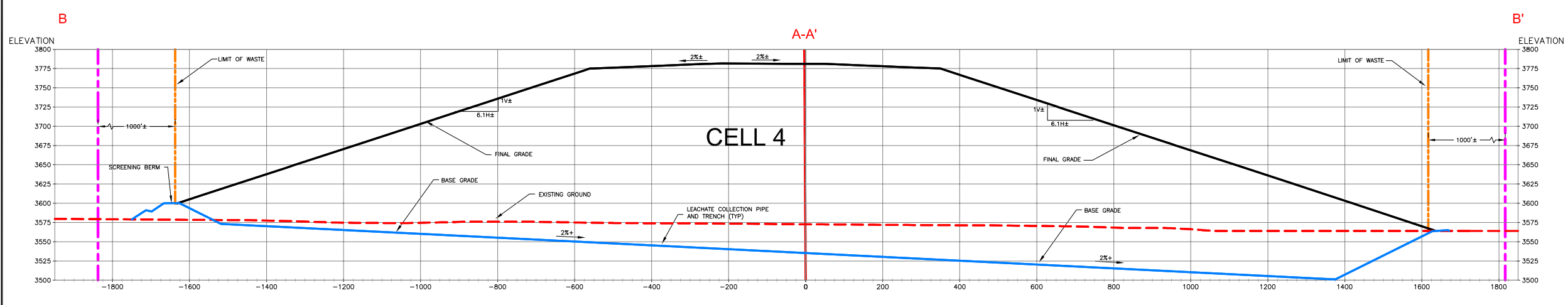
- A. "Geotechnical Aspects of Landfill Design and Construction", Xuede Qian, Robert M. Koerner, Donald H. Gray, Prentice Hall, 2002
- B. "Waste Containment Systems, Waste Stabilization, and Landfills", Hari D. Sharma and Sangeeta P. Lewis, John Wiley & Sons, 1994
- C. WDOE Landfill Design Manual, 1987
- D. "Design and Engineering Guide for Polyethylene Piping", Poly Pipe Industries, Inc, 2008
- E. "Polyethylene Piping Systems Manual", Driscopipe, Inc., 2008
- F. Chevron Phillips, "Bulletin: PP 900", Book 2 – Chapter 7, p. 112, 2003

LEGEND

- SITE BOUNDARY (559.5 ACRES±)
- SURFACE WASTE MANAGEMENT FACILITY BOUNDARY (500.0 ACRES)
- SOLID WASTE DISPOSAL AREA LIMITS (224.3 ACRES±)
- CELL BOUNDARY
- EXISTING GRADE
- BASE GRADE
- FINAL GRADE
- ↑ ↑ CROSS-SECTION LOCATION



1 LAND DISPOSAL EAST-WEST SECTION
8 SECTION A-A'

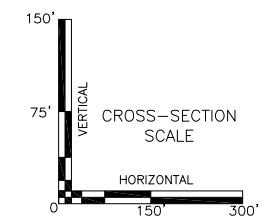


2 LAND DISPOSAL NORTH-SOUTH SECTION
8 SECTION B-B'



KEY MAP
N.T.S.

NOTE:
1. THE DESIGN OF THE FACILITIES SHOWN IS PRELIMINARY. CONSTRUCTION PLANS AND SPECIFICATIONS FOR EACH MAJOR ELEMENT WILL BE SUBMITTED TO OCD IN ADVANCE OF INSTALLATION.



I. KEITH GORDON, P.E.
N.M. PROFESSIONAL ENGINEER NO. 10984

All reports, drawings, specifications, computer files, field data, notes and other documents and instruments prepared by the Engineer as instruments of service shall remain the property of the Engineer. The Engineer shall retain all common law, statutory and other reserved rights, including the copyright thereto.

LANDFILL CROSS-SECTIONS
OWL LANDFILL SERVICES, LLC
LEA COUNTY, NEW MEXICO

<p>Gordon Environmental, Inc. Consulting Engineers</p>		213 S. Camino del Pueblo Bernalillo, New Mexico, USA Phone: 505-867-6990 Fax: 505-867-6991
		<p>DATE: 09/08/2016 CAD: WholeSI-2.DWG PROJECT #: 560.01.02 DRAWN BY: ASM REVIEWED BY: CRK APPROVED BY: IKG get@gordonenvironmental.com</p>

FIGURE III.5.1

**APPLICATION FOR PERMIT
OWL LANDFILL SERVICES, LLC**

**VOLUME III: ENGINEERING DESIGN AND CALCULATIONS
SECTION 5: PIPE LOADING CALCULATIONS**

ATTACHMENT III.5.A

**QIAN, XUEDE; KOERNER, ROBERT M.; AND GRAY, DONALD H. 2002.
GEOTECHNICAL ASPECTS OF LANDFILL DESIGN AND CONSTRUCTION.
NEW YORK: PRENTICE HALL**

GEOTECHNICAL ASPECTS OF LANDFILL DESIGN AND CONSTRUCTION

Xuede Qian

*Geotechnical Engineering Specialist
Michigan Department of Environmental Quality*

Robert M. Koerner

*H. L. Bowman Professor of Civil Engineering, Drexel University
Director, Geosynthetic Research Institute*

Donald H. Gray

*Professor of Civil and Environmental Engineering
The University of Michigan*



PRENTICE HALL
Upper Saddle River, New Jersey 07458

Number of Perforation Holes:

$$\begin{aligned}
 N &= Q_{in}/Q_b & (9.12) \\
 &= 0.0002184/0.00002114 \\
 &= 10.35 \text{ holes/ft (34 holes/m)}
 \end{aligned}$$

So, use 12 holes/ft (40 holes/m); that is 6 holes per foot (20 holes per meter) each side as shown in Figure 9.3.

9.4 DEFORMATION AND STABILITY OF LEACHATE COLLECTION PIPE

All components of the leachate collection and removal system must have sufficient strength to support the weight of the overlying waste, cover system, and post-closure loadings, as well as the stresses from operating equipment. The component that is perhaps the most vulnerable to compressive strength failure is the drainage layer piping. Leachate collection and removal system piping can fail by excessive deflection, which may lead to buckling or collapsing. Pipe strength calculations should include resistance to pipe deflection and critical buckling pressure. This situation is heightened by the current tendency to create extremely large landfills, sometimes called “megafills.”

9.4.1 Pipe Deflection

Leachate collection pipes may excessively deform during construction, during the active life of the landfill or under the post-closure loading. This deformation may lead to buckling and eventual collapse. Thus, leachate pipes should be handled carefully and brought on site only when the trench is ready. Passage of heavy equipment directly over a pipe must be avoided. A pipe can be installed in either a positive or negative projection mode. However, every effort should be made to install it in a negative projection mode (Figure 9.2), although at times it may be necessary to install a pipe in a positive projecting mode (Figure 9.5). The essential difference between these two con-

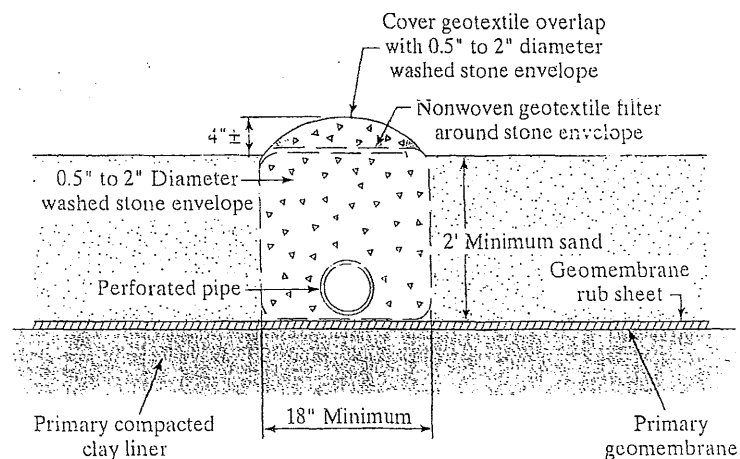


FIGURE 9.5 Leachate Collection Pipe in a Positive Projection Mode

cepts is that a negative projection allows for soil arching which limits the load on the pipe. Conversely, positive projection can actually add load to the pipe. Spangler (1960), among others, explains these concepts for deeply buried pipelines. The design of a pipe must be checked to ascertain whether it will be able to withstand the load during both preconstruction and postconstruction periods. Usually one of two types of pipes are used, HDPE or PVC. These are considered as flexible type pipes. This infers that they do not rupture or break under excessive load, they deform, and if excessively, buckle and/or collapse. The basic design approach consists of calculating the deflection of the pipe, which should not exceed the allowable value. The following formula, commonly known as the Modified Iowa formula, can be used to estimate pipe deflection (Spangler and Handy, 1973; Moser, 1990).

Modified Iowa Formula:

$$\Delta X = \frac{D_L \cdot K \cdot W_c \cdot r^3}{E \cdot I + 0.061 E' \cdot r^3} \tag{9.16}$$

where ΔX = horizontal deflection, in or m (Figure 9.6);

K = bedding constant, its value depending on the bedding angle (see Table 9.1 and Figure 9.7); also, as a general rule, a value of $K = 0.1$ is assumed;

D_L = deflection lag factor (see Table 9.2);

W_c = vertical load per unit length of the pipe, lb/in or kN/m;

r = mean radius of the pipe, $r = (D_o - t)/2$, in or m;

E = elastic modulus of the pipe material, lb/in² or kN/m²;

I = moment of inertia of the pipe wall per unit length,

$$I = t^3/12, \text{ in}^4/\text{in} = \text{in}^3 \text{ or } \text{m}^4/\text{m} = \text{m}^3;$$

t = thickness of pipe, in or m; and

E' = soil reaction modulus, lb/in² or kN/m², see Table 9.3.

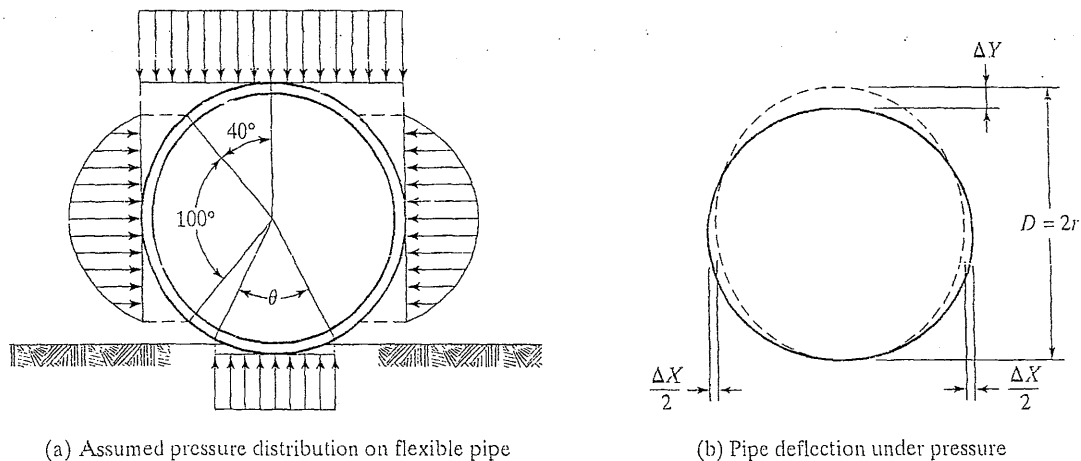


FIGURE 9.6 Buried Flexible Pipe

TABLE 9.1 Values of Bedding Constant, K

Bedding Angle, θ (degree)	Bedding Constant, K
0	0.110
30	0.108
45	0.105
60	0.102
90	0.096
120	0.090
180	0.083

The deflection of the pipe, ΔX , calculated from Equation 9.16 is the deflection in the horizontal direction, as shown in Figure 9.6. When the deflection of pipe is not large (e.g., less than 10%), the vertical deflection of pipe, ΔY , is usually assumed to be approximately equal to the horizontal deflection of pipe, ΔX .

Vertical Load per Unit Length of Pipe:

For Solid Pipe,

$$W_c = (\sum \gamma_i \cdot H_i) \cdot D_o \quad (9.17)$$

where W_c = vertical load per unit length of the pipe, lb/in or kN/m;
 γ_i = unit weight of material i on the pipe (sand, clay or solid waste),
 lb/in³ or kN/m³;
 H_i = thickness of material i , in or m; and
 D_o = outside diameter of the pipe, in or m.

For Perforated Pipe,

$$W_c = \frac{(\sum \gamma_i \cdot H_i) \cdot D_o}{(1 - n \cdot d/12)} \quad (9.18)$$

where W_c = vertical load per unit length of the pipe, lb/in or kN/m;
 γ_i = unit weight of material i (soils or solid waste), lb/in³ or
 kN/m³;
 H_i = thickness of material i , in or m;
 D_o = outside diameter of the pipe, in or m;
 d = diameter of perforated hole or width of perforated slot on the pipe, in
 or m; and
 n = number of perforated holes or slots per row per foot of pipe.

FIGURE 9.7 Pipe Bedding Angle

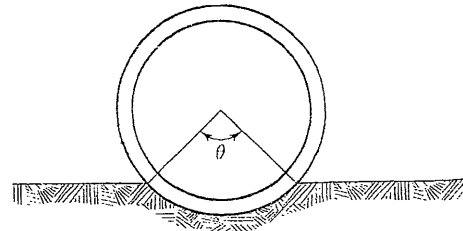


TABLE 9.2 Approximate Range of Values of D_L

Variable	Range	Remarks
D_L	1.5 to 2.5	If the soil in the trench is not compacted, then the higher value of D_L should be used.
	1.0	When deflection calculations are based on prism loads.

 TABLE 9.3 Average Values of Soil Reaction Modulus, E' (for Short Term Flexible Pipe Deflection) (Howard, 1977)

Soil type-pipe bedding material (United Classification System) ^a	E' for degree of compaction of bedding			
	Dumped	Slight, < 85% Proctor, < 40% relative density	Moderate, 85%–95% Proctor, 40%–70% relative density	High, > 95% Proctor, > 70% relative density
Fine-grained soils (LL > 50) ^b Soils with medium to high plasticity CH, MH, CH-MH	No data available; consult a competent soils engineer; Otherwise use $E' = 0$			
Fine-grained soils (LL < 50) Soils with medium to no plasticity CL, ML, ML-CL, with less than 25% coarse-grained particles	50 lb/in ² (345 kN/m ²)	200 lb/in ² (1,380 kN/m ²)	400 lb/in ² (2,760 kN/m ²)	1,000 lb/in ² (6,900 kN/m ²)
Fine-grained soils (LL < 50) Soils with medium to no plasticity CL, ML, ML-CL, with more than 25% coarse-grained particles	100 lb/in ² (690 kN/m ²)	400 lb/in ² (2,760 kN/m ²)	1,000 lb/in ² (6,900 kN/m ²)	2,000 lb/in ² (13,800 kN/m ²)
Coarse-grained soils with fines GM, GC, SM, SC contains more than 12% fines	200 lb/in ² (1,380 kN/m ²)	1,000 lb/in ² (6,900 kN/m ²)	2,000 lb/in ² (13,800 kN/m ²)	3,000 lb/in ² (20,700 kN/m ²)
Coarse-grained soils with little or no fines GW, GP, SW, SP ^c contains less than 12% fines	1,000 lb/in ² (6,900 kN/m ²)	3,000 lb/in ² (20,700 kN/m ²)	3,000 lb/in ² (20,700 kN/m ²)	3,000 lb/in ² (20,700 kN/m ²)
Crushed rock	1,000 lb/in ² (6,900 kN/m ²)	3,000 lb/in ² (20,700 kN/m ²)	3,000 lb/in ² (20,700 kN/m ²)	3,000 lb/in ² (20,700 kN/m ²)
Accuracy in term of percentage deflection ^d	± 2	± 2	± 1	± 0.5

^a ASTM Designation D2487, USBR Designation E-3

^b LL = Liquid Limit

^c or any borderline soil beginning with one of these symbols (i.e., GM-GC, GC-SC)

^d for ± 1% accuracy and predicted deflection of 3%, actual deflection would be between 2% and 4%

Note: Values applicable only for soil fills less than 50 ft (15 m). Table does not include any safety factor. For use in predicting initial deflections only—appropriate deflection lag factor must be applied for long-term deflections. If bedding falls on the borderline between two compaction categories, select lower E' value or average the two values. Percentage Proctor based on laboratory maximum dry density from test standards using about 12,500 ft-lb/ft³ (600 m-kN/m³) (ASTM D698, AASHTO T-99, USBR Designation E-11).

Used with permission of ASCE.

The parameter that controls the pipe deformation is known as the deflection ratio. The deflection ratio of a pipe is defined as the ratio of the vertical deflection of pipe and the mean diameter of the pipe.

Deflection Ratio:

$$\text{Deflection Ratio (\%)} = (\Delta Y/D) \times 100\% \quad (9.19)$$

where ΔY = vertical deflection of pipe, $\Delta Y \approx \Delta X$ when the deflection is less than 10%, in or m; and
 D = mean diameter of pipe, in or m.

Mean Diameter of Pipe:

$$D = (D_o + D_i)/2 = D_o - t = D_i + t \quad (9.20)$$

where D = mean diameter of pipe, in or m;
 D_o = outside diameter of pipe, in or m;
 D_i = inside diameter of pipe, in or m; and
 t = thickness of pipe, in or m.

There is another formula that can be used to estimate the deflection of the pipe. It is essentially an alternative version of the Modified Iowa formula and has been widely used in the engineering field. This formula is

$$\Delta X = \frac{D_L \cdot K \cdot W_c}{0.149 \cdot PS + 0.061 \cdot E'} \quad (9.21)$$

where ΔX = horizontal deflection, in or m (Figure 9.6);
 K = bedding constant, its value depending on the bedding angle (see Table 9.1 and Figure 9.7); as a general rule, a value of $K = 0.1$ is assumed;
 D_L = deflection lag factor, see Table 9.2;
 W_c = vertical load per unit length of the pipe, lb/in or kN/m;
 PS = pipe stiffness, lb/in² or kN/m²; and
 E' = soil reaction modulus, lb/in² or kN/m².

The vertical pressure on solid pipe is given by

$$P_{tp} = \sum \gamma_i \cdot H_i \quad (9.22)$$

The vertical pressure on perforated pipe is given by

$$P_{tp} = \frac{\sum \gamma_i \cdot H_i}{(1 - n \cdot d/12)} \quad (9.23)$$

where P_{tp} = vertical pressure on the pipe, $P_{tp} = W_c/D_o$, lb/in² or kN/m²;
 γ_i = unit weight of material i on the pipe (sand, clay or solid waste), lb/in³ or kN/m³;
 H_i = thickness of material i , in or m;

d = diameter of perforated hole or width of perforated slot on the pipe, in or m; and
 n = number of perforated holes or slots per row per foot of pipe.

Pipe stiffness is measured according to ASTM D2412 (Standard Test Method for External Loading Properties of Plastic Pipe by Parallel-Plate Loading). The elastic modulus of the pipe material depends on the type of resin and formulation being used. Three formulas that can be used to calculate pipe stiffness are

$$PS = \frac{E \cdot I}{0.149 \cdot r^3} \quad (9.24)$$

$$PS = 0.559 \cdot E \cdot (t/r)^3 \quad (9.25)$$

and

$$PS = 4.47 \cdot \frac{E}{(SDR - 1)^3} \quad (9.26)$$

where PS = pipe stiffness, lb/in² or kN/m²;
 E = elastic modulus of the pipe material, lb/in² or kN/m²;
 I = moment of inertia of the pipe wall per unit length,
 $I = t^3/12$, in⁴/in = in³ or m⁴/m = m³;
 r = mean radius of pipe, in or m;
 t = wall thickness of pipe, in or m; and
 SDR = standard dimension ratio, the same as the dimension ratio.

The allowable deflection ratios for a typical commercial polyethylene pipe are listed in Table 9.4.

Deflections of buried flexible pipe are commonly calculated using Equation 9.16 or 9.21. These equations use the soil reaction modulus, E' , as a surrogate parameter for soil stiffness. It should be noted that the values of E' in Table 9.3 only apply for soil fills of less than 50 ft (15 m). However, megafills built over leachate collection pipes often exceed 150 ft (46 m) in height. The soil reaction modulus is not a directly measurable soil parameter; instead it must be determined by back-calculation using observed pipe deflections. Research by Selig (1990) showed that E' is a function of the bedding condition and overburden pressure. Selig's studies were carried out to seek a correlation between the soil reaction modulus and soil stiffness parameters such as

TABLE 9.4 Allowable Deflection Ratio of Polyethylene Pipe

SDR	Allowable Deflection Ratio
11	2.7%
13.5	3.4%
15.5	3.9%
17	4.2%
19	4.7%
21	5.2%
26	6.5%
32.5	8.1%

Young's modulus of soil, E_s , and the constrained modulus of soil, M_s , where E_s and D_s are related through Poisson's ratio of soil, ν_s , by

$$M_s = \frac{E_s \cdot (1 - \nu_s)}{(1 + \nu_s)(1 - 2 \cdot \nu_s)} \quad (9.27)$$

where M_s = constrained modulus of soil, lb/ft² or kN/m²;
 E_s = elastic modulus of soil, lb/ft² or kN/m²; and
 ν_s = Poisson's ratio of soil.

The studies and analyses by Neilson (1967), Allgood and Takahashi (1972), and Hartely and Duncan (1987) indicated that for

$$E' = k \cdot M_s \quad (9.28)$$

the value of k may vary from 0.7 to 2.3. Using $k = 1.5$ as a representative value and $\nu_s = 0.3$, in addition to combining Equations 9.27 and 9.28 yields the following relationship between the elastic modulus of the pipe and soil (Selig, 1990):

$$E' = 2 \cdot E_s \quad (9.29)$$

The values of elastic parameters, E_s and ν_s , can be found in Table 9.5 according to different percents of density from a standard Proctor compaction test (ASTM D698).

TABLE 9.5 Elastic Soil Parameters (Selig, 1990)

Soil Type	Stress Level		85% Standard Density			95% Standard Density		
			E_s		ν_s	E_s		ν_s
	psi	kPa	psi	MPa		psi	MPa	
SW, SP, GW, GP	1	7	1,300	9	0.26	1,600	11	0.40
	5	35	2,100	14	0.21	4,100	28	0.29
	10	70	2,600	18	0.19	6,000	41	0.24
	20	140	3,300	23	0.19	8,600	59	0.23
	40	280	4,100	28	0.23	13,000	90	0.25
	60	420	4,700	32	0.28	16,000	110	0.29
GM, SM, ML, and GC, SC with < 20% fines	1	7	600	4	0.25	1,800	12	0.34
	5	35	700	5	0.24	2,500	17	0.29
	10	70	800	6	0.23	2,900	20	0.27
	20	140	850	6	0.30	3,200	22	0.29
	40	280	900	6	0.38	3,700	25	0.32
	60	420	1,000	7	0.41	4,100	28	0.35
CL, MH, GC, SC	1	7	100	1	0.33	400	3	0.42
	5	35	250	2	0.29	800	6	0.35
	10	70	400	3	0.28	1,100	8	0.32
	20	140	600	4	0.25	1,300	9	0.30
	40	280	700	5	0.35	1,400	10	0.35
	60	420	800	6	0.40	1,500	10	0.38

9.4.2 Pipe Wall Buckling

Buckling can occur because of insufficient stiffness. Buckling may govern design of flexible pipes subjected to internal vacuum, external hydrostatic pressure, or high soil pressures in compacted soil (Figure 9.8). As Moser (1990) notes the more flexible the conduit (e.g., high values of *SDR*), the more unstable the wall structure will be in resisting buckling.

Most conduits are buried in a soil medium that does offer considerable shear resistance. An exact rigorous solution to the problem of buckling of a cylinder in an elastic medium entails some advanced mathematics (Moser, 1990). However, because of uncertainties in the behavior and performance of the surrounding soil, an exact solution is not necessary. Meyerhof and Baikal (1963) developed the following empirical formula for computing the critical buckling pressure in a buried circular conduit:

$$P_{cr} = 2 \cdot \{ [E' / (1 - \mu^2)] (E \cdot I / r^3) \}^{1/2} \tag{9.30}$$

Where,

- P_{cr} = critical buckling pressure, lb/in² or kN/m²;
- E' = modulus of soil reaction, lb/in² or kN/m², see Table 9.3;
- μ = Poisson's ratio of pipe material;
- E = modulus of elasticity of the pipe material, lb/in² or kN/m²;
- I = moment of inertia of the pipe wall per unit length,
in⁴/in = in³ or m⁴/m = m³, $I = t^3/12$; and
- r = mean radius of the pipe, in or m.

Because $I = t^3/12$ and $r = D/2$, Equation 9.30 can be rewritten as

$$P_{cr} = 2 \cdot (G_b \cdot E')^{1/2} \tag{9.31}$$

where

$$G_b = \frac{2 \cdot E}{3 \cdot (1 - \mu^2)} \cdot (t/D)^3 \tag{9.32}$$

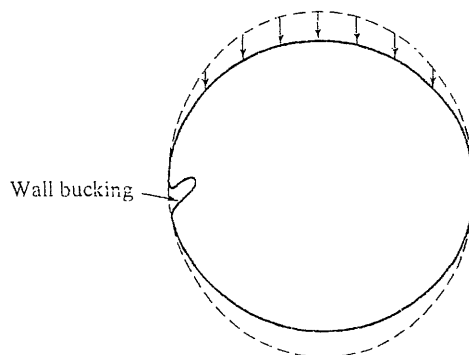


FIGURE 9.8 Localized Wall Buckling

in which

$$t = \text{thickness of pipe, in or m and}$$

$$D = \text{mean diameter of pipe, in or m}$$

The factor of safety for pipe wall buckling can be determined by

$$FS = P_{cr}/P_{ip} \quad (9.33)$$

where P_{ip} = actual vertical pressure at the top of the pipe, obtained from Equation 9.22 or 9.23, lb/in² or kN/m².

In both Equations 9.30 and 9.31 initial out-of-roundness is neglected but the reduction in P_{cr} because of this has been assumed to be no greater than 30% (Moser, 1990). As a result, a factor of safety ≥ 2 is recommended for use with Equation 9.33 in the design of a flexible conduit to resist buckling.

EXAMPLE 9.2

An 8-inch (200-mm) SDR 11 HDPE perforated pipe with 8, 0.25-inch (6-mm) holes per foot (i.e., 4 holes per side per foot) is selected as a primary leachate collection pipe. The maximum load acting on the pipe includes a 2-ft (0.6-m) protective sand layer ($\gamma_{\text{sand}} = 115 \text{ lb/ft}^3$ or 18 kN/m^3), 100-ft (30-m) solid waste ($\gamma_{\text{waste}} = 60 \text{ lb/ft}^3$ or 9.4 kN/m^3), 12-inch (0.3-m) gas venting layer ($\gamma_{\text{sand}} = 115 \text{ lb/ft}^3$ or 18 kN/m^3), 18-inch (0.45-m) compacted clay layer ($\gamma_{\text{clay}} = 110 \text{ lb/ft}^3$ or 17.3 kN/m^3), 24-inch (0.6-m) drainage and protective layer ($\gamma_{\text{silt}} = 110 \text{ lb/ft}^3$ or 17.3 kN/m^3), and 6-inch (0.15-m) topsoil ($\gamma_{\text{top}} = 90 \text{ lb/ft}^3$ or 14 kN/m^3). Assume bedding angle $\theta = 0^\circ$, deflection lag factor $D_L = 1.0$, elastic modulus of the pipe material for 50 years at 73°F (23°C) temperature $E = 28,200 \text{ lb/in}^2$, (194,000 kN/m²), Poisson's ratio of pipe material $\mu = 0.3$. The bedding material of the pipe is poorly graded gravel (GP) with 85% standard density. What will be the deflection ratio (%) and critical buckling pressure of the pipe?

Solution: The maximum load applied on the pipe is given by

$$W_c = \frac{\left(\sum \gamma_i \cdot H_i \right) \cdot D_o}{(1 - n \cdot d/12)} \quad (9.18)$$

$$= \frac{[(115)(2) + (60)(100) + (115)(1) + (110)(3.5) + (90)(0.5)] \times 8/12}{(1 - 4 \times 0.25/12)}$$

$$= \frac{(230 + 6,000 + 115 + 385 + 45) \times 8/12}{0.917}$$

$$= \frac{6,775 \times 8/12}{0.917}$$

$$= 4,925 \text{ lb/ft} = 410 \text{ lb/in} \text{ (72 kN/in)}$$

The maximum pressure applied on the pipe can be obtained from

$$P_{ip} = W_c/D_o = 410/8 = 51.3 \text{ lb/in}^2 \text{ (354 kN/m}^2\text{)}$$

From Table 9.5,

$$P_{ip} = 40 \text{ lb/in}^2, E_s = 4,100 \text{ lb/in}^2$$

and $P_{ip} = 60 \text{ lb/in}^2$, $E_s = 4,700 \text{ lb/in}^2$

For $P_{ip} = 51.3 \text{ lb/in}^2$,

$$E_s = 4,100 + (51.3 - 40)(4,700 - 4,400)/20 = 4,100 + 339 = 4,439 \text{ lb/in}^2$$

The soil reaction modulus is given by

$$E' = 2 \cdot E_s = 2 \times 4,439 = 8,878 \text{ lb/in}^2 (61,200 \text{ kN/m}^2) \quad (9.29)$$

The thickness of pipe is given by

$$\begin{aligned} t &= D_o / SDR \\ &= 8/11 = 0.73 \text{ in (0.0185 m)} \end{aligned} \quad (9.6)$$

The mean diameter of pipe is

$$\begin{aligned} D &= D_o - t \\ &= 8 - 0.73 = 7.27 \text{ in (0.1847 m)} \end{aligned} \quad (9.20)$$

Also,

Deflection lag factor, $D_L = 1.0$;

Bedding angle $\theta = 0^\circ$, $K = 0.11$;

Mean radius of the pipe, $r = 3.635 \text{ in (0.0923 m)}$;

Elastic modulus of the pipe material, $E = 28,200 \text{ lb/in}^2 (194,000 \text{ kN/m}^2)$;

Soil reaction modulus, $E' = 8,878 \text{ lb/in}^2 (61,200 \text{ kN/m}^2)$;

and

Inertia moment of the pipe wall per unit length, $\text{in}^4/\text{in} = \text{in}^3$, given by

$$I = t^3/12 = (0.73)^3/12 = 0.389/12 = 0.0324 \text{ in}^3 (5.276 \times 10^{-7} \text{ m}^3)$$

Modified Iowa Formula:

$$\begin{aligned} \Delta X &= \frac{D_L \cdot K \cdot W_c \cdot r^3}{E \cdot I + 0.061 E' \cdot r^3} \\ &= \frac{(1.0)(0.11)(410)(3.635)^3}{(28,200)(0.0324) + (0.061)(8,878)(3.635)^3} \\ &= \frac{(1.0)(0.11)(410)(48.03)}{(28,200)(0.0324) + (0.061)(8,878)(48.03)} \\ &= \frac{2,166}{914 + 26,011} \\ &= 0.08 \text{ in (2.0 mm)} \end{aligned} \quad (9.16)$$

Deflection Ratio:

$$\begin{aligned} \text{Deflection Ratio} &= (\Delta Y/D) \times 100\% \\ &= (0.08/7.27) \times 100\% \\ &= 1.1\% < 2.7\% \text{ (ok, as shown in Table 9.4)} \end{aligned} \quad (9.19)$$

Wall Buckling of Pipe:

Modulus of soil reaction, $E' = 8,878 \text{ lb/in}^2$, (61,200 kN/m²);

Poisson's ratio of pipe material, $\mu = 0.3$;
 Modulus of elasticity of the pipe material, $E = 28,200 \text{ lb/in}^2$ ($194,000 \text{ kN/m}^2$);
 Moment of inertia of the pipe wall per unit length, $I = 0.0324 \text{ in}^3$ ($5.276 \times 10^{-7} \text{ m}^3$);
 Mean radius of the pipe, $r = 3.635 \text{ in}$ (0.0923 m).
 Thus,

$$\begin{aligned}
 P_{cr} &= 2 \cdot \{ [E' / (1 - \mu^2)] (E \cdot I / r^3) \}^{1/2} & (9.30) \\
 &= 2 \times \{ [8,878 / (1 - 0.3^2)] [(28,200 \times 0.0324) / (3.635)^3] \}^{1/2} \\
 &= 2 \times [9,756 \times (913.68 / 48.03)]^{1/2} \\
 &= 2 \times (185,589)^{1/2} \\
 &= 2 \times 431 \\
 &= 862 \text{ lb/in}^2 \text{ (5,943 kN/m}^2\text{)}
 \end{aligned}$$

The factor of safety for pipe wall buckling is, then,

$$FS = P_{cr} / P_{tp} = 862 / 51.3 = 16.8 > 2 \text{ (OK)} \quad (9.33)$$

9.5 SUMP AND RISER PIPES

Leachate collection sumps are low points in the landfill liner constructed to collect and removal leachate. The sumps are filled with gravel to provide the maximum space (volume) for leachate accumulation, as well as to support the weight of the overlying waste, cover system, and post-closure loadings. Commonly, the composite liner system is slightly depressed or indented to create these sumps (shown in Figures 9.9 and 9.10). The absence of sketches illustrating continued gravity flow of leachate beyond the limits of the cells and/or landfill using liner penetrations is intentional. The authors do not recommend such practice due to the difficulty of making liner seams in this remote of all locations. With double liner systems, the situation is even more difficult. Even with the sketches of Figures 9.9 and 9.10 it is difficult to test the geomembrane seaming in such sumps because of the slope and corners at which the seams occur. Because of the difficulty in seam testing sumps, sump areas often are designed with an additional layer of geomembrane. Sulfates are one of the most common and abundant constituents in landfill leachate. Accordingly, all concrete components in a sump (e.g., riser pipe and foundation pad) must be constructed using low water/cement ratios and sulfate resistant, Class V Portland cement (ACI, 1998). Failure to observe this precaution can lead to sulfate attack and disintegration of the concrete. Sulfate attack occurs when calcium, alumina, and sulfate combine to form the mineral ettringite ($3\text{CaO} \cdot \text{Al}_2\text{O}_3 \cdot 32\text{H}_2\text{O}$) in the cement matrix. The volume of ettringite is over 200% that of the original constituents, which can result in massive swelling and cracking when sufficient ettringite forms by the sulfation of alumina. Alternatively, many sumps now are being constructed using premanufactured units made of HDPE, with large-diameter HDPE pipe or HDPE manholes. Although more costly, the factory manufactured sumps can be thoroughly tested and installed as a unit.

Figure 9.9 shows details of vertical riser (manhole) removal designs for primary and secondary leachate collection systems. The manhole riser extends vertically

**APPLICATION FOR PERMIT
OWL LANDFILL SERVICES, LLC**

**VOLUME III: ENGINEERING DESIGN AND CALCULATIONS
SECTION 5: PIPE LOADING CALCULATIONS**

ATTACHMENT III.5.B

SHARMA, HARI .D. AND SANGEETA P. LEWIS. 1994.

***WASTE CONTAINMENT SYSTEMS, WASTE STABILIZATION AND LANDFILLS:
DESIGN AND EVALUATION.***

NEW YORK: JOHN WILEY AND SONS

WASTE CONTAINMENT SYSTEMS, WASTE STABILIZATION, AND LANDFILLS: DESIGN AND EVALUATION

HARI D. SHARMA, PH.D., P.E.

Chief Engineer and Director
EMCON Associates
San Jose, California

SANGEETA P. LEWIS, P.E.

Project Manager
CH₂M Hill
Oakland, California



A Wiley-Interscience Publication

JOHN WILEY & SONS, INC.

New York / Chichester / Toronto / Brisbane / Singapore

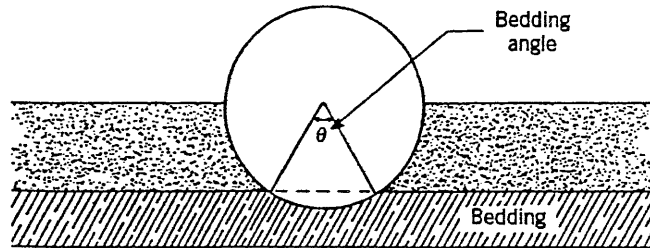


Figure 9.29 Bedding angle. (From Moser, 1990.)

approximately 1.5 times greater than the load determined using Marston’s equation. The bedding constant is dependent on the bedding angle, as depicted in Figure 9.29. Values for the bedding constant are given in Table 9.12.

In the preceding paragraphs on soil stiffness we discussed the modulus of passive resistance of the soil, e , and noted that the units for e were not dimensionally correct. The Iowa formula was therefore modified and the following equation is known as the modified Iowa formula:

$$\Delta X \approx \Delta Y = \frac{D_L K W_c r^3}{EI + 0.061 E' r^3} \tag{9.34}$$

where $E' = er$. E' is known as the modulus of soil reaction. Methods for establishing this value were given in the preceding soil stiffness paragraphs. Actual deflections may be estimated using the modified Iowa formula by assuming that horizontal and vertical deflections are equal.

WATKINS’ RING STABILITY EQUATION. Deflection may also be calculated using Watkins’ (1989) ring stability equation. The ring stability equation is based on assuming incipient collapse of the pipe; however, it is important to note that incipient collapse does not mean imminent collapse. Rather, it refers to a condition of possible col-

TABLE 9.12 Values of Bedding Constant, K

Bedding Angle (deg)	K
0	0.110
30	0.108
45	0.105
60	0.102
90	0.096
120	0.090
180	0.083

Source: Moser (1990).

**APPLICATION FOR PERMIT
OWL LANDFILL SERVICES, LLC**

**VOLUME III: ENGINEERING DESIGN AND CALCULATIONS
SECTION 5: PIPE LOADING CALCULATIONS**

ATTACHMENT III.5.C

WASHINGTON STATE DEPARTMENT OF ECOLOGY. 1987.

SOLID WASTE LANDFILL DESIGN MANUAL.

WASHINGTON: WDOE

TABLE OF CONTENTS

	<u>Page</u>
4C.1 COLLECTION PIPE MATERIALS	4C-1
4C.1.1 Pipe Perforations	4C-3
4C.2 STRUCTURAL REQUIREMENTS	4C-4
4C.2.1 Loading Conditions	4C-4
4C.2.2 Refuse and Earth Loads	4C-6
4C.2.3 Superimposed Loads	4C-13
4C.2.4 Design Safety Factor	4C-18
4C.3 RIGID PIPE DESIGN	4C-19
4C.3.1 Classes of Bedding and Bedding Factors	4C-19
4C.3.2 Selection of Pipe Strength	4C-23
4C.4 FLEXIBLE PIPE DESIGN.....	4C-23
4C.4.1 General Approach.....	4C-23
4C.4.2 Selection of Plastic Pipe.....	4C-25
4C.4.3 Selection of Other Flexible Pipes.....	4C-26
4C.4.4 Bedding Material.....	4C-26

LIST OF FIGURES

	<u>Page</u>
4C.1 Installation Conditions	4C-5
4C.2 Trench Condition-Values of Load Coefficient C_{us} (Trench Uniform Surcharge)	4C-8
4C.3 Trench Condition-Values of Load Coefficient C_d (Backfill).....	4C-10
4C.4 Diagram for Load Coefficient C_c for Positive Projecting Pipes	4C-11
4C.5 Diagrams for Load Coefficient C_n for Negative Projecting and Induced Trench Pipes	4C-14
4C.6 Trench Beddings: Circular Pipe	4C-20
4C.7 Positive Projecting Embankment Beddings: Circular Pipe	4C-21

LIST OF TABLES

	<u>Page</u>
4C.1 Maximum Value of K_u' for Typical Backfill Soils	4C-8
4C.2 Recommended Design Values of r_{sd} (Positive Projecting Embankment <i>Conditions</i>)	4C-12
4C.3 Values of Load Coefficients, C_s , for Concentrated and Distributed Superimposed Loads Vertically Centered over Sewer Pipe	4C-16
4C.4 Superimposed Concentrated Load Impact Factors, F	4C-17
4C.5 Equipment Loads	4C-17
4C.6 Values of N for Circular Pipe	4C-22
4C.7 Values of X for Circular Pipe	4C-22
4C.8 Values of Bedding Constant, K_b	4C-25

APPENDIX 4C

COLLECTION PIPE MATERIALS AND STRUCTURAL REQUIREMENTS

4C.1 COLLECTION PIPE MATERIALS

Pipe that may be suitable for leachate collection systems is manufactured to meet nationally recognized product specifications. Some materials are more appropriate than others for use in a leachate collection system and the various types of pipe should be evaluated carefully. Various factors to consider are:

- Intended use (type of leachate)
- Flow requirements
- Scour or abrasion conditions
- Corrosion conditions
- Product characteristics
- Physical properties
- Installation requirements
- Handling requirements
- Cost effectiveness

No single pipe product will provide optimum capability in every characteristic for all leachate collection system design conditions. Specific application requirements should be evaluated prior to selecting pipe materials.

Pipe materials for leachate collection applications fall within the two commonly accepted classifications of rigid pipe and flexible pipe. Rigid pipe materials derive a substantial part of their basic earth load carrying capacity from the structural strength inherent in the rigid pipe wall, while flexible pipe materials derive load carrying capacity from the interaction of the flexible pipe and the embedment soils. Products commonly available within these two classes are:

1. Rigid Pipe
 - a. Asbestos-cement pipe (ACP)
 - b. Cast iron pipe (CIP)
 - c. Concrete pipe (CP)
 - d. Vitrified clay pipe (VCP)
2. Flexible Pipe
 - a. Ductile iron pipe (DIP)
 - b. Steel pipe (SP)
 - c. Thermoplastic pipe
 - Acrylonitrile-butadiene-styrene (ABS)
 - ABS composite
 - Polyethylene (PE)
 - Polyvinyl chloride (PVC)
 - d. Thermoset plastic pipe
 - Reinforced plastic mortar (RPM)

- Reinforced thermosetting resin (RTR)

Within the rigid pipe classification, the suitability of cast iron and concrete pipe for leachate collection systems is limited by the difficulty of incorporating perforations in the pipe walls and their susceptibility to corrosion by acidic leachates. The use of asbestos-cement pipe is limited by its low beam strength. It is also susceptible to attack by acidic leachates. Vitrified clay pipe can be perforated and is highly resistant to chemical corrosion, but its relatively low beam strength limits the fill height that can be placed over it. For these reasons, rigid pipes have very limited use potential in leachate collection systems.

As a group, flexible pipes offer good potential for use in leachate collection systems. Within the flexible pipe group, however, only certain products are suitable. Ductile iron and steel pipe have little application for leachate collection systems primarily because of their susceptibility to attack by acidic leachates. Also, although ductile iron pipe has high load bearing capacity, incorporating perforations in the pipe walls is difficult. Thermoplastic and thermoset plastic pipe are more suitable products for leachate collection systems.

Thermoplastic materials are characterized by their ability to be repeatedly softened by heating and hardened by cooling through a temperature range characteristic for each plastic. Materials suitable for use in leachate collection systems include ABS pipe, ABS composite pipe, PE pipe, and PVC pipe. All of these materials are subject to attack by certain organic chemicals, so compatibility with the leachate must be considered in this selection. ABS is generally not as resistant to acids as PVC and neither of these two materials has good resistance to concentrated ketones and esters. Pipes manufactured from any of these materials are subject to excessive deflection when improperly bedded and haunched, so proper design and construction are important. With the exception of PVC pipe, these pipes are also subject to environmental stress cracking. Thermoplastic pipe product design should be based on long-term data.

Thermoset plastic materials, cured by heat or other means, are substantially infusible and insoluble. The two categories of thermoset plastic materials suitable for leachate collection systems include RPM pipe and RTR pipe. RPM pipe is manufactured containing reinforcements, such as fiberglass, and aggregates, such as sand, embedded in or surrounded by cured thermosetting resin. RTR pipe is manufactured using a number of methods including centrifugal casting, pressure laminating, and filament winding. In general, the product contains fibrous reinforcement materials, such as fiberglass, embedded in or surrounded by cured thermosetting resin. Pipes manufactured from both of these materials are subject to strain corrosion in some environments, attack by certain organic chemicals, and excessive deflection when improperly bedded and haunched. Therefore, leachate compatibility and proper design and construction are important when thermoset plastic pipe is used in leachate collection systems.

4C.1.1 Pipe Perforations

By nature of their intended use, leachate collection lines must be perforated. The size and spacing of the openings should be determined based on hydraulic considerations. The effects of the perforations should be considered in the structural design of the leachate collection pipes.

4C.1.1.1 Size and Spacing

A leachate collection line, to function correctly, must be capable of accepting all the leachate flowing to it through the gravel drainage layer. After the pipe is sized to handle the flow, the size and spacing of the perforations should be selected. The rate of flow into the leachate collection pipes through the perforations is dependent on several factors, including the hydraulic conductivity of the gravel material around the pipe and the head loss due to convergence of flow to the perforations in the pipe.

W.T. Moody, as cited in U.S. * Department of the Interior (1978) determined the theoretical relationship among the above factors and concluded that increasing the hydraulic conductivity of the gravel envelope around the pipe was a more effective method for increasing the rate of flow into the pipe than increasing the size of the openings. Therefore, the selection of the size and spacing of the perforations should be based on: consideration of standard perforated pipe commonly available from manufacturer; bedding and backfill requirements for the particular installation; and effects on pipe strength. For a given rate of leachate inflow and a perforated pipe, the minimum required hydraulic conductivity of the gravel envelope around the pipe can be determined using a procedure similar to that presented in U.S. Department of the Interior (1978).

4C.1.1.2 Effects on Load Capacity

The various design procedures for rigid and flexible pipes and the various pipe performance limits are based on solid wall pipe. Pacey, et al., as cited in Dietzler (1984) has suggested that the effect of perforations could be compensated by arbitrarily increasing the earth load on the pipe. Data presented in Dietzler (1984) indicated the inclusion of typical perforations in the lower quarters of 6-inch ABS and PVC pipe has little influence on pipe stiffness and deflection versus load performance. Others have stated there are indications that perforations will reduce the effective length of pipe available to carry loads and resist deflection suggest taking the effect of perforations into account by increasing the load in proportion to the reduction in the effective length. This latter method appears to be an adequately conservative approach. If L_p equals the cumulative length of the perforations per unit length of the pipe, L , then the actual load on the pipe should be increased as follows:

$$\text{Design Load} = \text{Actual Load} \times \frac{L}{L - L_p} \quad (4C-1)$$

Methods to determine the actual load are discussed in the following sections.

4C.2 STRUCTURAL REQUIREMENTS

Leachate collection systems installed underneath a landfill must be designed to withstand the anticipated height and weight of refuse to be placed over them. It is not uncommon to find heights in excess of 100 feet. Appropriately, leachate collection systems must be designed for vertical pressure acting at the base of the landfill, considering the height of the landfill and the weighted average density of the refuse, daily cover, final cover system, and any superimposed loads during the life of the landfill. Perimeter collection systems that generally lie outside the landfill should be designed for the earth loads acting on them along with any superimposed loads.

The supporting strength of a leachate collection pipe is a function of installation conditions as well as the strength of the pipe itself. Structural analysis and design of the collection system are problems of soilstructure interaction. This section presents general procedures for determining the structural requirements of the pipes in a leachate collection system. Detailed discussions concerning structural design of pipelines may be found in ASCE and WPCF (1982). The design procedure for the selection of pipe strength consists of the following:

- Determination of loading condition
- Determination of refuse and earth loads
- Determination of superimposed loads
- Selection of bedding and determination of bedding factor
- Application of factor of safety
- Selection of pipe strength

4C.2.1 Loading Conditions

The load transmitted to a pipe is largely dependent on the type of installation. The common types of installation conditions are shown in Figure 4C.1 and include trench, positive projecting embankment, negative projecting embankment, and induced trench. Jacked or tunneled is also an installation condition, but has little application for leachate collection systems. The difficulty in controlling the placement of the embankment material greatly limits the potential use of the induced trench condition for leachate collection systems.

Trench installation* conditions are defined as those in which the pipe is installed in a relatively narrow trench cut in undisturbed ground and covered with backfill to the original ground surface. Embankment conditions are defined as those in which the pipe is covered above the original ground surface or in which a trench in undisturbed soil is so wide that wall friction does not affect the load on the pipe. The embankment classification is further subdivided into positive projecting and negative projecting classification. Pipe is positive projecting when its top is above the adjacent original ground surface. Negative projecting pipe is installed with its top below the adjacent original ground surface in a trench that is narrow with respect to the pipe and depth of cover.

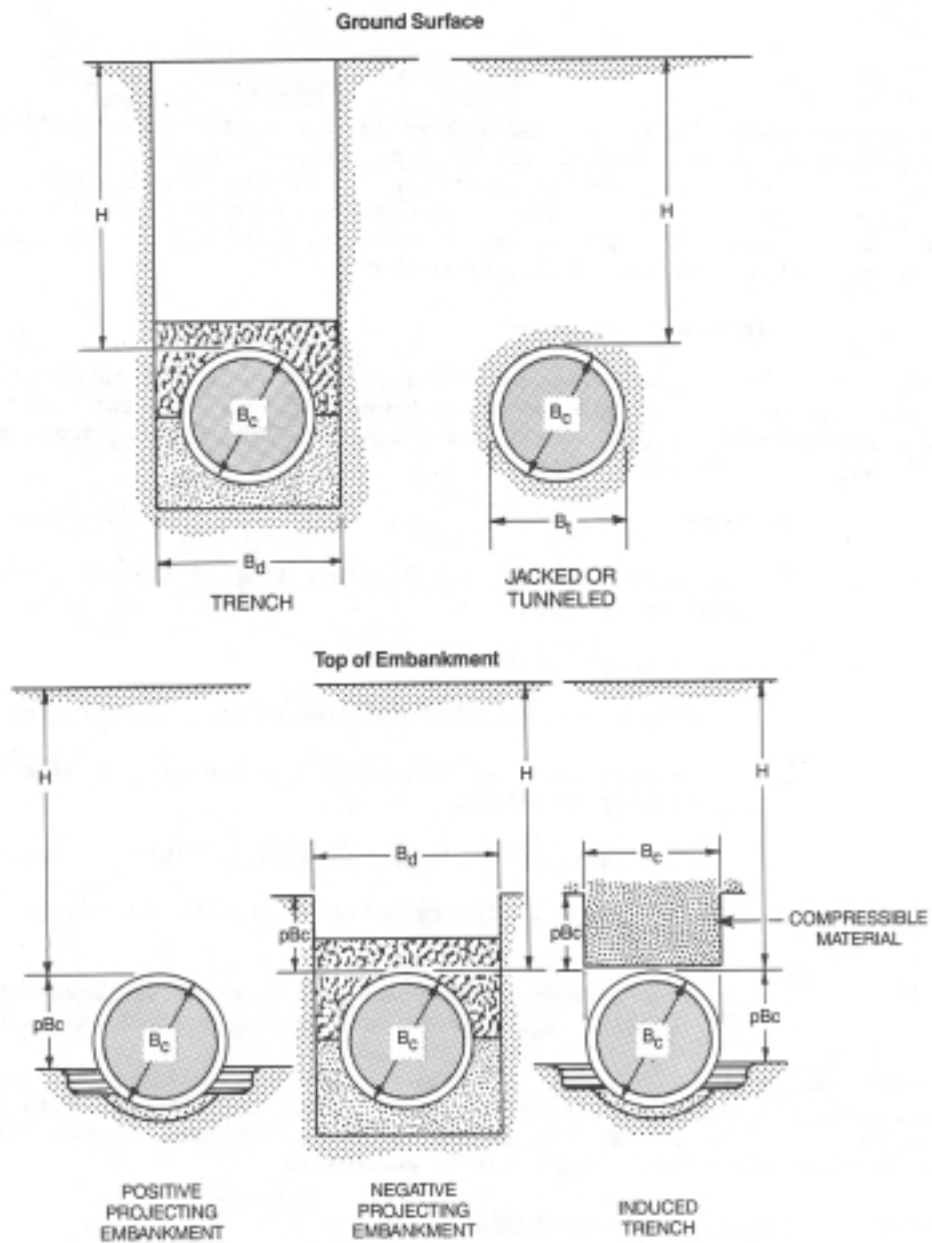


Figure 4C.1
Installation Conditions

Both the trench condition and either of the embankment conditions may be appropriate in the design of leachate collection systems. A perimeter collection system may be designed for either the trench condition or the negative projecting embankment condition, depending on trench width. Leachate collection systems underneath the landfill would generally be designed for one of the embankment conditions.

4C.2.2 Refuse and Earth Loads

The methods for determining the vertical load on buried conduits caused by soil forces were developed by Marston for all of the most commonly encountered construction conditions (ASCE and WPCF, 1982). The general form of the Marston equation is:

$$W = CWB^2 \quad (4C-2)$$

where: W = Vertical load per unit length acting on the pipe because of gravity soil loads

v = Unit weight of the soil

B = Trench or pipe width, depending on installation conditions

C = Dimensionless coefficient that measures the effects of the following variables:

- The ratio of the height of fill to width of trench or pipe
- The shearing forces between interior and adjacent soil prisms
- The direction and amount of relative settlement between interior and adjacent soil prisms for embankment conditions

While the general form of the Marston equation includes all the factors necessary to analyze all types of installation conditions, it is convenient to write a specialized form of the equation for each of the installation conditions described in the previous subsection.

4C.2.2.1 Loads for Trench Conditions

In the trench condition, the load on the pipe is caused by both the waste fill and the trench backfill (U.S. EPA, 1983). These two components of the total vertical pressure on the pipe are computed separately and then added to obtain the total vertical pressure acting on the top of the pipe.

The waste fill is assumed to develop a uniform surcharge pressure, O_f , at the base of the fill. The magnitude of Q_f is given by the expression:

where: $Q_f = (w_f)(H_f)$ (4C-3)
 $Q_f =$ Vertical pressure at the base of the waste fill (lbs/sq ft)

$w_f =$ Weighted average density of the waste fill including refuse, intermediate cover, and final cover system (lbs/cu ft)

$H_f =$ Height of waste fill including cover (ft)

The weighted average density of the waste fill, w_f is computed as follows:

$$\frac{w_r(H_r) + (w_i)(T) + (w_c)(T_c)}{H_f} \quad (4C-4)$$

where: $w_r =$ Average in-place wet density of the refuse (lbs/cu ft)

$H_r =$ Height of refuse excluding cover layers (ft)

$w_i =$ Wet density of intermediate cover (lbs/cu ft)

$T_i =$ Total thickness of intermediate cover layers (ft)

$w_c =$ Wet density of the final cover system (lbs/cu ft)

$T_c =$ Thickness of the final cover system (ft)

$H_f = H_r + T_i + T_c$

The value of the vertical pressure at the top of the pipe due to the waste fill, P_{vf} (in lbs/sq ft), is determined from the following:

$$P_{vf} = (Q_f)(C_{us}) \quad (4C-5)$$

where: $C_{us} =$ Dimensionless load coefficient that is a function of the ratio of the depth of the trench, H (measured from the original ground surface to the top of the pipe) to the trench width, B_d , and of the friction between the backfill and the sides of the trench.

The load coefficient, C_{us} , may be calculated from the following equation or obtained from Figure 4C.2:

$$C_{us} = e^{-2Ku'(H/B_d)} \quad (4C-6)$$

where: $e =$ Base of natural logarithms
 $K =$ Rankine's ratio of lateral pressure to vertical pressure
 $u' =$ Coefficient of friction between backfill material and the sides of the trench

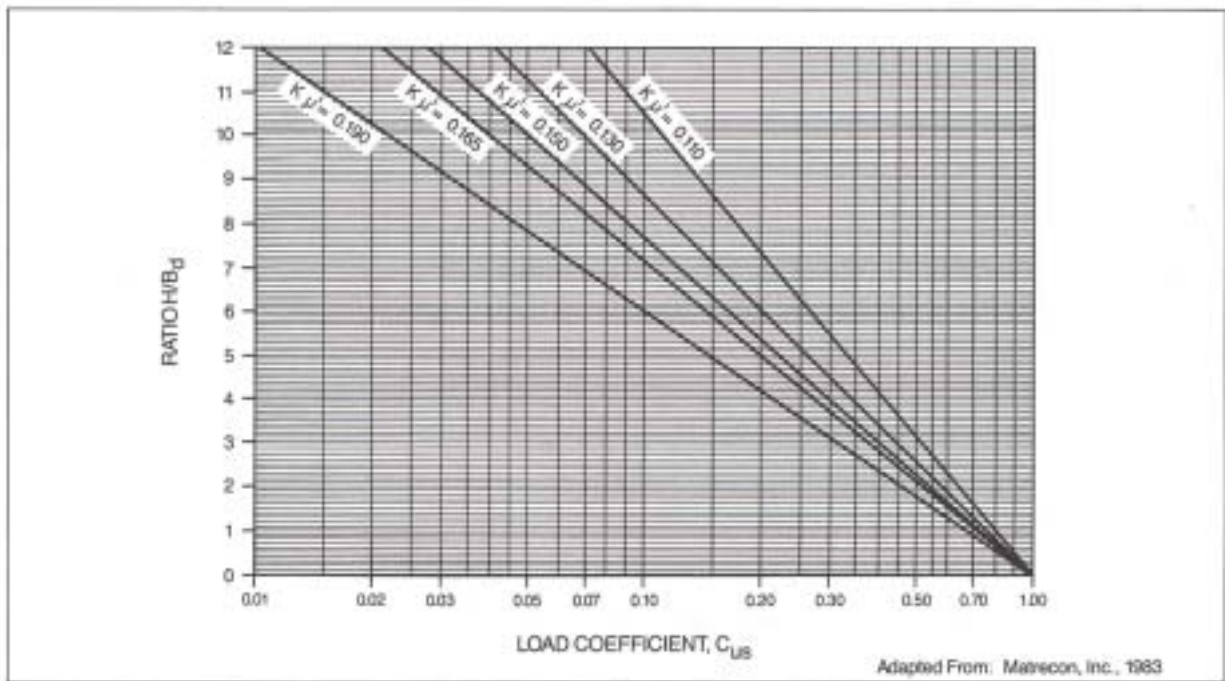


Figure 4C.2
Trench Condition—Values of Load Coefficient C_{US} (Trench Uniform Surcharge)

H = Depth of trench from original ground surface to top of pipe (ft)

B_d = Width of trench at top of pipe (ft)

The product of Ku' is characteristic for a given combination of backfills in natural, undisturbed soil. Maximum values of Ku' for typical soils are listed in Table 4C.1.

Table 4C.1. Maximum Value of Ku' for Typical Backfill Soils

<u>Type of Soil</u>	<u>Maximum Value of Ku'</u>
Granular Materials Without Cohesion	0.19
Sand and Gravel	0.165
Saturated Topsoil	0.150
Clay	0.130
Saturated Clay	0.110

Source: U.S. EPA (1983)

The value of the vertical pressure at the top of the pipe due to the trench backfill is determined from the following equation developed by Marston (see U.S. EPA, 1983):

$$P_{vt} = (B_d)(w)(C_d) \quad (4C-7)$$

where:

P_{vt} = Value of the vertical pressure at the top of the pipe (lbs/sq ft)

W = Unit weight of trench backfill (lbs/cu ft)

C_d = Dimensionless load coefficient which is a function of the ratio of the depth of the trench, H , to the trench width, B_d , and of the friction between the backfill and the sides of the trench

The load coefficient, C_d , may be computed from the following equation or obtained from Figure 4C.3:

$$C_d = \frac{1 - e^{-2Ku'(H/B_d)}}{2Ku'} \quad (4C-8)$$

in which the terms are as previously defined.

The total vertical pressure at the top of the pipe, P_v , is equal to:

$$P_v = P_{vf} + P_{vt} \quad (4C-9)$$

$$P_v = (Q_f)(C_{us}) + (B)(w)(C_d) \quad (4C-10)$$

Based on Marston's formula, the load on a rigid pipe in the trench condition would be:

$$w_e = P_v B_d \quad (4C-11)$$

or:

$$w_c = (B_d)(Q_f)(C_{us}) + (B_d)^2 (w)(C_d) \quad (4C-12)$$

where: w_c = Force per unit length of pipe (lb/ft)

For flexible pipe in the trench condition, the load as given by Marston's formula would be:

$$w_c = P_v B_c \quad (4C-13)$$

or:

$$w_c = (B)(Q_f)(C_{us}) + (B_d)(w)(C_d)(B_c) \quad (4C-14)$$

where: B_c = Outside diameter of pipe (ft)

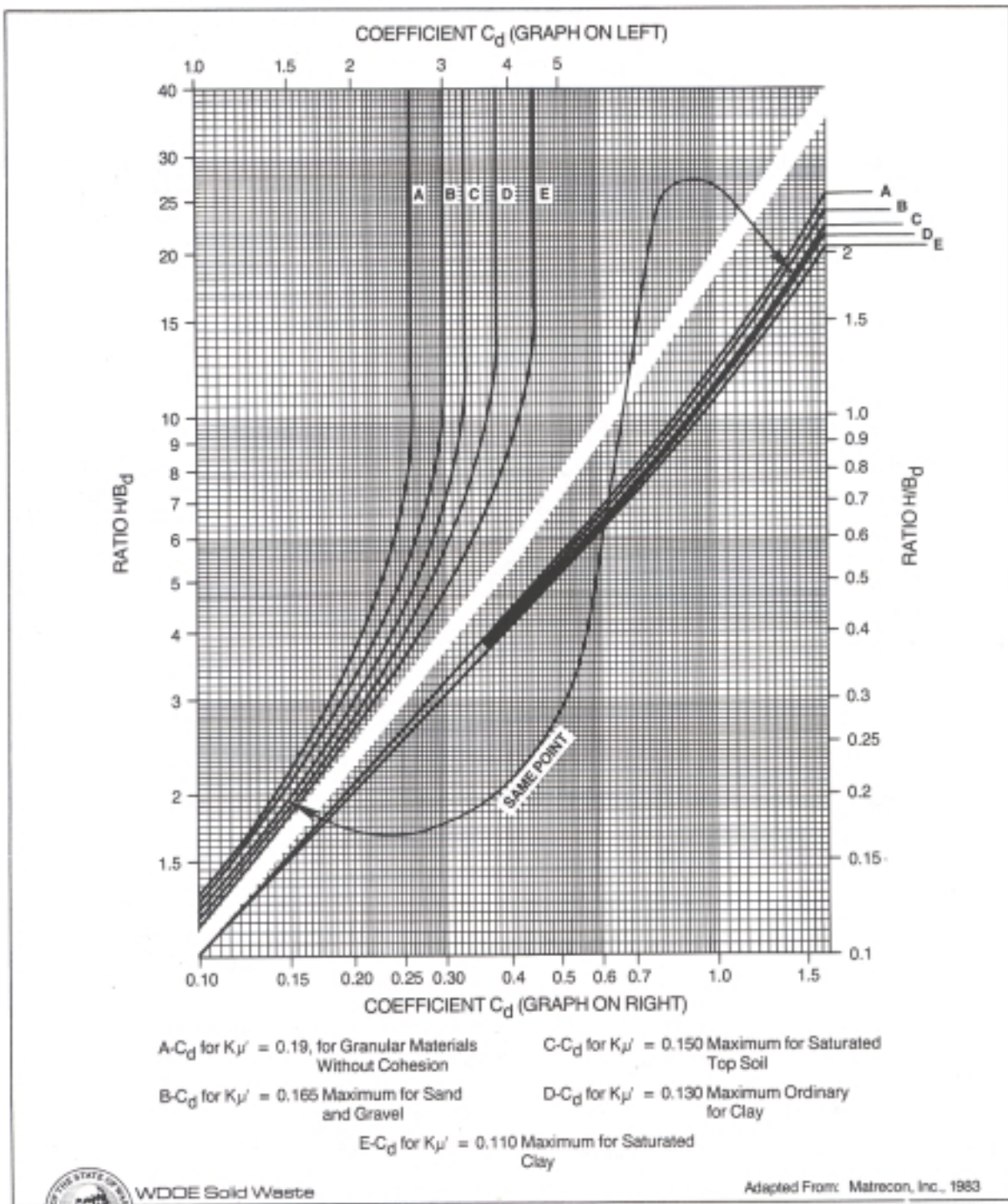


Figure 4C.3
Trench Condition—Values of Load Coefficient C_d (Backfill)

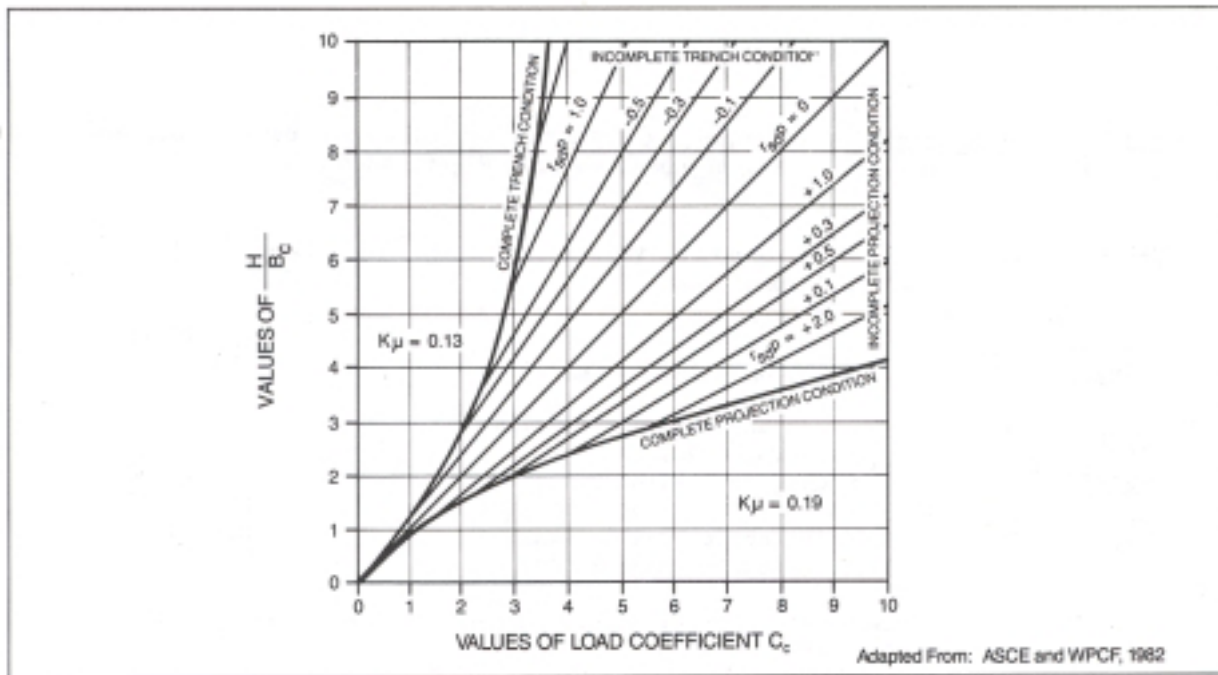


Figure 4C.4
Diagram for Load Coefficient C_c for Positive Projecting Pipes

This formula is applicable to flexible pipes only if the backfill material at the sides of the pipe is compacted so that it will deform under vertical load less than the pipe itself will deform. In this condition, the side fills between the sides of the pipe and the sides of the trench may be expected to carry their proportional share of the total load. If this condition does not exist, then the loads are determined as described below for the embankment conditions.

4C.2.2.2 Loads for Positive Protecting Embankment Conditions

Marston's formula for the fill load on a pipe in the positive projecting embankment condition is:

$$W_c = C_c w_f B_c^2 \quad (4C-15)$$

where: W_c = Load on the pipe (lbs/ft)

w_f = Weighted average density of the waste fill (lbs/cu ft)

B_c = Outside width of pipe (ft)

C_c = Load coefficient

A complete discussion of this load coefficient may be found in the Concrete Pipe Design Manual developed by the American Concrete Pipe Association (1980)

and Gravity Sanitary Sewer Design and Construction published by the ASCE and WPCF (1982). Values of C_c may be obtained from Figure 4C.4.

Table 4C.2. Recommended Design Values of r_{sd} (Positive, Projecting Embankment Conditions).

Type of Pipe	Soil Conditions	Settlement Ratio, r_{sd}
Rigid	Rock or unyielding foundation	+1.0
Rigid	Ordinary foundation	+0.5 to +0.8
Rigid	Yielding foundation	0 to +0.5
Rigid	Negative projecting installation	-0.3 to -0.5
Flexible	Poorly compacted side fills	-0.4 to 0
Flexible	Well compacted side fills	0

Source: ASCB and WPCF, 1982, p. 178

The fill load on a pipe installed in a positive projecting embankment condition is influenced by the product of the settlement ratio (r_{sd}) and the projecting ratio (p'). The settlement ratio is the relationship between the pipe deflection and the relative settlement between the prism of fill directly above the pipe and the adjacent material. Design values of the settlement ratio is the vertical distance the pipe projects above the original ground divided by the outside vertical height of the pipe, and can be determined when the size and elevation of pipe has been established.

In the last three cases shown in Table 4C.2, the settlement ratio may be conservatively assumed to be zero which results in designing for the weight of the prism of material directly above the pipe. In such cases, C_c is equal to H/B_c and Marston's formula for the prism load becomes:

$$W_c = (H)(w_f)(B_c) \quad (4C-16)$$

where: W_c = Load on pipe (lbs/ft)

H = Height of the fill above the pipe (ft)

w_f = Weighted average density of the waste fill, including gravel backfill above the pipe, refuse, intermediate cover, and final cover system (lbs/cu ft)

B_c = Outside diameter of the pipe (ft)

The load on the pipe is also influenced by the coefficient of internal friction of the embankment material. ASCE and WPCF (1982) recommends the following values of the product K_u for use in Figure 4C.4.

For a positive settlement ratio: $K_u = 0.19$

For a negative settlement ratio: $K_u = 0.13$

4C.2.2.3 Loads for Negative Projecting Embankment and Induced Trench Conditions

The formula for the fill load on a negative projecting pipe is:

$$W_c = C_n w B_d^2 \quad (4C-17)$$

where: W_c = Load on the pipe (lbs/ft)

w = Density of fill above pipe (lbs/cu ft)

B_d = Width of trench (ft)

C_n = Load coefficient

In the case of induced trench pipe, B_c is substituted for B_d in the preceding equation. B_c is the outside diameter of the sewer pipe which is assumed to be the width of the trench.

A complete discussion of the load coefficient, C_n , may be found in American Concrete Pipe Association (1980) and ASCE and WPCF (1982). Values of C_n may be obtained from Figure 4C.5.

As in the case of the positive projecting embankment condition, the fill load is influenced by the product of the settlement ratio (r_{sd}) and the projection ratio (p'). The settlement ratio for the negative projecting embankment condition is the quotient obtained by taking the difference between the settlement of the firm ground surface and the settlement of the plane in the trench backfill which was originally level with the ground surface and dividing this difference by the compression of the column of material in trench. Values for the negative projecting settlement ratio range from -0.1 for $P' = 0.5'$ to -1.0 for $P' = 2.0'$ for rigid pipe (American Concrete Pipe Association, 1980, p. 162). Induced trench settlement ratios range from -0.3 to 0.5 (ASCE and WPCF, 1982). The projection ratio for this condition, p' is equal to the vertical distance from the firm ground surface down to the top of the pipe, divided by the width of the trench, B_d .

4C.2.3 **Superimposed Loads**

Leachate collection pipes in a landfill may be subjected to two types of superimposed loads: concentrated loads and distributed loads. Loads of pipes caused by these loadings can be determined by application of the Boussinesq equations (ASCE and WPCF, 1982).

4C.2.3.1 Concentrated Loads

The formula for load caused by a superimposed concentrated load, such as a

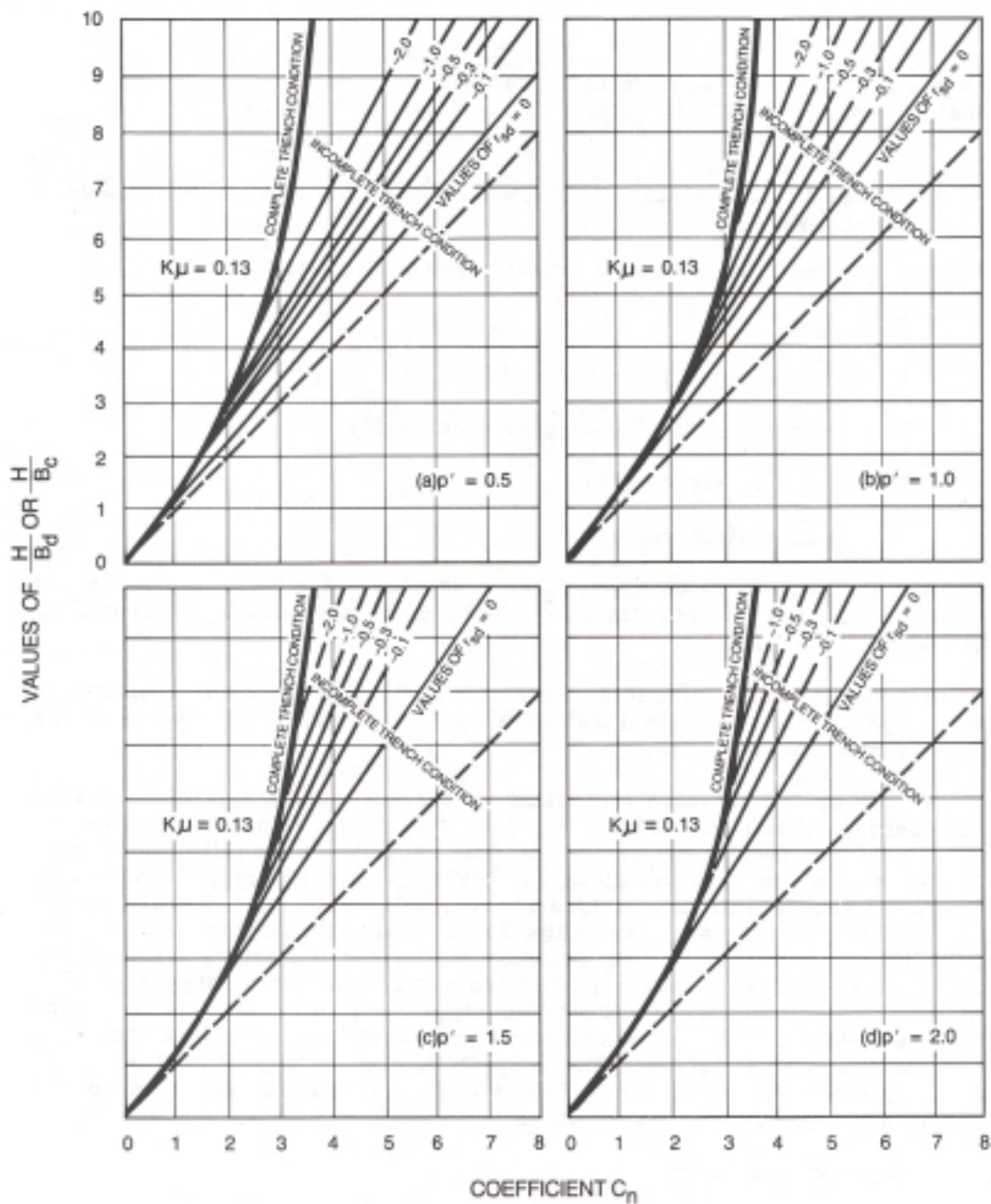


Figure 4C.5
Diagrams for Load Coefficient C_n for Negative
Projecting and Induced Trench Pipes

wheel load during construction, is given the following form (ASCE and WPCF, 1982):

$$W_{sc} = \frac{PF}{C_s L} \quad (4C-18)$$

where: W_{sc} = Load on pipe (lbs/ft)

P = Concentrated load (lbs)

F = Impact factor

L = Effective length of pipe (ft)

C_s = Load coefficient

The load coefficient, C_s , is a function of $B_c/2H$ and $L/2H$, in which B_c is the outside diameter of the pipe and H is the height of fill from the top of the pipe to the ground surface. Table 4C.3 lists values of the load coefficients for concentrated and distributed superimposed loads centered over the pipe.

The effective length, L , is the length over which the average load caused by surface wheels produces nearly the same stress in the pipe wall as does the actual load which varies in intensity from point to point. ASCE and WPCF (1982) recommends using an effective length equal to 3 feet for pipes greater than 3 feet long and using the actual length of pipes shorter than 3 feet.

The impact factor, F , reflects the influence of dynamic loads caused by traffic at ground surface. The impact factors recommended by AASHTO are listed in Table 4C.4 (American Concrete Pipe Association, 1980).

Various equipment loads that may occur during construction are listed in Table 4C.5.

Loads on pipes resulting from concentrated loads during construction may be greater than the loads caused by the refuse placed in the landfill. It is important that both construction loads and long-term loads be considered in determining the maximum load expected on pipes.

4C.2.3.2 Distributed Loads

Superimposed loads distributed over an area of considerable extent such as a truck load during construction may be determined from the following equation (ASCE and WPCF, 1982):

$$W_{sd} = CspFBc \quad (4C-19)$$

where: W_{sd} = Load on pipe (lbs/ft)

p = Intensity of distributed load (lbs/sq ft)

F = Impact factor

Table 4C.3. Values of Load Coefficients, C_g , for Concentrated and Distributed Superimposed Loads Vertically Centered over Sewer Pipe.

$\frac{D}{2H}$ or	$\frac{M}{2H}$ or $\frac{L}{2H}$													
	0.1	0.2	0.3	0.4	0.5	0.6	0.7	0.8	0.9	1.0	1.2	1.5	2.0	5.0
0.1	0.019	0.037	0.053	0.065	0.079	0.089	0.097	0.103	0.108	0.112	0.117	0.121	0.124	0.128
0.2	0.037	0.072	0.103	0.131	0.155	0.174	0.189	0.202	0.211	0.219	0.229	0.238	0.244	0.248
0.3	0.053	0.103	0.149	0.190	0.224	0.252	0.274	0.292	0.306	0.318	0.333	0.345	0.355	0.360
0.4	0.067	0.131	0.190	0.241	0.284	0.320	0.349	0.373	0.391	0.405	0.425	0.440	0.454	0.460
0.5	0.079	0.155	0.224	0.284	0.336	0.379	0.414	0.441	0.463	0.481	0.505	0.525	0.540	0.548
0.6	0.089	0.174	0.252	0.320	0.379	0.428	0.467	0.499	0.524	0.544	0.572	0.596	0.613	0.624
0.7	0.097	0.189	0.274	0.349	0.414	0.467	0.511	0.546	0.584	0.597	0.628	0.650	0.674	0.688
0.8	0.103	0.202	0.292	0.373	0.441	0.499	0.546	0.584	0.615	0.639	0.674	0.703	0.725	0.740
0.9	0.108	0.211	0.306	0.391	0.463	0.524	0.574	0.615	0.647	0.673	0.711	0.742	0.766	0.784
1.0	0.112	0.219	0.318	0.405	0.481	0.544	0.597	0.639	0.673	0.701	0.740	0.774	0.800	0.816
1.2	0.117	0.229	0.333	0.425	0.505	0.572	0.628	0.674	0.711	0.740	0.783	0.820	0.849	0.868
1.5	0.121	0.238	0.345	0.440	0.525	0.596	0.650	0.703	0.742	0.774	0.820	0.861	0.894	0.916
2.0	0.124	0.244	0.355	0.454	0.540	0.613	0.674	0.725	0.766	0.800	0.849	0.894	0.930	0.956

Bc = Outside diameter of pipe (ft)

Cs = Load coefficient

Table 4C.4 Superimposed Concentrated Load Impact Factors, F.

Height of Cover	Impact Factor
0 - 1.0 ft.	1.3
1.1 - 2.0 ft.	1.2
2.1 - 2.9 ft.	1.1
3.0 ft. and greater	1.0

Table 4C.5 Equipment Loads

<u>Equipment</u>	<u>Operating Weight (lbs)</u>	<u>Ground Contact</u>	<u>Track or Wheel Load (lbs)</u>
Caterpillar D-6	32,850	181101 9.011	16,425 Track Load
Caterpillar D-8	81,950	2211x 1016.5	40,975 Track Load
Scrapers, loaded 21/31 cu yd capacity (631 D)	168,410	Wheel load	45,470 Drive Wheel Load
Compactor Caterpillar 825-C	71,429	81 Width Coverage	35,715 Roller Load

Adapted From: Caterpillar Performance Handbook, 1984

The load coefficient, Cs, is a function of D/2H and M/2H, in which H is the height from the top of the pipe to the ground surface and D and M are the width and length, respectively, or the area over which the distributed load acts. Table 4C.3 lists the values of the load coefficients for loads centered over the pipe. A method for determining the loads on the pipe from offset uniform loads may be found in ASCE and WPCF, 1982. A typical offset uniform load would be the waste fill placed inside and adjacent to a perimeter leachate collection system.

4C.2.4 Design Safety Factor

The factor of safety for a pipe is defined as the ratio of the maximum performance limit to the design or service performance limit. The selection of a suitable safety factor is an essential part of the structural design of leachate collection pipes. The factor of safety should be related either to an allowable working stress or to a pre-established ultimate failure condition. Factors of safety compensate for poor construction practice or for inadequate inspection. Properly established design performance values and adequate factors of safety must be realized in installation and operation to provide reasonable assurance of long-term leachate collection system performance.

The relationship between safety factors and design performance values is similar for rigid and flexible pipes. However, there are differences in the design requirements for each type of pipe and these affect the form of the safety factor associated with each.

4C.2.4.1 Rigid Pipe

Design performance limits for rigid pipes are expressed in terms of strength under load. Testing is generally used to determine the service strength for rigid pipe. Strengths of rigid pipe are measured in terms of 1) the ultimate three-edge bearing strength, and 2) the ultimate and 0.01-inch crack, three-edge bearing strengths for reinforced concrete pipe. A safety factor of 1.0 should be applied to the specified minimum ultimate three-edge bearing strength to determine the working strength for other rigid pipes (ASCE and WPCF, 1982). Common practice is to use a factor of safety of 1.25 for the ultimate load of reinforced concrete pipe, and up to 1.50 for vitrified clay.

4C.2.4.2 Flexible Pipe

Design performance limits for flexible pipes are most commonly expressed in terms of deflection. The design limit varies with different pipe materials and the pipe manufacturing process. Flexible pipes must be able to deflect without experiencing cracking, liner failure, or other distress; and they should be designed with a reasonable factor of safety.

Manufacturers should be consulted on the value of the deflection limits for various types of flexible pipes. The PVC pipe manufacturers suggest limiting the deflection of buried PVC pipe to 7-1/2 percent. This strain is one-fourth the minimum strain level at which cracking and reverse curvature reportedly occurs when subjecting PVC pipe to testing in accordance with ASTM D 2412. To maintain this same factor of safety (FS-4.0) with ABS pipe, the allowable strain for ABS pipe should be limited to 5-1/2 percent. The high safety factor of 4.0 is intended to compensate for the long-term effects of creep of the plastic. Dietzler (1984) suggests that deflections of ABS and PVC pipe should be limited to one-third the deflection at which reverse curvature of splitting occurs in ASTM D 2412, including a deflection lag factor.

4C.3 RIGID PIPE DESIGN

For reasons previously indicated rigid pipes have limited use potential in leachate collection systems. In situations where they are used, their structural design should follow the recognized procedures for the various rigid pipe products available. The design of rigid pipe systems relates to the product's performance limit, expressed in terms of strength of the installed pipe. When determining field strength of rigid pipes, it is convenient to classify the *installation conditions* as either trench or embankment. For each of these conditions, bedding classes and corresponding bedding factors have been developed for use in determining and the required pipe strength.

4C-3-1 Classes of Bedding and Bedding Factors

4C.3-1.1 Trench Beddings

Four general classes of bedding for installation of rigid pipes in a trench condition are illustrated in Figure 4C.6. The bedding factor for each of the classes of pipe bedding are also listed in Figure 4C.6. Because leachate collection pipes are normally installed with granular material *surrounding* the pipe, the appropriate bedding class is usually Class B with a bedding factor of 1.9.

4C.3.1.2 Embankment Beddings

Four general classes of bedding for the installation of rigid pipes in a positive projecting embankment condition are illustrated in Figure 4C.7. Most leachate collection lines installed in a positive projecting embankment condition would have Class B or C bedding, depending on the projection ratio, p , of the actual installation. For pipe installed in a positive projecting embankment condition, active lateral pressure is exerted against the sides of the pipe. The bedding factor, L_f , for this type of installation is computed by the equation:

$$L_f = \frac{A}{N-xq} \quad (4C-20)$$

where:	A	Pipe shape factor
	N	A parameter that is a function of the bedding class
	x	A parameter dependent on the area over which lateral pressure effectively acts
	q	Ratio of total lateral pressure to total vertical load on the pipe

For circular pipe, A has a value of 1.431. Values of N for various classes of bedding are given in Table 4C.6. Values of x are listed in Table 4C.7.

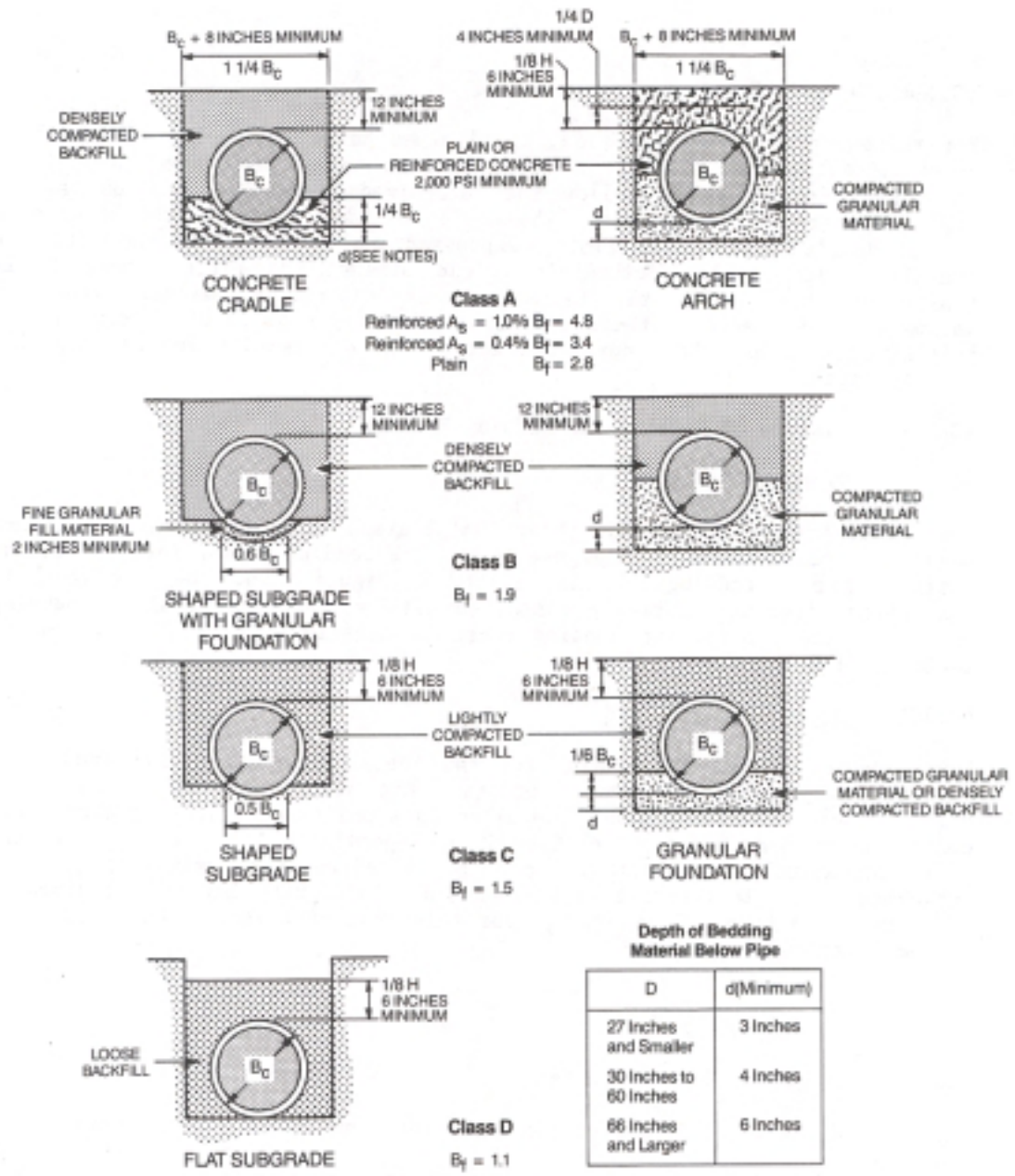


Figure 4C.6
Trench Beddings:
Circular Pipe

B_c = Outside Diameter D = Inside Diameter
 H = Backfill Cover Above Top of Pipe A_s = Area of Transverse Steel in the Cradle of Arch Expressed as a Percentage of Area of Concrete at Invert or Crown
 d = Depth of Bedding Material Below Pipe

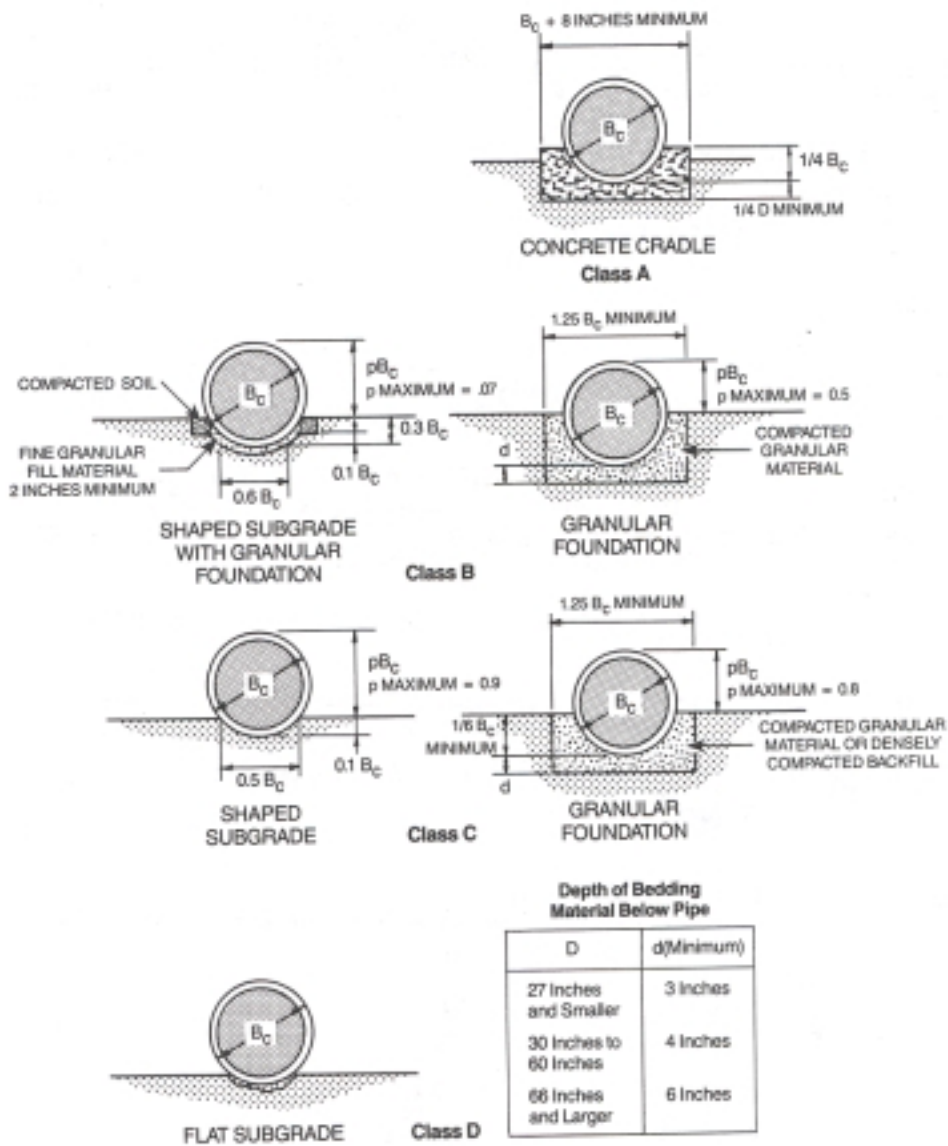


Figure 4C.7
Positive Projecting Embankment Beddings:
Circular Pipe

- B_c = Outside Diameter
- H = Backfill Cover Above Top of Pipe
- D = Inside Diameter
- d = Depth of Bedding Material Below Pipe

Table 4C.6 Values of N for Circular Pipe

<u>Class of Bedding</u>	<u>N</u>
A (reinforced cradle)	0.421 to 0.505
Aa (unreinforced cradle)	0.505 to 0.636
B	0.707
C	0.840
D	1.310

Adapted from: ASCE and WPCF (1982)

The projection ratio, m , in Table 4C.7 refers to the fraction of the vertical pipe diameter over which lateral pressure is effective. For pressure acting on the top half of the pipe above the horizontal diameter, m equals 0.5. Values for q may be estimated by the formula:

$$q = \frac{mk}{C_c} \left[\frac{H}{B_c} + \frac{m}{2} \right] \quad (4C-21)$$

where: k Ratio of unit lateral pressure to unit vertical pressure (Rankine's ratio)

A value of k equal to 0.33 usually be sufficiently accurate. Values of C_c may be found in Figure 4C.4.

Table 4C.7 Values of x for Circular Pipe

<u>Fraction of Pipe Subjected to Lateral Pressure, m</u>	<u>Class A Bedding</u>	<u>Other Than Class A Bedding</u>
0	0.150	0
0.3	0.743	0.217
0.5	0.856	0.423
0.7	0.811	0.594
0.9	0.678	0.655
1.0	0.638	0.638

Adapted from: ASCE and WPCF (1982)

The classes of bedding for rigid pipes installed in a negative projecting embankment condition are the same as those for the trench condition. The trench condition bedding factors listed in Figure 4C.6 should be used for

negative projecting embankment installations. For leachate collection lines, this would generally be Class B bedding and a bedding factor of 1.9.

4C.3.2 Selection of Pipe Strength

The design strength of rigid pipes is commonly related to a three-edge bearing strength measured at the manufacturing plant in accordance with recognized national testing standards. For pipes installed under specified conditions of bedding and backfilling, the required three-edge bearing strength for a given class of bedding and design load can be determined from the following:

$$\text{Required Three Edge Bearing Strength (lb/ft)} = \frac{\text{Design Load (lb/ft)} \times \text{Factor of Safety}}{\text{Bedding Factor}}$$

The strength of reinforced concrete pipe at either the 0.01-inch crack or ultimate load divided by the internal diameter of the pipe is defined as the D-load strength. The D-load concept provides strength classification of pipe independent of pipe diameter. The required three-edge bearing strength of reinforced concrete pipe expressed as D-load is determined by the following equation:

$$\text{D-Load (lbs)} = \frac{\text{Design Load (lbs/ft)} \times \text{Safety Factor}}{\text{Bedding Factor} \times \text{Diameter (ft)}}$$

The above equations are applicable to rigid pipes installed in both trench conditions and embankment conditions. After determining the design load, the selection of the pipe strength involves applying the appropriate safety factor and bedding factor for the installation conditions in either of the above equations.

4C.4 FT BLE PIPE DESIGN

4C.4.1 General Approach

Flexible pipes derive the majority of their load supporting ability from the passive resistance of the soil in side fills as the pipe deflects under load. Because of this resistance, it is important to examine the interaction between the bedding or fill material and the pipe, rather than simply studying pipe characteristics. The extent to which flexible pipe deflects as installed is most commonly used as a basis for design since it reflects this interaction. The approximate long-term deflection of flexible pipe in place can be calculated using the Modified Iowa Formula developed by Spangler and Watkins (ASCE and WPCF, 1982):

$$Y = \frac{D_i K_b W_c r^3}{EI + 0.061 E' r^3} \quad (4C-22)$$

where: Y = Vertical deflection (inches), assumed to approximately equal horizontal deflection

- D_1 = Deflection lag factor
- K_b = Bedding constant
- W_c = Load (lbs/inch)
- r = Mean radius of pipe (inches)
- E = Modulus of tensile elasticity (lbs/sq in)
- I = Moment of inertia per length (in⁴/ft)
- E' = Modulus of soil reaction (lbs/sq in)

The above equation can be rewritten to express pipe deflection as a decimal fraction of the pipe outside diameter, B_c , and relate it to the vertical stress on the pipe, P_v , as follows:

$$\frac{W_c}{B_c} = P_v = \frac{Y(EI + 0.061 E'n^3)}{B_c(D_1K_b r^3)} \quad (4C-23)$$

Pipe manufacturers may establish limits for pipe deflection or vertical stress on the pipe (P_v). Maximum vertical stress is often referred to as critical buckling pressure.

The deflection lag factor, D_1 , compensates for time consolidation of the bedding, which may permit flexible pipes to continue to deform after installation. Long-term deflection will be greater with low degrees of compaction of the bedding in the side fills compared to higher degrees of compaction. Values recommended for this factor range from 1.25 to 1.50 (ASCE and WPCF, 1982), although values over 2.5 have been recorded in dry soil. A deflection lag factor of 2.0 may be realistic for design of leachate collection pipes if weathering and/or softening of the bedding material is likely to occur over the life of the landfill or if the bedding material is rounded or may be placed with minimal compaction (Dietzler, 1984).

Values for the bedding constant, K_b , are listed in Table 4C.8. Spangler's data suggested a K_b value of 0.10 for pipe embedded in native soil with no bedding and a K_b value of 0.083 for pipe embedded in gravel up to the spring line. The installation of leachate collection pipes is more closely represented by the latter case, and a K_b value of 0.083 should therefore be used in lieu of actual field data.

Table 4C.8. Values of Bedding Constant, K_b -

Bedding Angle (Degrees)	K_b
0	0.110
30	0.108
45	0.105
60	0.102
90	0.096
120	0.090
180	0.083

Source: ASCE and WPCF (1982)

Values for the soil reaction modulus, EI , range from 0 to 3,000, depending on the soil type of the bedding material and relative degree of compaction (ASCE and WPCF, 1982). The use of a high value for EI is not realistic for leachate collection pipes in many localities (Dietzler, 1984). In a situation where a rounded river gravel will be used for the bedding material and a high degree of compaction may be unobtainable in the bedding around the leachate collection pipe, a realistic value for E , of 400 may be appropriate (Dietzler, 1984).

The first term in the denominator (EI) of the Modified Iowa Formula is the stiffness factor and reflects the influence of the inherent stiffness of the pipe on deflection. The second term, $0.061 EI d$, reflects the influence of the passive pressure on the side of the pipe. With flexible pipes, the second term is normally predominant.

After the allowable strain level in the pipe has been determined, the design procedure for flexible pipes is to perform a trial and adjustment analysis to find a class of pipe that will result in deflections less than the established limit. There are slight variations in the procedure for the various types of flexible pipe.

4C.4.2 Selection of Plastic Pipe

The standard test to determine pipe stiffness or the load deflection characteristic of plastic pipe is the parallel-plate loading test conducted in accordance with ASTM D 2412. The test determines the pipe stiffness, PS , at a prescribed deflection, Y , which for convenience in testing is arbitrarily set at 5 percent. The pipe stiffness is defined as the value obtained by dividing the load per unit length, F , by the resulting deflection at the prescribed percentage deflection:

$$PS = \frac{F}{Y} \quad (4C-.24)$$

The stiffness factor, SF, in the Modified Iowa Formula is related to the pipe stiffness by the following expression:

$$SF = EI = 0.149r^3(PS) \quad (4C-25)$$

in which the terms are as previously defined.

For circular plastic pipes, the approximate deflection based on pipe stiffness can be determined by using the following simplified version of the Modified Iowa Formula:

$$Y = \frac{D_1 K_b W_c}{0.149(PS) + 0.061 E'} \quad (4C-26)$$

The pipe stiffness for the various plastic pipe materials and diameters of pipe may be obtained from the manufacturer or may be determined by tests performed in accordance with ASTM D 2412.

4C.4.3 Selection of Other Flexible Pipes

Flexible pipes of material other than plastic, such as ductile iron and corrugated metal, have little potential for general use in leachate collection systems for reasons previously discussed. However, if they are found suitable for a specific installation, their structural design should follow recognized procedures for the particular flexible pipe being considered. Procedures for designing ductile iron and corrugated metal pipes are described in ASCE and WPCF (1982). Manufacturers of the specific products should also be consulted.

4C.4.4 Bedding Material

Bedding provides a: contact between a pipe and the foundation on which it rests. The total load that a pipe will support depends on the width of the contact area and the quality of the contact between the pipe and the bedding material. The influence of the bedding on the supporting strength of the pipe is a factor that must be considered in the design of a leachate collection pipe. This section discusses bedding material considerations. More detailed requirements are given in previous sections of this Appendix.

An important consideration in selecting a material for bedding is positive contact between the bed and the pipe. A well-graded crush stone or a well-graded gravel are suitable bedding materials based on supporting strength considerations, and both are more suitable than a uniformly graded pea gravel (ASCE and WPCF, 1982). Larger particle sizes give greater stability; however, the maximum size and shape of the bedding material should be related to the pipe material and the recommendations of the manufacturer. For small pipes, the maximum size of the bedding material should be limited to about 10 percent of the pipe diameter and, in general, well-graded crush stone or gravel ranging in size from 3/4 inch to the No. 4 sieve will provide the most satisfactory pipe bedding (ASCE and WPCF, 1982).

In addition to providing support, bedding for leachate collection pipes must allow unrestricted flow of leachate through the bedding into the perforated leachate collection pipes. The bedding material must also be resistant to attack from the leachate. Redundancy in the design of leachate collection systems is important to minimize the effects of failures when they occur. One of the primary ways to provide redundancy is to design the bedding to meet drainage requirements through the gravel layer alone if flow through the pipe is restricted (Bass, 1984).

A well-graded material with 100 percent passing the 1-1/2 inch clear, square screen openings and not more than 5 percent passing the No. 50 U.S. Standard Series sieve is recommended for drainage purposes (U.S. Department of the Interior, 1978). To determine whether the material is well-graded, the coefficient of uniformity which describes the slope of the gradation curve must be greater than 4 for gravels and greater than 6 for sands. In addition, the coefficient of curvature that describes the shape of the curve must be between 1 and 3 for both gravels and sands. These coefficients are defined as follows:

$$\text{Coefficient of uniformity, } C_u, = \frac{D_{60}}{D_{10}} \quad (4C-27)$$

and

$$\text{Coefficient of curvature, } C_c, = \frac{(D_{30})^2}{(D_{10})(D_{60})} \quad (4C-28)$$

where: D_{10} , D_{30} , and D_{60} Diameter of particles in millimeters passing the 10, 30, and 60 percent points, respectively, on the base material gradation curve.

Based on the above criteria for supporting strength and drainage, a bedding material for leachate collection pipes should be well-graded gravel with the following properties:

- Gradation: 100% passing 1-1/2" sieve
 5% maximum passing No. 50 sieve
- C_u : 4.0 or greater
- C_c : 1.0 to 3.0

The actual bedding material should be selected within these limits after consideration of the pipe material, availability of bedding material, and its resistance to leachate attack.

**APPLICATION FOR PERMIT
OWL LANDFILL SERVICES, LLC**

**VOLUME III: ENGINEERING DESIGN AND CALCULATIONS
SECTION 5: PIPE LOADING CALCULATIONS**

ATTACHMENT III.5.D

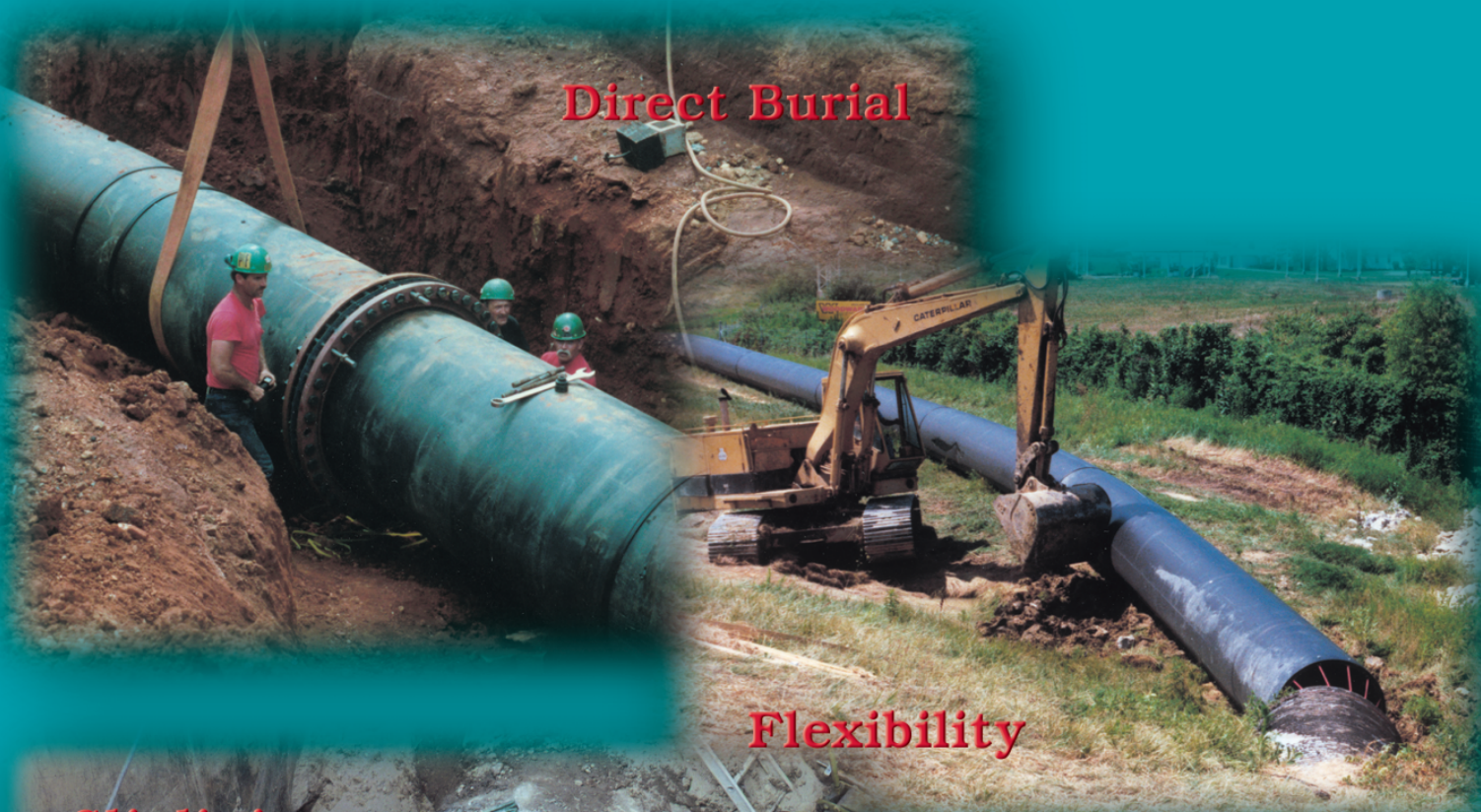
POLY PIPE INDUSTRIES, INC. 2008.

DESIGN AND ENGINEERING GUIDE FOR POLYETHYLENE PIPING.

WWW.PLASTICPIPE.ORG

PolyPipe®

Direct Burial



Flexibility



Sliplining

Marine Applications



*Design and Engineering Guide
for Polyethylene Piping*

Table A-2 (cont'd)
PIPE WEIGHTS AND DIMENSIONS (IPS)
PE3608 (BLACK)

OD			SDR	Nominal ID		Minimum Wall		Weight	
Nominal in.	Actual			in.	mm.	in.	mm.	lb. per foot	kg. per meter
	in.	mm.							
			7	2.44	61.98	0.500	12.70	2.047	3.047
			7.3	2.48	63.08	0.479	12.18	1.978	2.943
			9	2.68	67.96	0.389	9.88	1.656	2.464
			9.3	2.70	68.63	0.376	9.56	1.609	2.395
			11	2.83	71.77	0.318	8.08	1.387	2.065
3	3.500	88.90	11.5	2.85	72.51	0.304	7.73	1.333	1.984
			13.5	2.95	74.94	0.259	6.59	1.153	1.716
			15.5	3.02	76.74	0.226	5.74	1.015	1.511
			17	3.06	77.81	0.206	5.23	0.932	1.386
			21	3.15	79.93	0.167	4.23	0.764	1.136
			26	3.21	81.65	0.135	3.42	0.623	0.927
			7	3.14	79.68	0.643	16.33	3.384	5.037
			7.3	3.19	81.11	0.616	15.66	3.269	4.865
			9	3.44	87.38	0.500	12.70	2.737	4.073
			9.3	3.47	88.24	0.484	12.29	2.660	3.958
			11	3.63	92.27	0.409	10.39	2.294	3.413
4	4.500	114.30	11.5	3.67	93.23	0.391	9.94	2.204	3.280
			13.5	3.79	96.35	0.333	8.47	1.906	2.836
			15.5	3.88	98.67	0.290	7.37	1.678	2.497
			17	3.94	100.05	0.265	6.72	1.540	2.292
			21	4.05	102.76	0.214	5.44	1.262	1.879
			26	4.13	104.98	0.173	4.40	1.030	1.533
			32.5	4.21	106.84	0.138	3.52	0.831	1.237
			7	3.88	98.51	0.795	20.19	5.172	7.697
			7.3	3.95	100.27	0.762	19.36	4.996	7.435
			9	4.25	108.02	0.618	15.70	4.182	6.224
			9.3	4.29	109.09	0.598	15.19	4.065	6.049
			11	4.49	114.07	0.506	12.85	3.505	5.216
5	5.563	141.30	11.5	4.54	115.25	0.484	12.29	3.368	5.012
			13.5	4.69	119.11	0.412	10.47	2.912	4.334
			15.5	4.80	121.97	0.359	9.12	2.564	3.816
			17	4.87	123.68	0.327	8.31	2.353	3.502
			21	5.00	127.04	0.265	6.73	1.929	2.871
			26	5.11	129.78	0.214	5.43	1.574	2.343
			32.5	5.20	132.08	0.171	4.35	1.270	1.890
			7	4.62	117.31	0.946	24.04	7.336	10.917
			7.3	4.70	119.41	0.908	23.05	7.086	10.545
			9	5.06	128.64	0.736	18.70	5.932	8.827
			9.3	5.11	129.92	0.712	18.09	5.765	8.579
			11	5.35	135.84	0.602	15.30	4.971	7.398
6	6.625	168.28	11.5	5.40	137.25	0.576	14.63	4.777	7.109
			13.5	5.58	141.85	0.491	12.46	4.130	6.147
			15.5	5.72	145.26	0.427	10.86	3.637	5.413
			17	5.80	147.29	0.390	9.90	3.338	4.967
			21	5.96	151.29	0.315	8.01	2.736	4.072
			26	6.08	154.55	0.255	6.47	2.233	3.322
			32.5	6.19	157.30	0.204	5.18	1.801	2.680

See ASTM D3035, F714 and AWWA C-901/906 for OD and wall thickness tolerances.
Weights are calculated in accordance with PPI TR-7.

EARTHLOADING

PolyPipe®, due to its flexibility, will deflect when it is buried. The degree of deflection will depend upon the soil conditions, burial conditions, trench width, and the depth of burial. The degree of deflection of the pipe is limited by the soil around its periphery, especially in the lateral direction. When the soil compacts around the pipe, there is a supportive effect from the soil itself, and as compaction occurs, there is soil friction and cohesion over the pipe that reduces the direct load on the pipe.

PolyPipe®, as do other flexible conduits, depends on the surrounding soil for support, and has to be considered as one component in a pipe/soil system. The presence of the soil arch and the support derived from the lateral movement limitations are highly beneficial to the efficiency of the system. Therefore, the flexibility of **PolyPipe®** is the major reason for these advantages. As has been stated, the durability of polyethylene is the reason for its resistance to high levels of mechanical abuse, and this is no less true for buried systems where forced deflections may occur due to subsidence, washout and settlement.

External loading analysis must be conducted to determine the application's feasibility. There are two loading calculations necessary when designing or engineering below ground applications of **PolyPipe®**. These calculations are ring deflection and wall buckling. Wall crushing, calculated using the allowable compressive strength of the PE material, is usually not critical when using solid wall **PolyPipe®**, as ring deflection and wall buckling are predominant parameters.

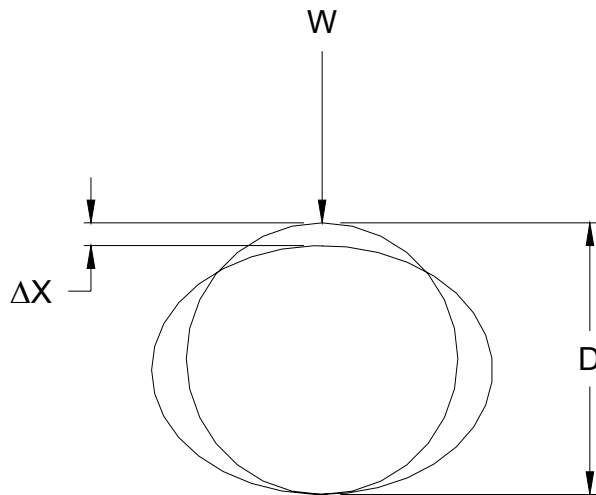
RING DEFLECTION

PolyPipe®, when buried in loose soil conditions, will exhibit the tendency to deflect, called ring deflection. Listed below are the recommended maximum allowable design limits for ring deflection of **PolyPipe®** for the different available Dimension Ratios (DR).

Table C-1
Design Limits for Ring Deflection

DR	Safe Deflection, % of Diameter
32.5	8.0
26	7.0
21	6.0
17	5.0

Figure C-1



PolyPipe®, due to its inherent physical properties of flexibility, resilience and toughness can withstand significant deflection without failure. It can be flattened without causing a fracture of the pipe wall. However, this condition is unacceptable as far as service is concerned. A deflection of 15% would be acceptable for a butt fused polyethylene system, although a reduction in flow would be noted. It would also be difficult to utilize conventional cleaning equipment with this severity of deflection. Ring deflection resulting in hydraulic flow area reductions should be taken into account when engineering the flow characteristics. Refer to Table C-2 for the percentage of area reduction based on percent of ring deflection.

Table C-2
AREA REDUCTION DUE TO RING DEFLECTION

Ring Deflection, %	Area Reduction, %
2	0.04
4	0.16
5	0.25
6	0.36
8	0.64
10	1.00
12	1.44
14	1.96
15	2.25
16	2.56

In calculating the soil load placed on a buried pipe, the designer must be able to calculate to some degree of accuracy the type and condition of the backfill material. Saturated clay would be more difficult to place and adequately compact than would coarse granular material that would not stick together. It is important in the pipe/soil system that the backfill material utilized for haunching and initial backfill (see Installation, Section F, for explanation of terminology) be granular and non-cohesive, free of debris, organic matter, frozen earth and rocks larger than 1½ inch in diameter. This material can be described as Class I or II of ASTM D2321 "Angular ¼ to 1½ inch Graded Stone, Slag, Cinders, Crushed Shells and Stone or Sands and Gravel Containing Small Percentages of Fines, Generally Granular and Non-Cohesive, Wet or Dry." This material can easily be worked into the pipe haunch, and compacted in approximately 4-6 inch lifts.

To determine the ring deflection of externally loaded **PolyPipe®**, you must first determine the earthload in pounds per linear inch of pipe by use of the following modified Marston formula⁵:

$$W = \frac{C_d \cdot \rho \cdot B_d \cdot D}{144} \tag{17}$$

- Where
- W = Earthload per unit length of pipe, lbs/in
 - C_d = Trench Coefficient, (dimensionless) (See Figure C-2)
 - ρ = Soil density, lbs/ft³
 - D = Outside diameter, inches
 - B_d = Trench width at top of pipe, feet

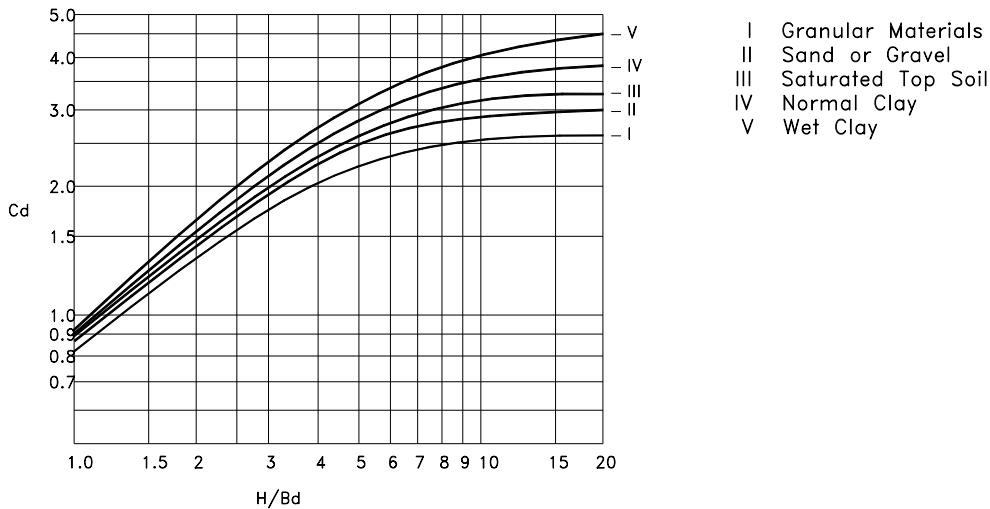
⁵ Moser, A.P. Buried Pipe Design. 2nd Edition. New York: McGraw-Hill, 2001.

**Table C-3
CLASSIFICATION OF BACKFILL MATERIAL
PER ASTM D2321***

Class	Comments
<u>Class I</u> - Angular graded stone, ¼" to 1½", including a number of fill materials that have regional significance such as coral, slag, cinders, crushed stone, crushed gravel and crushed shells.	100 - 200 pounds per cubic foot. Pipe sizes less than 10" should limit maximum particle size to ½" to ¾" for ease of placement.
<u>Class II</u> - Coarse sands and gravel with maximum particle size of 1½", including variously graded sands and gravel containing small percentages of fines, generally granular and non-cohesive, wet or dry.	110 - 130 pounds per cubic foot. Pipe sizes less than 10" should limit maximum particle size to ½" to ¾" inch for ease of placement.
<u>Class III</u> - Fine sand and clay gravel, including fine sands, sand-clay mixtures, and gravel-clay mixtures.	140 - 150 pounds per cubic foot.
<u>Class IV</u> - Silt, silty clays, and clays, including inorganic clays and silts of medium to high plasticity and liquid limits.	150 - 180 pounds per cubic foot.
<u>Class V</u> - Includes organic soils as well as soils containing frozen earth, debris, rocks larger than 1½" in diameter, and other foreign materials.	Not recommended for backfill except in the final backfill zone.

* For further classification of soils the designer may want to review ASTM D2487, "Standard Test Method for Classification of Soil for Engineering Purposes."

**Figure C-2
TRENCH COEFFICIENT, C_d
DEPENDENT ON SOIL TYPE AND DITCH CONFIGURATION**



In general practice, the trench width can be kept to a minimum of six inches per side greater than the pipe diameter itself. Although this may seem narrow in comparison to trenching of conventional materials, it must be noted that **PolyPipe®** can be pre-assembled above ground and later placed into the trench. The trench width should be maintained as narrow as possible as the soil loading on the pipe is a relationship of the trench width.

The linear deflection of the pipe can be calculated from the following modified Spangler equation⁶:

$$\Delta x = \frac{D_i \cdot K \cdot W}{\left(\frac{2E}{3(DR-1)^3} \right) + 0.061E'} \quad (18)$$

Where

- Δx = Horizontal deflection or change in diameter, inches
- D_i = Deflection lag factor, **PolyPipe**[®] recommends 1.0 (dimensionless)
- K = Bedding constant, **PolyPipe**[®] recommends 0.1 (dimensionless)
- W = Earthload, lbs/inch (See Equation (17))
- E = Modulus of elasticity of pipe, 30,000 psi
- E' = Soil modulus, psi
- DR = Dimension ratio, (dimensionless)

* For further values of K see reference.

The percent deflection can be calculated by use of the following formula⁶:

$$d = \frac{\Delta x}{D} \cdot 100 \quad (19)$$

Where

- d = Percent deflection, %
- Δx = Horizontal deflection, inches (See Equation (18))
- D = Outside diameter, inches

**Table C-4
TYPICAL SOIL MODULUS VALUES (PSI)**

Type of Soil	Depth of Cover		Standard AASHTO relative compaction			
	ft	m	85%	90%	95%	100%
Fine-grained soils with less than 25% sand content (CL, ML, CL-ML)	0-5	0-1.5	500	700	1000	1500
	5-10	1.5-3.1	600	1000	1400	2000
	10-15	3.0-4.6	700	1200	1600	2300
	15-20	4.6-6.1	800	1300	1800	2600
Coarse-grained soils with fines (SM., SC)	0-5	0-1.5	600	1000	1200	1900
	5-10	1.5-3.0	900	1400	1800	2700
	10-15	3.0-4.6	1000	1500	2100	3200
	15-20	4.6-6.1	1100	1600	2400	3700
Coarse-grained soils with little or no fines (SP, SW, GP, GW)	0-5	0-1.5	700	1000	1600	2500
	5-10	1.5-3.0	1000	1500	2200	3300
	10-15	3.0-4.6	1050	1600	2400	3600
	15-20	4.6-6.1	1100	1700	2500	3800

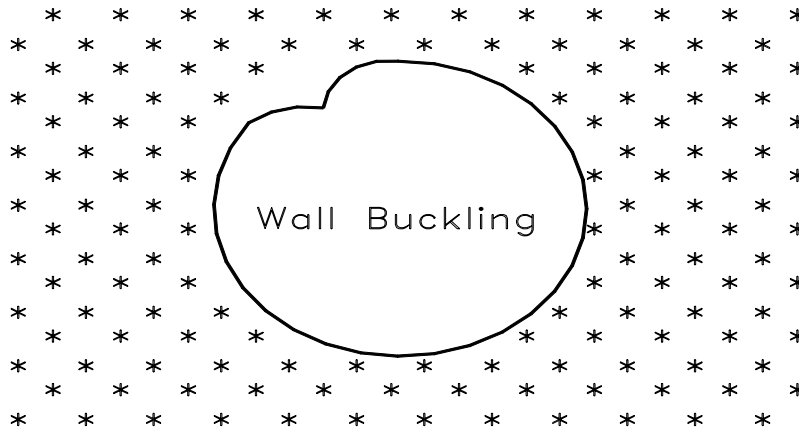
⁶ Plastics Pipe Institute. Underground Installation of Polyethylene Pipe, 1996.

Values of modulus of soil reaction, E' (psi) based on depth of cover, type of soil, and relative compaction. Soil type symbols are from the United Classifications System. Source: Hartley, James D. and Duncan, James M., "E' and its Variation with Depth," Journal of Transportation, Division of ASCE, Sept. 1987.

WALL BUCKLING

PolyPipe[®], when buried in dense soil conditions and subjected to excessive external loading, will exhibit the tendency of wall buckling. As seen in Figure C-3, wall buckling is a longitudinal wrinkle that usually occurs between the 10:00 and 2:00 positions. Wall buckling should become a design consideration when the total vertical load exceeds the critical buckling stress of **PolyPipe**[®].

Figure C-3



Vertical loading can be determined by the summation of the calculated dead load (load resulting from backfill overburden and static surface loads) and live load (loads resulting from cars, trucks, trains, etc.).

BACKFILL LOAD¹

$$P_b = \frac{\rho_{soil} \cdot H}{144} \tag{20}$$

- Where
- P_b = Backfill load, psi
 - ρ_{soil} = Backfill density, lbs/ft³
 - H = Height of backfill above pipe, feet

SURFACE LOAD

Surface loads are those forces exerted by permanent structures in close proximity to buried **PolyPipe**[®]. These loads can be buildings, storage tanks, or other structures of significant weight that could add to the backfill loading. The force exerted on **PolyPipe**[®] by structural surface loads can be approximated by use of the following Boussinesq¹⁷ formulation:

$$P_s = \frac{3Lz^3}{144 \cdot 2\pi R^5} \tag{21}$$

- Where
- P_s = Surface load on pipe, psi
 - L = Static surface load, lbs.
 - z = Vertical distance from top of pipe to surface load level, feet
 - R = Straight line distance from the top of pipe to surface load, feet

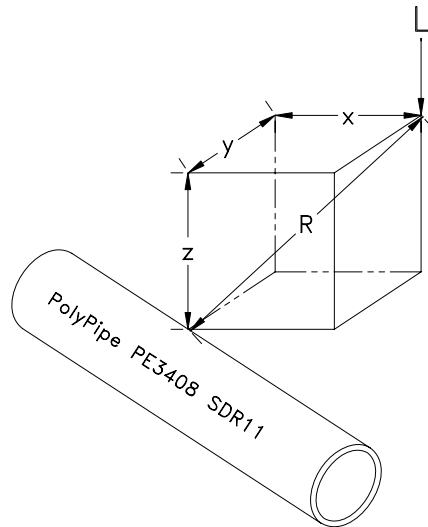
Where,

¹ Nayyar, Mohinder L. Ed. Piping Handbook, 6th Edition. New York: McGraw-Hill, Inc., 1992.
¹⁷ Chen, W. F., Liew, Richard L. Y. The Civil Engineering Handbook. New York: CRC Press, 2003. 2nd Edition.

$$R = \sqrt{x^2 + y^2 + z^2} \quad (22)$$

Where x = Horizontal distance from surface load, feet (Refer to Figure C-4)
 y = Horizontal distance from surface load, feet (Refer to Figure C-4)
 z = Vertical distance from top of pipe to surface load level, feet (Refer to Figure C-4)

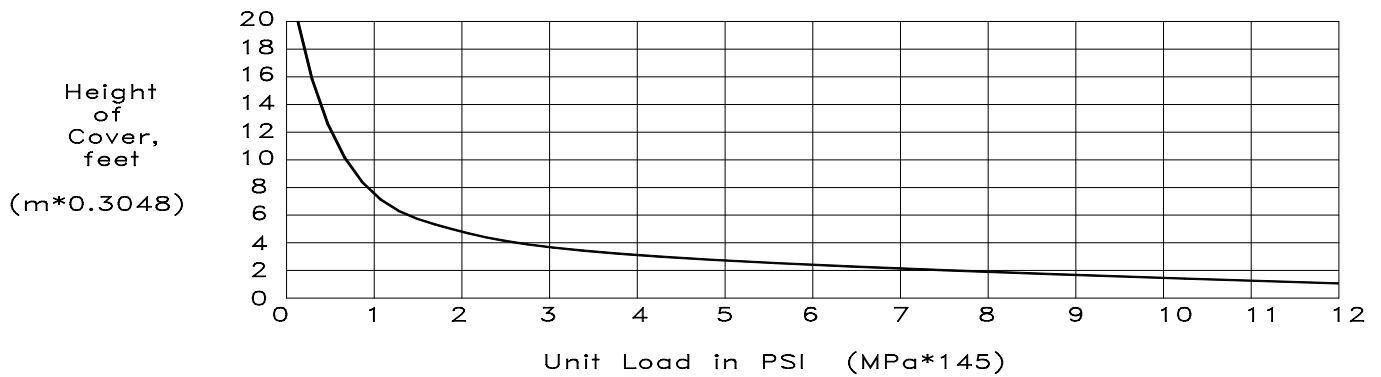
Figure C-4
RESULTANT SURFACE LOAD



LIVE LOAD

Live loading can be determined by extracting the load from Figure C-5 for H20 highway loading or from Figure C-6 for Cooper E-80 loading or by estimating, using available analytical techniques.

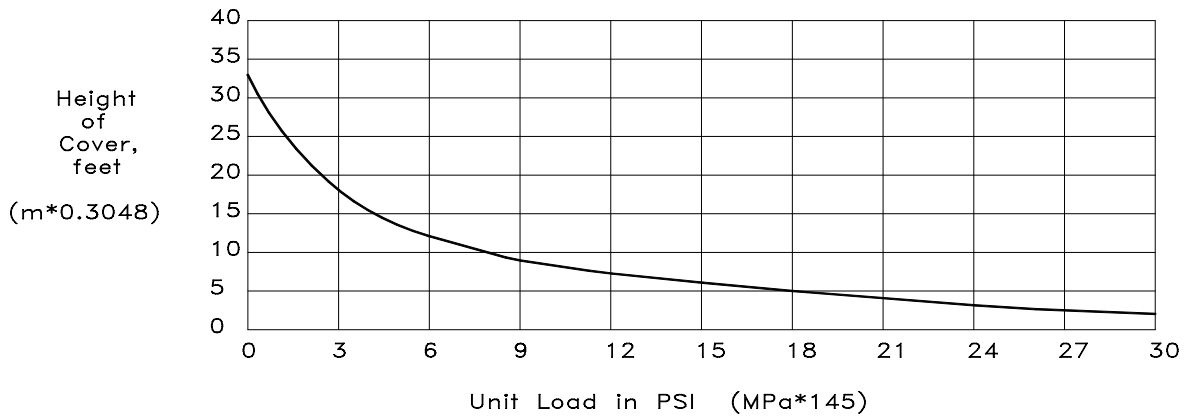
Figure C-5
H20 HIGHWAY LOADING



Note: The H20 live load assumes two 16,000 lb. loads applied to two 18" x 20" areas, one located over the point in question, and the other located at a distance of 72" away. In this manner, a truckload of 20 tons is simulated.

Source: American Iron and Steel Institute, Washington, DC

**Figure C-6
COOPER E-80**



Note: The Cooper E-80 live load assumes 80,000 pounds applied to three 2' x 6' areas on 5' centers, such as might be encountered through live loading from a locomotive with three 80,000 pounds axle loads.

Source: American Iron and Steel Institute, Washington, DC

TOTAL EXTERNAL LOADING

Total Load = Live Load + Backfill Load + Surface Load

$$P_t = P_l + P_b + P_s \tag{23}$$

Once the external loading on buried **PolyPipe**[®] has been determined, it will be necessary to calculate the critical buckling stress for contained **PolyPipe**[®] to determine if the pipe can withstand the external loading. The external loading capacity, or critical buckling stress, can be determined by the use of the following Von Mises formula:

$$P_{cb} = \frac{1}{SF} \cdot \left(\frac{2.67 \cdot R_w \cdot B \cdot E_s \cdot E}{DR^3} \right)^{1/2} \tag{24}$$

- Where P_{cb} = Critical buckling stress, psi
- SF = Safety factor, **PolyPipe**[®] recommends SF=2
- R_w = Water buoyancy factor, (dimensionless)
- B = Empirical Coefficient of Elastic Support, (dimensionless)
- E_s = Soil modulus, (See Table C-4)
- E = Pipe modulus of elasticity, psi
- DR = Dimension Ratio

Where,

$$R_w = 1 - \left(0.33 \cdot \frac{H_w}{H} \right) \tag{25}$$

- H_w = Height of water table above pipe, feet
- H = Height of soil cover above pipe, feet

Note: H_w must be less than H

and,

$$B = \frac{1}{1 + 4 \cdot e^{-0.065 \cdot H}} \quad (26)$$

Where $e = 2.718$
 $H =$ Height of soil cover above pipe, feet

If the total external loading, Equation (23), is less than the critical buckling stress ($P_t < P_{cb}$), then the application should be considered safe. However, if this is not the case ($P_t > P_{cb}$), then the required parameters can be determined for a safe application from the following variations of the above equation:

$$DR = \left(\frac{2.67 \cdot R_w \cdot B \cdot E_s \cdot E}{SF^2 \cdot P_{cb}^2} \right) \quad (27)$$

or

$$E_s = \frac{P_{cb}^2 \cdot SF^2 \cdot DR^3}{2.67 \cdot R_w \cdot B \cdot E} \quad (28)$$

NOTICE:

The data contained herein is a guide to the use of **PolyPipe**[®] polyethylene pipe and fittings and is believed to be accurate and reliable. However, general data does not adequately cover specific applications, and its suitability in particular applications should be independently verified. In all cases, the user should assume that additional safety measures might be required in the safe installation or operation of the project. Due to the wide variation in service conditions, quality of installation, etc., no warranty or guarantee, expressed or implied, is given in conjunction with the use of this material.

**APPLICATION FOR PERMIT
OWL LANDFILL SERVICES, LLC**

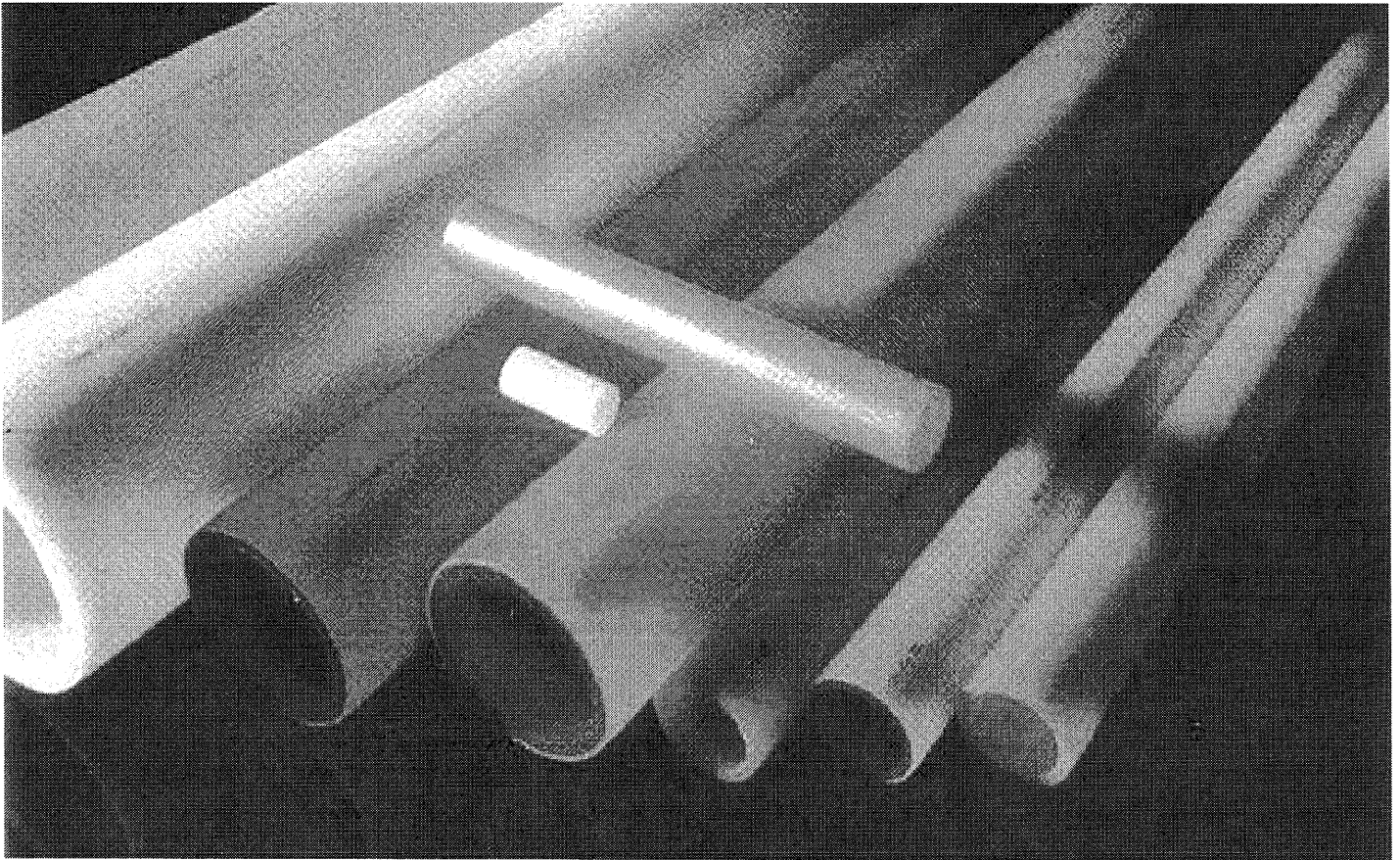
**VOLUME III: ENGINEERING DESIGN AND CALCULATIONS
SECTION 5: PIPE LOADING CALCULATIONS**

**ATTACHMENT III.5.E
DRISCOPIPE, INC. 2008.
*POLYETHYLENE PIPING SYSTEMS MANUAL***

www.driscopipe.com



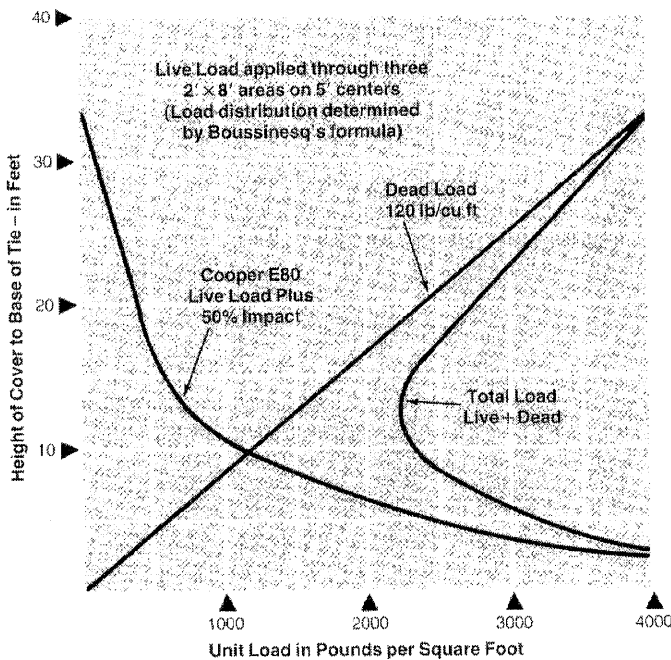
Polyethylene Piping Systems Manual



*Innovative Supplier of
Quality Piping Systems.*



FIGURE 6: COOPER E-80 LIVE LOADING



Note: Cooper E-80 live load assumes 80,000 pounds applied to three 2' x 8' areas on 5' centers such as might be encountered through live loading from a locomotive with three 80,000 pound axle loads.

Source: American Iron and Steel Institute, Washington, DC

APPARENT EXTERNAL PRESSURE DUE TO INTERNAL VACUUM, P_1 Vacuum generates a compressive hoop stress in the wall of a pipe and acts to collapse the pipeline. Under vacuum conditions, the value of P_1 is positive. P_1 is added to the other two external pressure components, P_S and P_L , to obtain the total external pressure, P_T , acting on the pipe. An internal vacuum generates pressure equal to the absolute value of the vacuum. The maximum apparent external pressure due to a vacuum inside the pipe is 14.7 psi (2,117 psf).

BURIAL DESIGN GUIDELINES The design engineer must select the proper pipe DR and specify the backfill conditions to obtain the desired performance of the “pipe-soil” system.

DESIGN BY WALL CRUSHING Wall crushing occurs when external vertical pressure causes the compressive stress in the pipe wall to exceed the long-term compressive strength of the pipe material. To design for wall crushing, the following check should be made:

$$S_A = \frac{(SDR - 1)}{2} P_T$$

Where: S_A = Actual compressive stress, psi
 SDR = Standard Dimension Ratio
 P_T = Total external pressure on the top of the pipe, psi

Safety Factor = 1500 psi / S_A (where 1500 psi is the compressive yield strength of Driscopipe HDPE pipe)

DESIGN BY WALL BUCKLING Local wall buckling is a longitudinal wrinkling of the pipe wall. Buckling can occur over the long term in non-pressurized pipe if the total external soil pressure, P_T , exceeds the pipe-soil system’s critical buckling pressure, P_{cb} . Although wall buckling is seldom the limiting factor in the design of a Driscopipe system, a check of non-pressurized pipelines can be made according to the following steps to insure $P_T < P_{cb}$. All pipe diameters with the same DR in the same burial situation have the same critical collapse and critical buckling endurance.

1. Calculate or estimate the total soil pressure, P_T , at the top of the pipe.
2. Calculate the stress, S_a , in the pipe wall:

$$S_a = \frac{(SDR - 1)P_T}{2}$$

3. Based upon the stress S_a and the estimated time duration of non-pressurization, find the value of the pipe's modulus of elasticity, E , in psi (approximate value for E is 35,000 psi).
4. Calculate the pipes hydrostatic, critical-collapse differential pressure, P_c

$$P_c = \frac{2E(t/D)^3 (D_{MIN} / D_{MAX})^3}{(1 - \mu^2)} \quad \text{or} \quad P_c = \frac{2.32(E)}{SDR^3}$$

Where: $(D_{MIN}/D_{MAX}) = 0.95$
 μ = Poission's Ratio = 0.45 for polyethylene pipe
 E = stress and time dependent tensile modulus of elasticity, psi
 $E = 35,000$ psi (approximate)
 D = Outside Diameter, in.
 t = thickness, in.

- 5 Calculate the soil modulus, E' , by plotting the total external soil pressure, P_T , against a specified soil density to derive the soil strain as shown in the example problem below Figure 7.
6. Calculate the critical buckling pressure at the top of the pipe by the formula:

$$P_{cb} = 0.8\sqrt{(E')(P_c)}$$

Where: P_{cb} = Critical buckling soil pressure at the top of the pipe, psi
 E' = Soil Modulus, psi
 P_c = Hydrostatic critical-collapse differential pressure, psi

7. Calculate the Safety Factor: $SF = P_{cb} / P_T$.
8. The above procedures can be reversed to calculate the minimum pipe DR required for a given soil pressure and an estimated soil density.

In a direct burial pressurized pipeline, the internal pressure is usually great enough to exceed the external critical-buckling soil pressure. When a pressurized line is to be shut down for a period, wall buckling should be examined.

**APPLICATION FOR PERMIT
OWL LANDFILL SERVICES, LLC**

**VOLUME III: ENGINEERING DESIGN AND CALCULATIONS
SECTION 5: PIPE LOADING CALCULATIONS**

ATTACHMENT III.5.F

CHEVRON PHILLIPS CHEMICAL COMPANY, LP. 2003.

PERFORMANCE PIPE ENGINEERING MANUAL.

BULLETIN: PP 900

DriscoPlex™ 2000 SPIROLITE® pipe is manufactured to ASTM F 894, which states that profile pipe designed for 7.5% deflection will perform satisfactorily when installed in accordance with ASTM D 2321. Deflection is measured at least 30 days after installation.

Manufacturing processes for DriscoPlex™ 2000 SPIROLITE® and DriscoPlex™ OD controlled pipe differ. Deflection limitations for OD controlled pipe are controlled by long-term material strain.

Ring Bending Strain

As pipe deflects, bending strains occur in the pipe wall. For an elliptically deformed pipe, the pipe wall ring bending strain, ε , can be related to deflection:

$$\varepsilon = f_D \frac{\Delta X}{D_M} \frac{2C}{D_M} \quad (7-39) \leftarrow$$

Where

- ε = wall strain
- f_D = deformation shape factor
- ΔX = deflection, in
- D_M = mean diameter, in
- C = distance from outer fiber to wall centroid, in

For DriscoPlex™ 2000 SPIROLITE® pipe

$$C = h - z \quad (7-40)$$

For DriscoPlex™ OD Controlled pipe

$$C = 0.5(1.06t) \quad (7-41) \leftarrow$$

Where

- h = pipe wall height, in
- z = pipe wall centroid, in
- t = pipe minimum wall thickness, in

For elliptical deformation, $f_D = 4.28$. However, buried pipe rarely has a perfectly elliptical shape. Irregular deformation can occur from installation forces such as compaction variation alongside the pipe. To account for the non-elliptical shape many designers use $f_D = 6.0$.

Lytton and Chua report that for high performance polyethylene materials such as those used by Performance Pipe, 4.2% ring bending strain is a conservative value for non-pressure pipe. Jansen reports that high performance polyethylene material at an 8% strain level has a life expectancy of at least 50 years.

When designing non-pressure heavy wall OD controlled pipe (DR less than 17), and high RSC (above 200) DriscoPlex™ 2000 SPIROLITE® pipe, the ring bending strain at the predicted deflection should be calculated and compared to the allowable strain.

In pressure pipe, the combined stress from deflection and internal pressure should not exceed the material's long-term design stress rating. Combined stresses are incorporated into Table 7-9 values, which presumes deflected pipe at full pressure. At reduced pressure, greater deflection is allowable.

**APPLICATION FOR PERMIT
OWL LANDFILL SERVICES, LLC**

**VOLUME III: ENGINEERING DESIGN AND CALCULATIONS
SECTION 6: GEOSYNTHETICS APPLICATION AND
COMPATIBILITY DOCUMENTATION**

TABLE OF CONTENTS

Section No.	Title	Page
1.0	INTRODUCTION	III.6-1
1.1	Site Location	III.6-1
1.2	Description	III.6-1
2.0	SUMMARY	III.6-2

LIST OF TABLES

Table No.	Title	Page
III.6.1	GEOSYNTHETIC APPLICATIONS AND COMPATIBILITY DOCUMENTATION	III.6-4

LIST OF ATTACHMENTS

Attachment No.	Title
III.6.A	HDPE GEOMEMBRANES REFERENCE DOCUMENTATION
III.6.B	GEOTEXTILE REFERENCE DOCUMENTATION
III.6.C	GEONET REFERENCE DOCUMENTATION
III.6.D	GEOSYNTHETIC CLAY LINER (GCL) REFERENCE DOCUMENTATION
III.6.E	HDPE PIPE REFERENCE DOCUMENTATION
III.6.F	PVC PIPE REFERENCE DOCUMENTATION

**APPLICATION FOR PERMIT
OWL LANDFILL SERVICES, LLC**

**VOLUME III: ENGINEERING DESIGN AND CALCULATIONS
SECTION 6: GEOSYNTHETICS APPLICATION AND
COMPATIBILITY DOCUMENTATION**

1.0 INTRODUCTION

OWL Landfill Services, LLC (OWL) is proposing to permit, construct, and operate a “Surface Waste Management Facility” for oil field waste processing and disposal services. The proposed OWL Facility is subject to regulation under the New Mexico (NM) Oil and Gas Rules, specifically 19.15.36 NMAC, administered by the Oil Conservation Division (OCD). The Facility has been designed in compliance with the requirements of 19.15.36 NMAC, and will be constructed, operated, and closed in compliance with a Surface Waste Management Facility Permit issued by the OCD.

The OWL Facility is one of the first designed to the new more stringent standards that, for instance, mandate double liners and leak detection for land disposal. The new services that OWL will provide fill a necessary void in the market for technologies that exceed current OCD requirements.

1.1 Site Location

The OWL site is located approximately 22 miles northwest of Jal, adjacent to the south of NM 128 in Lea County, NM. The OWL site is comprised of a 560-acre ± tract of land located within a portion of Section 23, Township 24 South, Range 33 East, Lea County, NM (**Figure IV.1.1**). Site access will be provided on the south side of NM 128. The coordinates for the approximate center of the OWL site are Latitude 32.203105577 and Longitude - 103.543122319 (surface coordinates).

1.2 Description

The OWL Surface Waste Management Facility will comprise approximately 500 acres of the 560-acre site, and will include two main components: an oil field waste Processing Area and an oil field waste Landfill Disposal Area, as well as related infrastructure. Oil field wastes are anticipated to be delivered to the OWL Facility from oil and gas exploration and production operations in southeastern NM and west Texas. The Permit Plans (**Attachment III.1.A**)

identify the locations of the Processing Area and Landfill Disposal Area.

2.0 SUMMARY

19.15.36.14 NMAC *Specific requirements applicable to Landfills:*

D. *Liner specifications and requirements.*

(1) *General requirements.*

(a) *Geomembrane liner specifications. Geomembrane liners shall consist of a 30-mil flexible PVC or 60-mil HDPE liner, or an equivalent liner approved by the division. Geomembrane liners shall have a hydraulic conductivity no greater than 1×10^{-9} cm/sec. Geomembrane liners shall be composed of impervious, geosynthetic material that is resistant to petroleum hydrocarbons, salts and acidic and alkaline solutions. Liners shall also be resistant to ultraviolet light, or the operator shall make provisions to protect the material from sunlight. Liner compatibility shall comply with EPA SW-846 method 9090A.*

19.15.36.17 NMAC *Specific requirements applicable to evaporation, storage, treatment, and skimmer ponds:*

B. *Construction, standards.*

(3) *Liner specifications. Liners shall consist of a 30-mil flexible PVC or 60-mil HDPE liner, or an equivalent liner approved by the division. Synthetic (geomembrane) liners shall have a hydraulic conductivity no greater than 1×10^{-9} cm/sec. Geomembrane liners shall be composed of an impervious, synthetic material that is resistant to petroleum hydrocarbons, salts and acidic and alkaline solutions. Liner materials shall be resistant to ultraviolet light, or the operator shall make provisions to protect the material from sunlight. Liner compatibility shall comply with EPA SW-846 method 9090A.*

Geosynthetics have a proven track record in a variety of civil engineering applications, primarily over the past 30 years. Fluid Containment design provides a unique opportunity to incorporate a range of engineered materials that exceed the equivalent performance of soils.

EPA SW-846 Method 9090A (July 1992 and subsequent revisions; the latest being June 2005) references ASTM methods for the majority of the physical properties of geosynthetics. Subsequent to the publication of EPA Method 9090A, the Geosynthetic Research Institute (GRI) published GRI-GM13 “*Test Methods, Test Properties and Testing Frequency for High Density Polyethylene (HDPE) Smooth and Textured Geomembranes*” (Revision 11: 12/14/12). Although this specification is not mandatory, the geosynthetics manufacturing industry has used this specification in the manufacturing of geosynthetics; and have used the noted ASTM methods for determining the adequacy of the geosynthetic physical properties for its intended use in landfills.

Compatibility testing of membrane liners has been completed by geosynthetic manufacturers in accordance with EPA method 9090A (July 1992) and subsequent updates. Additionally, the

EPA promulgated the Methods Innovation Rule in the June 2005. This Rule provides greater flexibility by allowing the use of alternate test procedures other than SW-846 that are considered “appropriate” as long as they fall within EPA’s mission to safeguard human health and the environment, and meet the goals, data quality objectives, and quality control parameters of the project.

The design of the OWL Facility includes several examples of geosynthetics and plastics deployed for their superior characteristics, usually applied in conjunction with soil layers:

- Geomembranes (flexible membrane liners) provided as barrier layer in the primary and secondary liner system (**Attachment III.6.A**).
- Geotextiles serving as cushioning layers and as filters to maintain flow (**Attachment III.6.B**).
- Geonets deployed as drainage layers and in leak detection systems (**Attachment III.6.C**).
- Geosynthetic clay liners (GCLs) employed as secondary composite layers for liners (**Attachment III.6.D**).
- The use of HDPE (High Density Polyethylene; **Attachment III.6.E**) or PVC (Polyvinyl Chloride; **Attachment III.6.F**) piping systems.

Geosynthetics are selected in the design process for their performance characteristics in the project’s environmental setting. These materials must be able to withstand the physical forces that they will experience, as documented in this section. **Attachment III.6.A** includes recent research results that indicate the functional longevity of HDPE liners in similar installations is in the hundreds of years.

This section provides demonstrations, as required by 19.15.36.14.D.1 and 19.15.36.17.B NMAC that the geosynthetic components are compatible with the materials to be contained within the cells and basins. The attached compatibility documentation includes published reports and test results; and is further endorsed by industry experience and proven installations by the design engineer. For the performance criteria of both soil and geosynthetic components to be achieved, they must be constructed in strict accordance with the **Permit Plans (Volume III.1)** and the Liner Construction Quality Assurance (CQA) Plan, (**Volume II.7**) of this Application for Permit.

Table III.6.1 provides an index of compatibility data provided for each of the prescribed geosynthetic materials and their function in the engineering design.

**TABLE III.6.1
Geosynthetic Applications and Compatibility Documentation
OWL Landfill Services, LLC**

MATERIAL	FUNCTION	ATTACHED REFERENCE DOCUMENTATION
HDPE Geomembrane	Primary and secondary barrier layer for landfill liner	<i>Geomembrane Lifetime Prediction: Unexposed and Exposed Conditions</i>
		<i>Cold Temperature and Free-Thaw Cycling Behavior of Geomembranes and Their Seams</i>
		<i>Chemical Compatibility of Poly-Flex Liners</i>
		<i>Chemical Resistance Table Low Density and High Density Polyethylene</i>
Geotextile (upper & lower component of geocomposite)	Filter layer around leachate collection piping	<i>NSC, Contaminant Solutions for Industrial Waste; HDPE Geomembrane</i>
		<i>Liner Longevity Article: Geosynthetics Magazine, Oct/Nov 2008</i>
		<i>Amoco Technical Note No. 7, Chemical Resistance of Amoco Polypropylene Geotextiles</i>
Geonet (middle component of geocomposite)	Drainage layer between primary and secondary liner	<i>Amoco Technical Note No. 14, Geotextile Polymers for Waste Applications</i>
		<i>GSE TenDrain 275 mil Geocomposite</i>
GCL	Secondary layer in composite liner	<i>Evaluation on Stress Cracking Resistance of Various HDPE Drainage Geonets</i>
		<i>The Effects of Leachate on the Hydraulic Conductivity of Bentomat Bench-scale Hydraulic Conductivity Tests of Bentonitic Blanket Materials for Liner and Cover Systems (Thesis by Paula Estornell)</i>
HDPE Pipe	Solid and slotted piping, leachate collection system and GCCS	<i>Chemical Resistance of Plastics and Elastomers Used in Pipeline Construction</i>
		<i>Driscopipe Engineering Characteristics</i>
		<i>Plexco Chemical Resistance Information</i>
PVC Pipe	Solid and slotted piping, leachate collection system and GCCS	<i>Certainteed - PVC Chemical Resistance</i>

Acronyms used:

GCL: Geosynthetic Clay Liner
 FML: Flexible Membrane Liner
 GSE: Gundle Schlegel Environmental
 PVC: Polyvinyl Chloride
 HDPE: High Density Polyethylene
 NSC: National Seal Company

**APPLICATION FOR PERMIT
OWL LANDFILL SERVICES, LLC**

**VOLUME III: ENGINEERING DESIGN AND CALCULATIONS
SECTION 6: GEOSYNTHETICS APPLICATION AND
COMPATIBILITY DOCUMENTATION**

**ATTACHMENT III.6.A
HDPE GEOMEMBRANES REFERENCE DOCUMENTATION**

Geosynthetic Institute

475 Kedron Avenue
Folsom, PA 19033-1208 USA
TEL (610) 522-8440
FAX (610) 522-8441



GRI White Paper #6

- on -

**Geomembrane Lifetime Prediction:
Unexposed and Exposed Conditions**

by

**Robert M. Koerner, Y. Grace Hsuan and George R. Koerner
Geosynthetic Institute
475 Kedron Avenue
Folsom, PA 19033 USA**

**Phone (610) 522-8440
Fax (610) 522-8441**

**E-mails:
robert.koerner@coe.drexel.edu
grace.hsuan@coe.drexel.edu
gkoerner@dca.net**

Original: June 7, 2005

Updated: February 8, 2011

Geomembrane Lifetime Prediction: Unexposed and Exposed Conditions

1.0 Introduction

Without any hesitation the most frequently asked question we have had over the past thirty years' is "how long will a particular geomembrane last".* The two-part answer to the question, largely depends on whether the geomembrane is covered in a timely manner or left exposed to the site-specific environment. Before starting, however, recognize that the answer to either covered or exposed geomembrane lifetime prediction is neither easy, nor quick, to obtain. Further complicating the answer is the fact that all geomembranes are formulated materials consisting of (at the minimum), (i) the resin from which the name derives, (ii) carbon black or colorants, (iii) short-term processing stabilizers, and (iv) long-term antioxidants. If the formulation changes (particularly the additives), the predicted lifetime will also change. See Table 1 for the most common types of geomembranes and their approximate formulations.

Table 1 - Types of commonly used geomembranes and their approximate formulations
(based on weight percentage)

Type	Resin	Plasticizer	Fillers	Carbon Black	Additives
HDPE	95-98	0	0	2-3	0.25-1
LLDPE	94-96	0	0	2-3	0.25-3
fPP	85-98	0	0-13	2-4	0.25-2
PVC	50-70	25-35	0-10	2-5	2-5
CSPE	40-60	0	40-50	5-10	5-15
EPDM	25-30	0	20-40	20-40	1-5

HDPE = high density polyethylene	PVC = polyvinyl chloride (plasticized)
LLDPE = linear low density polyethylene	CSPE = chlorosulfonated polyethylene
fPP = flexible polypropylene	EPDM = ethylene propylene diene terpolymer

* More recently, the same question has arisen but focused on geotextiles, geogrids, geopipe, turf reinforcement mats, fibers of GCLs, etc. This White Paper, however, is focused completely on geomembranes due to the tremendous time and expense of providing such information for all types of geosynthetics.

The possible variations being obvious, one must also address the degradation mechanisms which might occur. They are as follows accompanied by some generalized commentary.

- Ultraviolet Light - This occurs only when the geosynthetic is exposed; it will be the focus of the second part of this communication.
- Oxidation - This occurs in all polymers and is the major mechanism in polyolefins (polyethylene and polypropylene) under all conditions.
- Ozone - This occurs in all polymers that are exposed to the environment. The site-specific environment is critical in this regard.
- Hydrolysis - This is the primary mechanism in polyesters and polyamides.
- Chemical - Can occur in all polymers and can vary from water (least aggressive) to organic solvents (most aggressive).
- Radioactivity - This is not a factor unless the geomembrane is exposed to radioactive materials of sufficiently high intensity to cause chain scission, e.g., high level radioactive waste materials.
- Biological - This is generally not a factor unless biologically sensitive additives (such as low molecular weight plasticizers) are included in the formulation.
- Stress State – This is a complicating factor which is site-specific and should be appropriately modeled in the incubation process but, for long-term testing, is very difficult and expensive to achieve.
- Temperature - Clearly, the higher the temperature the more rapid the degradation of all of the above mechanisms; temperature is critical to lifetime and furthermore is the key to

time-temperature-superposition which is the basis of the laboratory incubation methods which will be followed.

2.0 Lifetime Prediction: Unexposed Conditions

Lifetime prediction studies at GRI began at Drexel University under U. S. EPA contract from 1991 to 1997 and was continued under GSI consortium funding until ca. 2002. Focus to date has been on HDPE geomembranes placed beneath solid waste landfills due to its common use in this particular challenging application. Incubation of the coupons has been in landfill simulation cells (see Figure 1) maintained at 85, 75, 65 and 55°C. The specific conditions within these cells are oxidation beneath, chemical (water) from above, and the equivalent of 50 m of solid waste mobilizing compressive stress. Results have been forthcoming over the years insofar as three distinct lifetime stages; see Figure 2.

Stage A - Antioxidant Depletion Time

Stage B - Induction Time to the Onset of Degradation

Stage C - Time to Reach 50% Degradation (i.e., the Half-life)

2.1 Stage A - Antioxidant Depletion Time

The dual purposes of antioxidants are to (i) prevent polymer degradation during processing, and (ii) prevent oxidation reactions from taking place during Stage A of service life, respectively. Obviously, there can only be a given amount of antioxidants in any formulation. Once the antioxidants are depleted, additional oxygen diffusing into the geomembrane will begin to attack the polymer chains, leading to subsequent stages as shown in Figure 2. The duration of the antioxidant depletion stage depends on both the type and amount of the various antioxidants, i.e., the precise formulation.

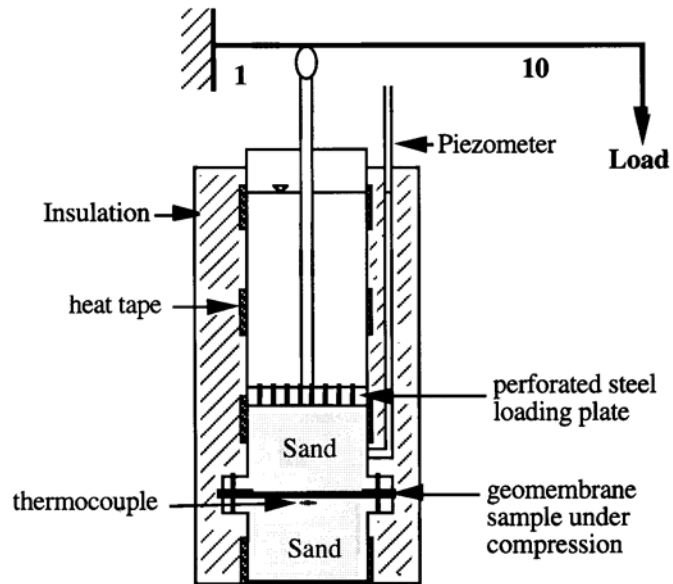


Figure 1. Incubation schematic and photograph of multiple cells maintained at various constant temperatures.

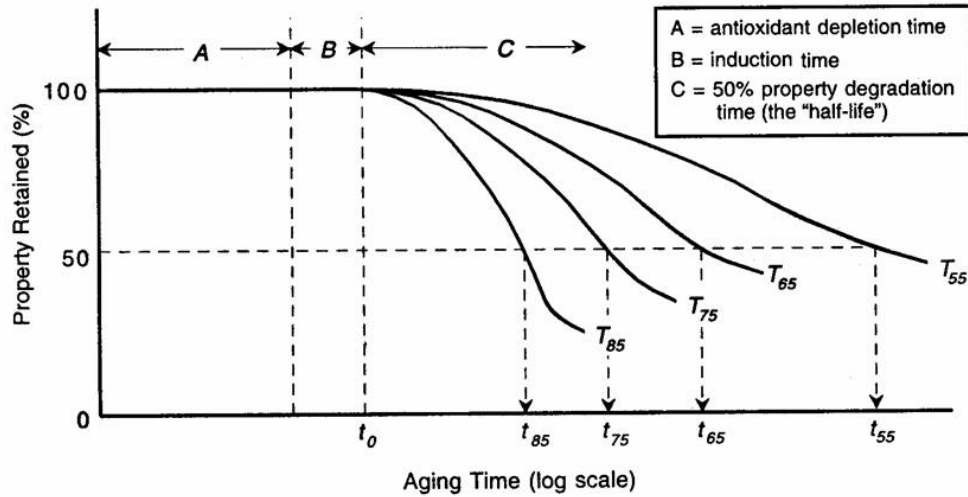


Figure 2. Three individual stages in the aging of most geomembranes.

The depletion of antioxidants is the consequence of two processes: (i) chemical reactions with the oxygen diffusing into the geomembrane, and (ii) physical loss of antioxidants from the geomembrane. The chemical process involves two main functions; the scavenging of free radicals converting them into stable molecules, and the reaction with unstable hydroperoxide (ROOH) forming a more stable substance. Regarding physical loss, the process involves the distribution of antioxidants in the geomembrane and their volatility and extractability to the site-specific environment.

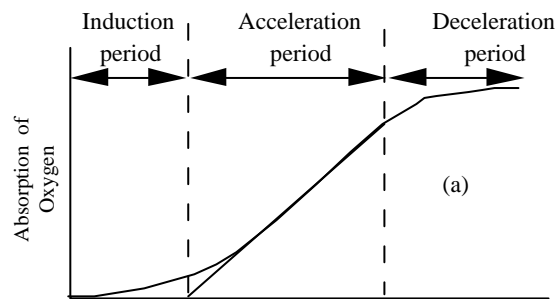
Hence, the rate of depletion of antioxidants is related to the type and amount of antioxidants, the service temperature, and the nature of the site-specific environment. See Hsuan and Koerner (1998) for additional details.

2.2 Stage B - Induction Time to Onset of Degradation

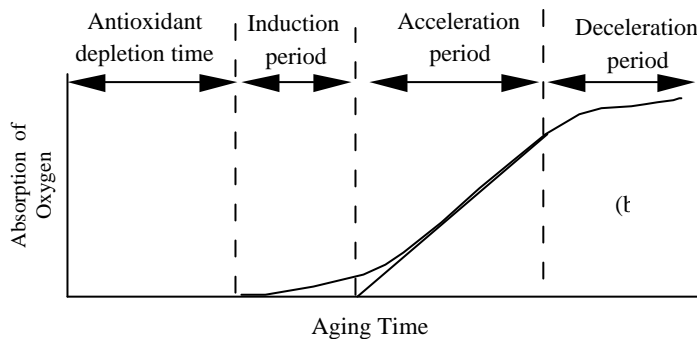
In a pure polyolefin resin, i.e., one without carbon black and antioxidants, oxidation occurs extremely slowly at the beginning, often at an immeasurable rate. Eventually, oxidation occurs more rapidly. The reaction eventually decelerates and once again becomes very slow.

This progression is illustrated by the S-shaped curve of Figure 3(a). The initial portion of the curve (before measurable degradation takes place) is called the induction period (or induction time) of the polymer. In the induction period, the polymer reacts with oxygen forming hydroperoxide (ROOH), as indicated in Equations (1)-(3). However, the amount of ROOH in this stage is very small and the hydroperoxide does not further decompose into other free radicals which inhibits the onset of the acceleration stage.

In a stabilized polymer such as one with antioxidants, the accelerated oxidation stage takes an even longer time to be reached. The antioxidants create an additional depletion time stage prior to the onset of the induction time, as shown in Figure 3(b).



(a) Pure unstabilized polyethylene



(b) Stabilized polyethylene

Figure 3. Curves illustrating various stages of oxidation.



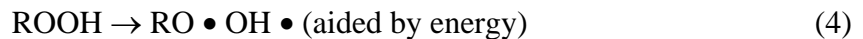
(aided by energy or catalyst residues in the polymer)



In the above, RH represents the polyethylene polymer chains; and the symbol “•” represents free radicals, which are highly reactive molecules.

2.3 Stage C - Time to Reach 50% Degradation (Half-life)

As oxidation continues, additional ROOH molecules are being formed. Once the concentration of ROOH reaches a critical level, decomposition of ROOH begins, leading to a substantial increase in the amount of free radicals, as indicated in Equations (4) to (6). The additional free radicals rapidly attack other polymer chains, resulting in an accelerated chain reaction, signifying the end of the induction period, Rapoport and Zaikov (1986). This indicates that the concentration of ROOH has a critical control on the duration of the induction period.



A series of oxidation reactions produces a substantial amount of free radical polymer chains (R•), called alkyl radicals, which can proceed to further reactions leading to either cross-linking or chain scission in the polymer. As the degradation of polymer continues, the physical and mechanical properties of the polymer start to change. The most noticeable change in physical properties is the melt index, since it relates to the molecular weight of the polymer. As for mechanical properties, both tensile break stress (strength) and break strain (elongation) decrease.

Ultimately, the degradation becomes so severe that all tensile properties start to change (tear, puncture, burst, etc.) and the engineering performance is jeopardized. This signifies the end of the so-called “service life” of the geomembrane.

Although quite arbitrary, the limit of service life of polymeric materials is often selected as a 50% reduction in a specific design property. This is commonly referred to as the half-life time, or simply the “half-life”. It should be noted that even at half-life, the material still exists and can function, albeit at a decreased performance level with a factor-of-safety lower than the initial design value.

2.4 Summary of Lifetime Research-to-Date

Stage A, that of antioxidant depletion for HDPE geomembranes as required in the GRI-GM13 Specification, has been well established by our own research and corroborated by others, e.g., Sangram and Rowe (2004). The GRI data for standard and high pressure Oxidative Induction Time (OIT) is given in Table 2. The values are quite close to one another. Also, as expected, the lifetime is strongly dependent on the service temperature; with the higher the temperature the shorter the lifetime.

Table 2 - Lifetime prediction of HDPE (nonexposed) at various field temperatures

In Service Temperature (°C)	Stage “A” (years)			Stage “B” (years)	Stage “C” (years)	Total Prediction* (years)
	Standard OIT	High Press. OIT	Average OIT			
20	200	215	208	30	208	446
25	135	144	140	25	100	265
30	95	98	97	20	49	166
35	65	67	66	15	25	106
40	45	47	46	10	13	69

*Total = Stage A (average) + Stage B + Stage C

Stage “B”, that of induction time, has been obtained by comparing 30-year old polyethylene water and milk containers (containing no long-term antioxidants) with currently

produced containers. The data shows that degradation is just beginning to occur as evidenced by slight changes in break strength and elongation, but not in yield strength and elongation. The lifetime for this stage is also given in Table 2.

Stage “C”, the time for 50% change of mechanical properties is given in Table 2 as well. The data depends on the activation energy, or slope of the Arrhenius curve, which is very sensitive to material and experimental techniques. The data is from Gedde, et al. (1994) which is typical of the HDPE resin used for gas pipelines and is similar to Martin and Gardner (1983).

Summarizing Stages A, B, and C, it is seen in Table 2 that the half-life of covered HDPE geomembranes (formulated according to the current GRI-GM13 Specification) is estimated to be 449-years at 20°C. This, of course, brings into question the actual temperature for a covered geomembrane such as beneath a solid waste landfill. Figure 4 presents multiple thermocouple monitoring data of a municipal waste landfill liner in Pennsylvania for over 10-years, Koerner and Koerner (2005). Note that for 6-years the temperature was approximately 20°C. At that time and for the subsequent 4-years the temperature increased to approximately 30°C. Thus, the half-life of this geomembrane is predicted to be from 166 to 446 years within this temperature range. The site is still being monitored, see Koerner and Koerner (2005).

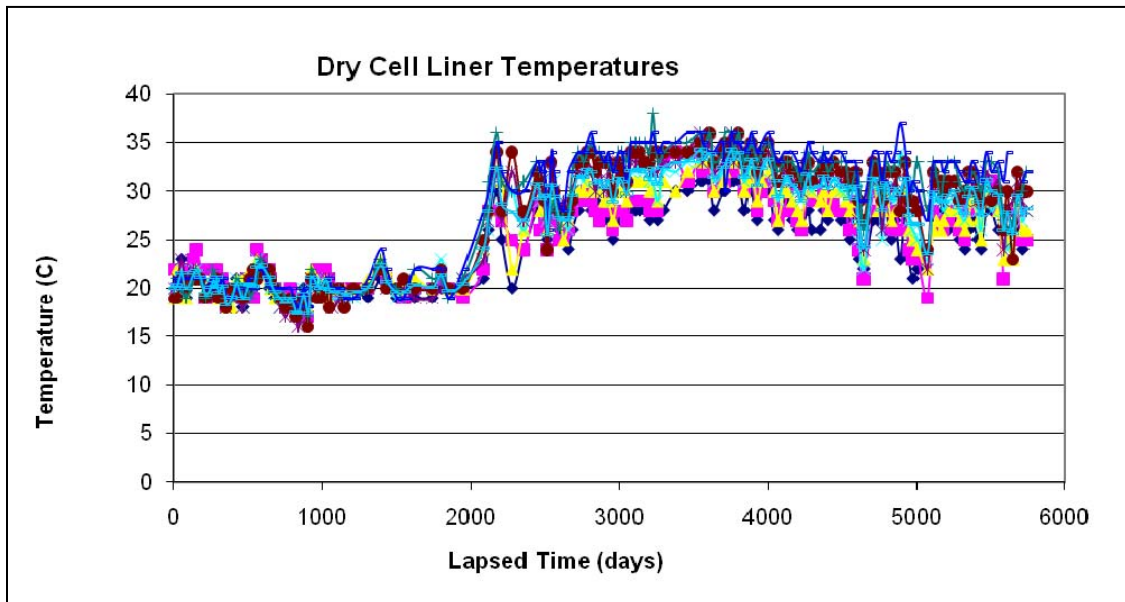


Figure 4. Long-term monitoring of an HDPE liner beneath a municipal solid waste landfill in Pennsylvania.

2.5 Lifetime of Other Covered Geomembranes

By virtue of its widespread use as liners for solid waste landfills, HDPE is by far the widest studied type of geomembrane. Note that in most countries (other than the U.S.), HDPE is the required geomembrane type for solid waste containment. Some commentary on other-than HDPE geomembranes (recall Table 1) follows:

2.5.1 Linear Low Density Polyethylene (LLDPE) geomembranes

The nature of the LLDPE resin and its formulation is very similar to HDPE. The fundamental difference is that LLDPE is a lower density, hence lower crystallinity, than HDPE; e.g., 10% versus 50%. This has the effect of allowing oxygen to diffuse into the polymer structure quicker, and likely decreases Stages A and C. How much is uncertain since no data is available, but it is felt that the lifetime of LLDPE will be somewhat reduced with respect to HDPE.

2.5.2 Plasticizer migration in PVC geomembranes

Since PVC geomembranes necessarily have plasticizers in their formulations so as to provide flexibility, the migration behavior must be addressed for this material. In PVC the plasticizer bonds to the resin and the strength of this bonding versus liquid-to-resin bonding is significant. One of the key parameters of a stable long-lasting plasticizer is its molecular weight. The higher the molecular weight of the plasticizer in a PVC formulation, the more durable will be the material. Conversely, low molecular weight plasticizers have resulted in field failures even under covered conditions. See Miller, et al. (1991), Hammon, et al. (1993), and Giroud and Tisinger (1994) for more detail in this regard. At present there is a considerable difference (and cost) between PVC geomembranes made in North America versus Europe. This will be apparent in the exposed study of durability in the second part of this White Paper.

2.5.3 Crosslinking in EPDM and CSPE geomembranes

The EPDM geomembranes mentioned in Table 1 are crosslinked thermoset materials. The oxidation degradation of EPDM takes place in either ethylene or propylene fraction of the co-polymer via free radical reactions, as expressed in Figure 5, which are described similarly by Equations (4) to (6).

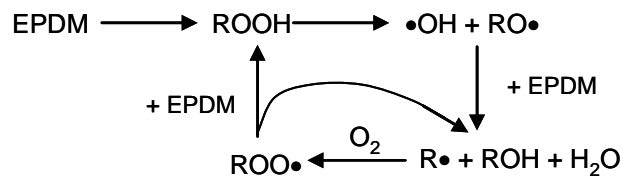


Figure 5. Oxidative degradation of crosslinked EPDM geomembranes, (Wang and Qu, 2003).

For CSPE geomembranes, the degradation mechanism is dehydrochlorination by losing chlorine and generating carbon-carbon double bonds in the main polymer chain, as shown in Figure 6.

The carbon-carbon double bonds become the preferred sites for further thermodegradation or cross-linking in the polymer, leading to eventual brittleness of the geomembrane.

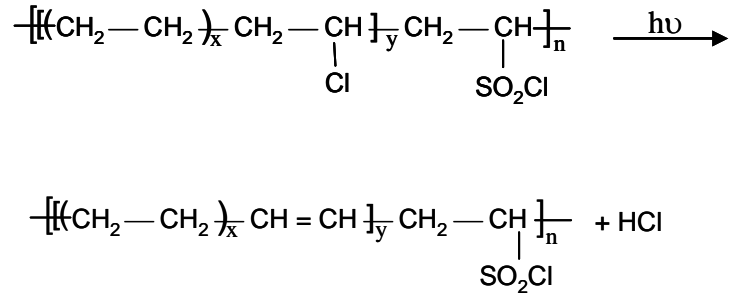


Figure 6. Dechlorination degradation of crosslinked CSPE geomembranes (Chailan, et al., 1995).

Neither EPDM nor CSPE has had a focused laboratory study of the type described for HDPE reported in the open literature. Most of lifetime data for these geomembranes is antidotal by virtue of actual field performance. Under covered conditions, as being considered in this section, there have been no reported failures by either of these thermoset polymers to our knowledge.

3.0 Lifetime Prediction: Exposed Conditions

Lifetime prediction of exposed geomembranes have taken two very different pathways; (i) prediction from anecdotal feedback and field performance, and (ii) from laboratory weathering device predictions.

3.1 Field Performance

There is a large body of anecdotal information available on field feedback of exposed geomembranes. It comes from two quite different sources, i.e., dams in Europe and flat roofs in the USA.

Regarding exposed geomembranes in dams in Europe, the original trials were using 2.0 mm thick polyisobutylene bonded directly to the face of the dam. There were numerous problems encountered as described by Scuero (1990). Similar experiences followed using PVC

geomembranes. In 1980, a geocomposite was first used at Lago Nero which had a 200 g/m² nonwoven geotextile bonded to the PVC geomembrane. This proved quite successful and led to the now-accepted strategy of requiring drainage behind the geomembrane. In addition to thick nonwoven geotextiles, geonets, and geonet composites have been successful. Currently over 50 concrete and masonry dams have been rehabilitated in this manner and are proving successful for over 30-years of service life. The particular type of PVC plasticized geomembranes used for these dams is proving to be quite durable. Tests by the dam owners on residual properties show only nominal changes in properties, Cazzuffi (1998). As indicated in Miller, et al. (1991) and Hammond, et al. (1993), however, different PVC materials and formulations result in very different behavior; the choice of plasticizer and the material's thickness both being of paramount importance. An excellent overview of field performance is recently available in which 250 dams which have been waterproofed by geomembranes is available from ICOLD (2010).

Regarding exposed geomembranes in flat roofs, past practice in the USA is almost all with EPDM and CSPE and, more recently, with fPP. Manufacturers of these geomembranes regularly warranty their products for 20-years and such warrants appear to be justified. EPDM and CSPE, being thermoset or elastomeric polymers, can be used in dams without the necessity of having seams by using vertical attachments spaced at 2 to 4 m centers, see Scuro and Vaschetti (1996). Conversely, fPP can be seamed by a number of thermal fusion methods. All of these geomembrane types have good conformability to rough substrates as is typical of concrete and masonry dam rehabilitation. It appears as though experiences (both positive and negative) with geomembranes in flat roofs should be transferred to all types of waterproofing in civil engineering applications.

3.2 Laboratory Weatherometer Predictions

For an accelerated simulation of direct ultraviolet light, high temperature, and moisture using a laboratory weatherometer one usually considers a worst-case situation which is the solar maximum condition. This condition consists of global, noon sunlight, on the summer solstice, at normal incidence. It should be recognized that the UV-A range is the target spectrum for a laboratory device to simulate the naturally occurring phenomenon, see Hsuan and Koerner (1993), and Suits and Hsuan (2001).

The Xenon Arc weathering device (ASTM D4355) was introduced in Germany in 1954. There are two important features; the type of filters and the irradiance settings. Using a quartz inner and borosilicate outer filter (quartz/boro) results in excessive low frequency wavelength degradation. The more common borosilicate inner and outer filters (boro/boro) shows a good correlation with solar maximum conditions, although there is an excess of energy below 300 nm wavelength. Irradiance settings are important adjustments in shifting the response although they do not eliminate the portion of the spectrum below 300 nm frequency. Nevertheless, the Xenon Arc device is commonly used method for exposed lifetime prediction of all types of geosynthetics.

UV Fluorescent devices (ASTM D7238) are an alternative type of accelerated laboratory test device which became available in the early 1970's. They reproduce the ultraviolet portion of the sunlight spectrum but not the full spectrum as in Xenon Arc weatherometers. Earlier FS-40 and UVB-313 lamps give reasonable short wavelength output in comparison to solar maximum. The UVA-340 lamp was introduced in 1987 and its response is seen to reproduce ultraviolet light quite well. This device (as well as other types of weatherometers) can handle elevated temperature and programmed moisture on the test specimens.

Research at the Geosynthetic Institute (GSI) has actively pursued both Xenon and UV Fluorescent devices on a wide range of geomembranes. Table 3 gives the geomembranes that were incubated and the number of hours of exposure as of 12 July 2005.

Table 5 - Details of the GSI laboratory exposed weatherometer study on various types of geomembranes

Geomembrane Type	Thickness (mm)	UV Fluorescent Exposure*	Xenon Exposure*	Comment
1. HDPE (GM13)	1.50	8000 hrs.	6600 hrs.	Basis of GRI-GM13 Spec
2. LLDPE (GM17)	1.00	8000	6600	Basis of GRI-GM-17 Spec
3. PVC (No. Amer.)	0.75	8000	6600	Low Mol. Wt. Plasticizer
4. PVC (Europe)	2.50	7500	6600	High Mol. Wt. Plasticizer
5. fPP (BuRec)	1.00	2745**	4416**	Field Failure at 26 mos.
6. fPP-R (Texas)	0.91	100	100	Field Failure at 8 years
7. fPP (No. Amer.)	1.00	7500	6600	Expected Good Performance

*As of 12 July 2005 exposure is ongoing

**Light time to reach half-life of break and elongation

3.3 Laboratory Weatherometer Acceleration Factors

The key to validation of any laboratory study is to correlate results to actual field performance. For the nonexposed geomembranes of Section 2 such correlations will take hundreds of years for properly formulated products. For the exposed geomembranes of Section 3, however, the lifetimes are significantly shorter and such correlations are possible. In particular, Geomembrane #5 (flexible polypropylene) of Table 3 was an admittedly poor geomembrane formulation which failed in 26 months of exposure at El Paso, Texas, USA. The reporting of this failure is available in the literature, Comer, et al. (1998). Note that for both UV Fluorescent and Xenon Arc laboratory incubation of this material, failure (half-life to 50% reduction in strength and elongation) occurred at 2745 and 4416 hours, respectively. The comparative analysis of laboratory and field for this case history allows for the obtaining of acceleration factors for the two incubation devices.

3.3.1 Comparison between field and UV Fluorescent weathering

The light source used in the UV fluorescent weathering device is UVA with wavelengths from 295-400 nm. In addition, the intensity of the radiation is controlled by the Solar Eye irradiance control system. The UV energy output throughout the test is 68.25 W/m².

The time of exposure to reach 50% elongation at break was as follows:

$$\begin{aligned} &= 2745 \text{ hr. of light} \\ &= 9,882,000 \text{ seconds} \end{aligned}$$

$$\begin{aligned} \text{Total energy in MJ/m}^2 &= 68.25 \text{ W/m}^2 \times 9,882,000 \\ &= 674.4 \text{ MJ/m}^2 \end{aligned}$$

The field site was located at El Paso, Texas. The UVA radiation energy (295-400 nm) at this site is estimated based on data collected by the South Florida Testing Lab in Arizona (which is a similar atmospheric location). For 26 months of exposure, the accumulated UV radiation energy is 724 MJ/m² which is very close to that generated from the UV fluorescent weatherometer. Therefore, direct comparison of the exposure time between field and UV fluorescent is acceptable.

Field time vs. Fluorescent UV light time: **Thus, the acceleration factor is 6.8.**
= 26 Months = 3.8 Months

3.3.2 Comparison between field and Xenon Arc weathering

The light source of the Xenon Arc weathering device simulates almost the entire sunlight spectrum from 250 to 800 nm. Depending of the age of the light source and filter, the solar energy ranges from 340.2 to 695.4 W/m², with the average value being 517.8 W/m².

The time of exposure to reach 50% elongation at break

$$\begin{aligned} &= 4416 \text{ hr. of light} \\ &= 15,897,600 \text{ seconds} \end{aligned}$$

$$\begin{aligned} \text{Total energy in MJ/m}^2 &= 517.8 \text{ W/m}^2 \times 15,897,600 \\ &= 8232 \text{ MJ/m}^2 \end{aligned}$$

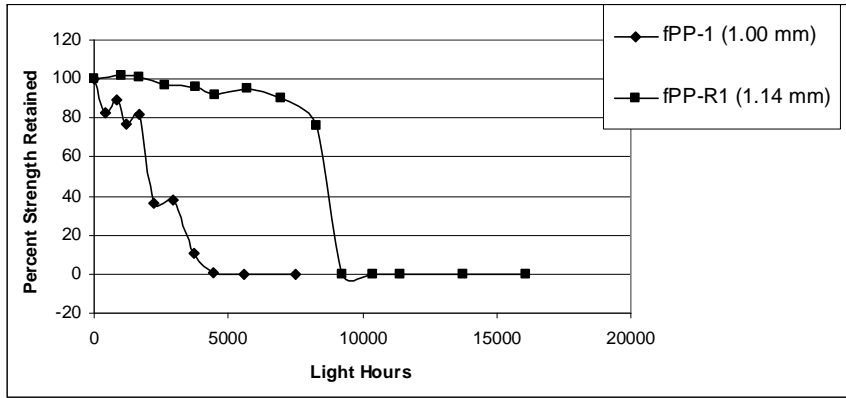
The solar energy in the field is again estimated based on data collected by the South Florida Testing Lab in Arizona. For 26 months of exposure, the accumulated solar energy (295-800 nm) is 15,800 MJ/m², which is much higher than that from the UV Fluorescent device. Therefore, direct comparison of half-lives obtained from the field and Xenon Arc device is not anticipated to be very accurate. However, for illustration purposes the acceleration factor based on Xenon Arc device would be as follows:

Field vs. Xenon Arc : **Thus, the acceleration factor is 4.3.**
= 26 Months = 6.1 Months

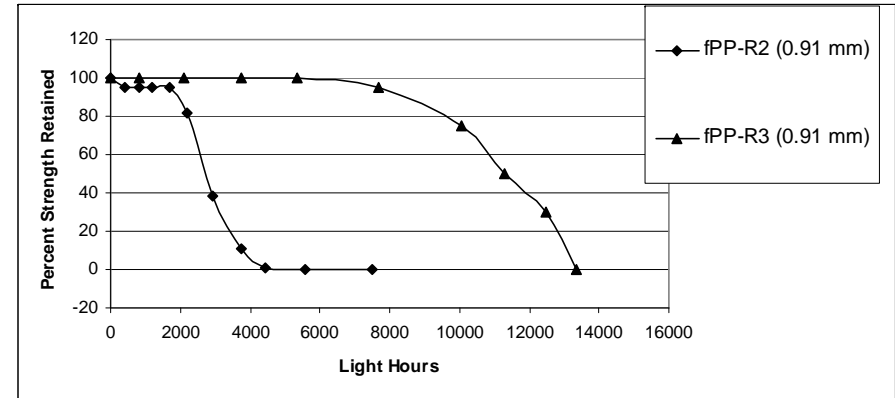
The resulting conclusion of this comparison of weathering devices is that the UV Fluorescent device is certainly reasonable to use for long-term incubations. When considering the low cost of the device, its low maintenance, its inexpensive bulbs, and ease of repair it (the UV Fluorescent device) will be used exclusively by GSI for long-term incubation studies.

3.3.3 Update of exposed lifetime predictions

There are presently (2011) four field failures of flexible polypropylene geomembranes and using unexposed archived samples from these sites their responses in laboratory UV Fluorescent devices per ASTM D7328 at 70°C are shown in Figure 5. From this information we deduce that the average correlation factor is approximately *1200 light hours* \simeq *one-year in a hot climate*. This value will be used accordingly for other geomembranes.



(a) Two Sites in West Texas



(b) Two Sites in So. Calif.

Lab-to-Field Correlation Factors
(ASTM D7238 @ 70°C)

Method	Thickness (mm)	Field (yrs.)	Location	Lab (lt. hr.)	Factor (lt. hrs./1.0 yr.)
fPP-1	1.00	≈ 2	W. Texas	1800	900
fPP-R1	1.14	≈ 8	W. Texas	8200	1025
fPP-R2	0.91	≈ 2	So. Calif.	2500	1250
fPP-R3	0.91	≈ 8	So. Calif.	11200	1400
					1140*

*Use 1200 lt. hr. = 1.0 year in hot climates

Figure 5. Four field failures of fPP and fPP-R exposed geomembranes.

Exposure of a number of different types of geomembranes in laboratory UV Fluorescent devices per ASTM D7238 at 70°C has been ongoing for the six years (between 2005 and 2011) since this White Paper was first released. Included are the following geomembranes:

- Two black 1.0 mm (4.0 mil) unreinforced flexible polypropylene geomembranes formulated per GRI-GM18 Specification; see Figure 6a.
- Two black unreinforced polyethylene geomembranes, one 1.5 mm (60 mil) high density per GRI-GM13 Specification and the other 1.0 mm (40 mil) linear low density per GRI-GM17 Specification; see Figure 6b.
- One 1.0 (40 mil) black ethylene polypropylene diene terpolymer geomembrane per GRI-GM21 Specification; see Figure 6c.
- Two polyvinyl chloride geomembranes, one black 1.0 mm (40 mil) formulated in North America and the other grey 1.5 mm (60 mil) formulated in Europe; see Figure 6d.

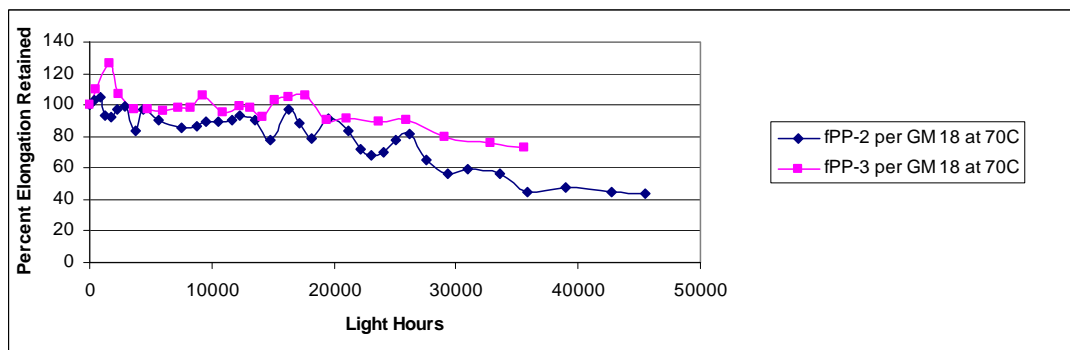
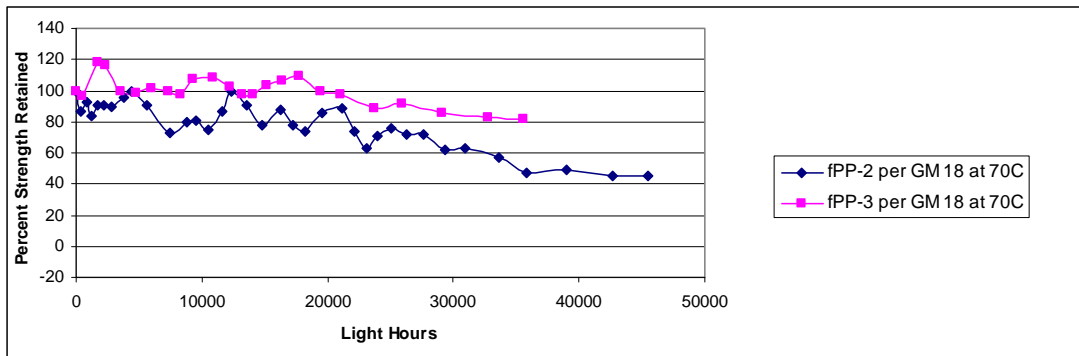


Figure 6a. Flexible polyethylene (fPP) geomembrane behavior.

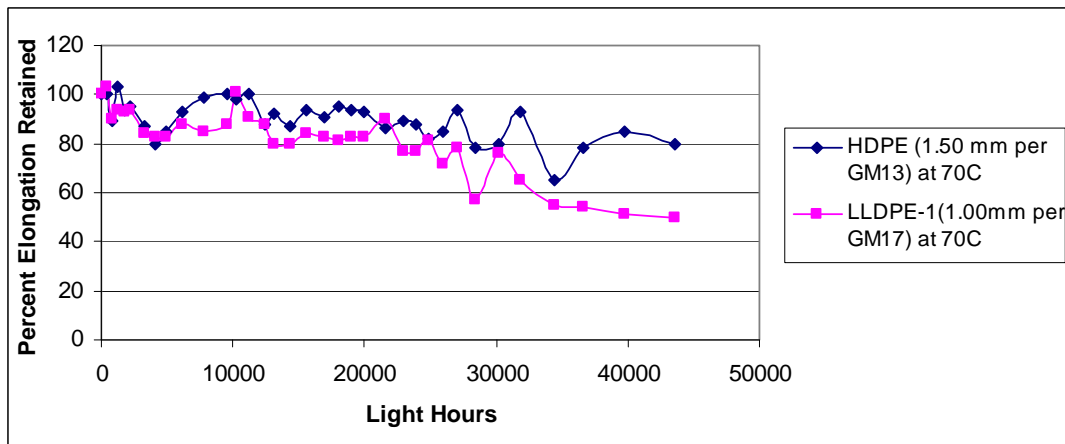
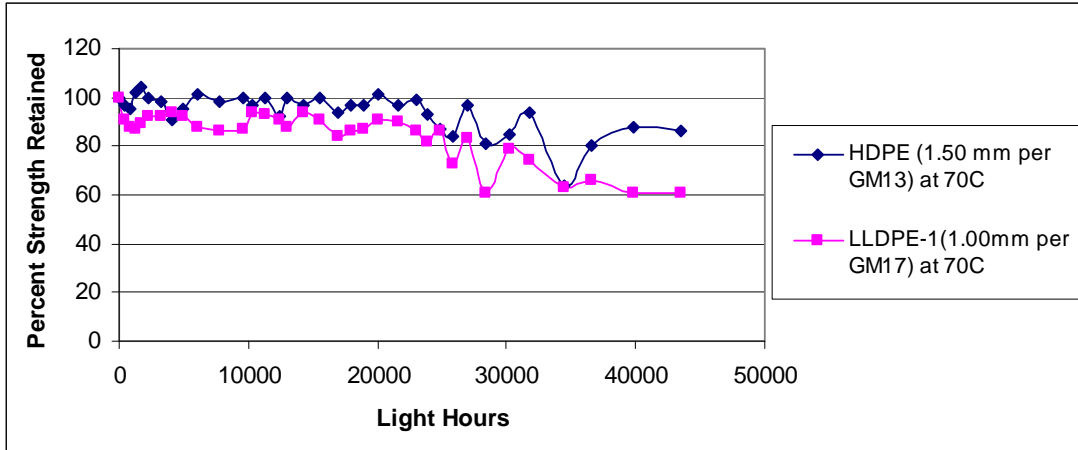


Figure 6b. Polyethylene (HDPE and LLDPE) geomembrane behavior.

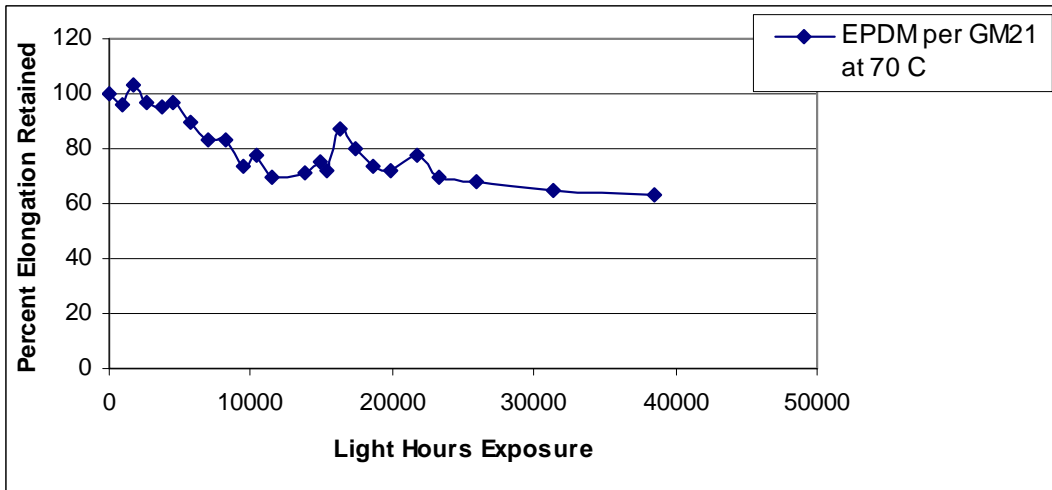
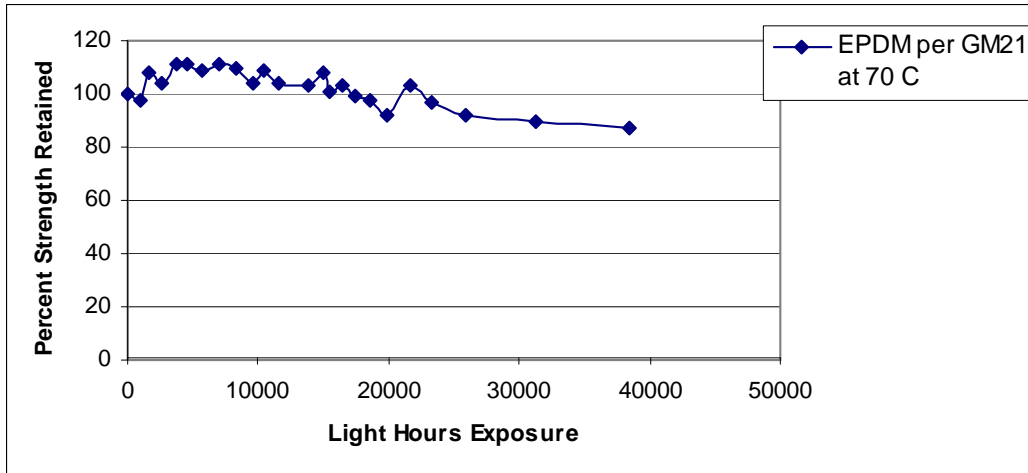


Figure 6c. Ethylene polypropylene diene terpolymer (EPDM) geomembrane.

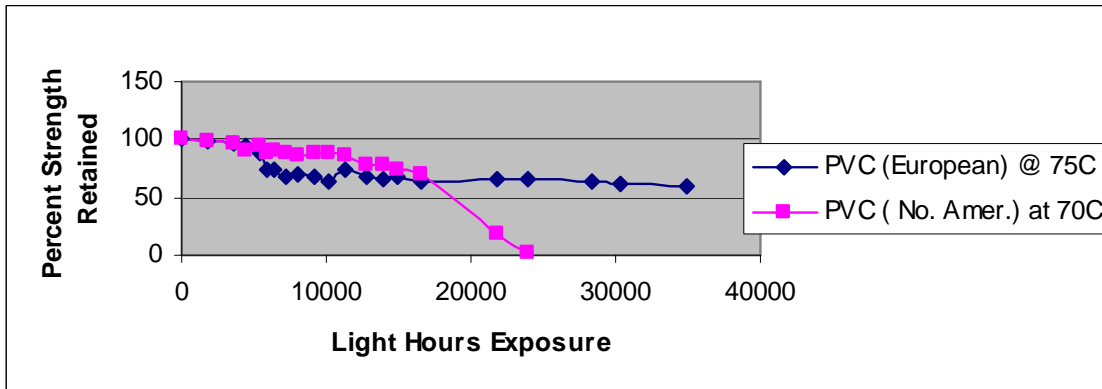


Figure 6d. Polyvinyl chloride (PVC) geomembranes.

From the response curves of the various geomembranes shown in Figure 6a-d, the 50% reduction value in strength or elongation (usually elongation) was taken as being the “half-life”. This value is customarily used by the polymer industry as being the materials lifetime prediction value. We have done likewise to develop Table 6 which is our predicted values for the designated exposed geomembrane lifetimes to date.

Table 6 – Exposed lifetime prediction results of selected geomembranes to date

Type	Specification	Prediction Lifetime in a Dry and Arid Climate
HDPE	GRI-GM13	> 36 years (ongoing)
LLDPE	GRI-GM17	≈ 36 years (half-life)
EPDM	GRI-GM21	> 27 years (ongoing)
fPP-2	GRI-GM18	≈ 30 years (half-life)
fPP-3	GRI-GM18	> 27 years (ongoing)
PVC-N.A.	(see FGI)	≈ 18 years (half-life)
PVC-Eur.	proprietary	> 32 years (ongoing)

4.0 Conclusions and Recommendations

This White Paper is bifurcated into two very different parts; covered (or buried) lifetime prediction of HDPE geomembranes and exposed (to the atmosphere) lifetime prediction of a number of geomembrane types. In the covered geomembrane study we chose the geomembrane type which has had the majority of usage, that being HDPE as typically used in waste containment applications. Invariably whether used in landfill liner or cover applications *the geomembrane is covered*. After ten-years of research Table 2 (repeated here) was developed which is the conclusion of the covered geomembrane research program. Here it is seen that HDPE decreases its predicted lifetime (as measured by its half-life) from 446-years at 20°C, to 69-years at 40°C. Other geomembrane types (LLDPE, fPP, EPDM and PVC) have had

essentially no focused effort on their covered lifetime prediction of the type described herein. That said, all are candidates for additional research in this regard.

Table 2 - Lifetime prediction of HDPE (nonexposed) at various field temperatures

In Service Temperature (°C)	Stage "A" (years)			Stage "B" (years)	Stage "C" (years)	Total Prediction* (years)
	Standard OIT	High Press. OIT	Average OIT			
20	200	215	208	30	208	446
25	135	144	140	25	100	265
30	95	98	97	20	49	166
35	65	67	66	15	25	106
40	45	47	46	10	13	69

*Total = Stage A (average) + Stage B + Stage C

Exposed geomembrane lifetime was addressed from the perspective of field performance which is very unequivocal. Experience in Europe, mainly with relatively thick PVC containing high molecular weight plasticizers, has given 25-years of service and the geomembranes are still in use. Experience in the USA with exposed geomembranes on flat roofs, mainly with EPDM and CSPE, has given 20⁺-years of service. The newest geomembrane type in such applications is fPP which currently carries similar warranties.

Rather than using the intricate laboratory setups of Figure 1 which are necessary for covered geomembranes, exposed geomembrane lifetime can be addressed by using accelerating laboratory weathering devices. Here it was shown that the UV fluorescent device (per ASTM D7238 settings) versus the Xenon Arc device (per ASTM D 4355) is equally if not slightly more intense in its degradation capabilities. As a result, all further incubation has been using the UV fluorescent devices per D7238 at 70°C.

Archived flexible polypropylene geomembranes at four field failure sites resulted in a correlation factor of 1200 light hours equaling one-year performance in a hot climate. Using this

value on the incubation behavior of seven commonly used geomembranes has resulted in the following conclusions (recall Figure 6 and Table 6);

- HDPE geomembranes (per GRI-GM13) are predicted to have lifetimes greater than 36-years; testing is ongoing.
- LLDPE geomembranes (per GRI-GM17) are predicted to have lifetimes of approximately 36-years.
- EPDM geomembranes (per GRI-GM21) are predicted to have lifetimes of greater than 27-years; testing is ongoing.
- fPP geomembranes (per GRI-GM18) are predicted to have lifetimes of approximately 30-years.
- PVC geomembranes are very dependent on their plasticizer types and amounts, and probably thicknesses as well. The North American formulation has a lifetime of approximately 18-years, while the European formulation is still ongoing after 32-years.

Regarding continued and future recommendations with respect to lifetime prediction, GSI is currently providing the following:

- (i) Continuing the exposed lifetime incubations of HDPE, EPDM and PVC (European) geomembranes at 70°C.
- (ii) Beginning the exposed lifetime incubations of HDPE, LLDPE, fPP, EPDM and both PVC's at 60°C and 80°C incubations.
- (iii) With data from these three incubation temperatures (60, 70 and 80°C), time-temperature-superposition plots followed by Arrhenius modeling will eventually provide information such as Table 2 for covered geomembranes. This is our ultimate goal.

- (iv) Parallel lifetime studies are ongoing at GSI for four types of geogrids and three types of turf reinforcement mats at 60, 70 and 80°C.
- (v) GSI does not plan to duplicate the covered geomembrane study to other than the HDPE provided herein. In this regard, the time and expense that would be necessary is prohibitive.
- (vi) The above said, GSI is always interested in field lifetime behavior of geomembranes (and other geosynthetics as well) whether covered or exposed.

Acknowledgements

The financial assistance of the U. S. Environmental Protection Agency for the covered HDPE lifetime study and the member organizations of the Geosynthetic Institute and its related institutes for research, information, education, accreditation and certification is sincerely appreciated. Their identification and contact member information is available on the Institute's web site at <<geosynthetic-institute.org>>.

References

- Cazzuffi, D., "Long-Term Performance of Exposed Geomembranes on Dams in the Italian Alps," Proc. 6th Intl. Conf. on Geosynthetics, IFAI, 1998, pp. 1107-1114.
- Chailan, J.-F., Boiteux, C., Chauchard, J., Pinel, B. and Seytre, G., "Effect of Thermal Degradation on the Viscoelastic and Dielectric Properties of Chlorosulfonated Polyethylene (CSPE) Compounds," Journal of Polymer Degradation and Stability, Vol. 48, 1995, pp. 61-65.
- Comer, A. I., Hsuan, Y. G. and Konrath, L., "The Performance of Flexible Polypropylene Geomembranes in Covered and Exposed Environments," 6th International Conference on Geosynthetics, Atlanta, Georgia, USA, March, 1998, pp. 359-364.
- Gedde, U. W., Viebke, J., Leijstrom, H. and Ifwarson, M., "Long-Term Properties of Hot-Water Polyolefin Pipes - A Review," Polymer Engineering and Science, Vol. 34, No. 24, 1994, pp. 1773-1787.
- Giroud, J.-P. and Tisinger, L. G., "The Influence of Plasticizers on the Performance of PVC Geomembranes," PVC GRI-17 Conference, IFAI, Roseville, MN, 1994, pp. 169-196.
- Hammon, M., Hsuan, G., Levin, S. B. and Mackey, R. E., "The Re-examination of a Nine-Year-Old PVC Geomembrane Used in a Top Cap Application," 31st Annual SWANA Conference, San Jose, CA, 1993, pp. 93-108.

- Hsuan, Y. G. and Guan, Z., "Evaluation of the Oxidation Behavior of Polyethylene Geomembranes Using Oxidative Induction Time Tests," ASTM STP 1326, Riga and Patterson, Eds., ASTM, 1997, pp. 138-149.
- Hsuan, Y. G. and Koerner, R. M., "Can Outdoor Degradation be Predicted by Laboratory Acceleration Weathering?," GFR, November, 1993, pp. 12-16.
- Hsuan, Y. G. and Koerner, R. M., "Antioxidant Depletion Lifetime in High Density Polyethylene Geomembranes," Jour. Geotech. and Geoenviron. Engr., ASCE, Vol. 124, No. 6, 1998, pp. 532-541.
- ICOLD (2010), "Geomembrane Sealing Systems for Dams: Design Principles and Return of Experience," Intl. Committee on Large Dams, Bulletin 135, Paris, France.
- Koerner, G. R. and Koerner, R. M., "In-Situ Temperature Monitoring of Geomembranes," Proc. GRI-18 Conf. at GeoFrontiers, Austin, TX, 2005, 6 pgs.
- Martin, J. R. and Gardner, R. J. (1983), "Use of Plastics in Corrosion Resistant Instrumentation," 1983 Plastics Seminar, NACE, October 24-27.
- Miller, L. V., Koerner, R. M., Dewyea, J. and Mackey, R. E., "Evaluation of a 30 mil PVC Liner and Leachate Collection System," Proc. 29th Annual GRCDA/SWANA Conf., Cincinnati, OH, 1991.
- Müeller, W. and Jakob, I., "Oxidative Resistance of High-Density Polyethylene Geomembranes," Jour. Polymer Degradation and Stability," Elsevier Publ. Co., No. 79, 2003, pp. 161-172.
- Rapoport, N. Y. and Zaikov, G. E., "Kinetics and Mechanisms of the Oxidation of Stressed Polymer," Developments in Polymer Stabilization—4, G. Scott, Ed., Applied Science Publishers Ltd., London, U.K., 1986, pp. 207-258.
- Sangam, H. P. and Rowe, R. K., "Effects of Exposure Conditions on the Depletion of Antioxidants from HDPE Geomembranes", Canadian Geotechnical Journal, Vol. 39, 2002, pp. 1221-1230.
- Scuero, A., "The Use of Geocomposites for the Rehabilitation of Concrete Dams," Proc. 4th Intl. Conf. on Geosynthetics, The Hague, Balkema Publ. Co., 1990, pg. 474.
- Scuero, A. M. and Vaschetti, G. L., "Geomembranes for Masonry and Concrete Dams: State-of-the-Art Report," Proc. Geosynthetics Applications, Design and Construction, M. B. deGroot, et al., Eds., A. A. Balkema, 1996, pp. 889-898.
- Suits, L. D. and Hsuan, Y. G., "Assessing the Photo Degradation of Geosynthetics by Outdoor Exposure and Laboratory Weatherometers," Proc. GRI-15 Conference, Hot Topics in Geosynthetics II, GII Publ., Folsom, PA, 2001, pp. 267-279.
- Wang, W. and Qu, B., "Photo and Thermo-Oxidative Degradation of Photocrosslinked Ethylene-Propylene-Diene Terpolymer," Journal of Polymer Degradation and Stability, Vol. 81, 2003, pp. 531-537.

Geosynthetic Institute
475 Kedron Avenue
Folsom, PA 19033-1208 USA
TEL (610) 522-8440
FAX (610) 522-8441



GSI White Paper #28

“Cold Temperature and Free-Thaw Cycling Behavior of Geomembranes and Their Seams”

by

Y. (Grace) Hsuan, Ph.D.
Professor of Civil, Architectural and
Environmental Engineering
Drexel University
215-895-2785
ghsuan@coe.drexel.edu

Robert M. Koerner, Ph.D., P.E., NAE
Director Emeritus – Geosynthetic Institute
Director Emeritus – Geosynthetic Institute
610-522-8440
robert.koerner@coe.drexel.edu

Alice I. Comer, P.E.
Project Manager
Formally With U. S. Bureau of Reclamation
Denver, Colorado

June 17, 2013

“Cold Temperature and Free-Thaw Cycling Behavior of Geomembranes and Their Seams”

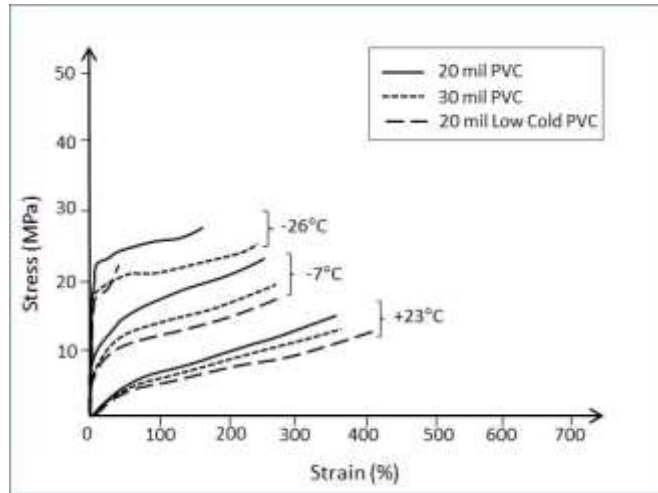
Introduction

It is common knowledge that materials in general, and polymeric materials in particular, will somewhat soften and increase in flexibility under high temperatures and will conversely somewhat harden and decrease in flexibility under cold temperatures. While there are indeed circumstances where high ambient temperatures are important, this white paper focuses entirely on cold ambient temperatures. Even further, it addresses cold temperature behavior of the various geomembranes by themselves and, most importantly, the freeze-thaw cycling behavior of a large number of geomembrane sheets and their seams.

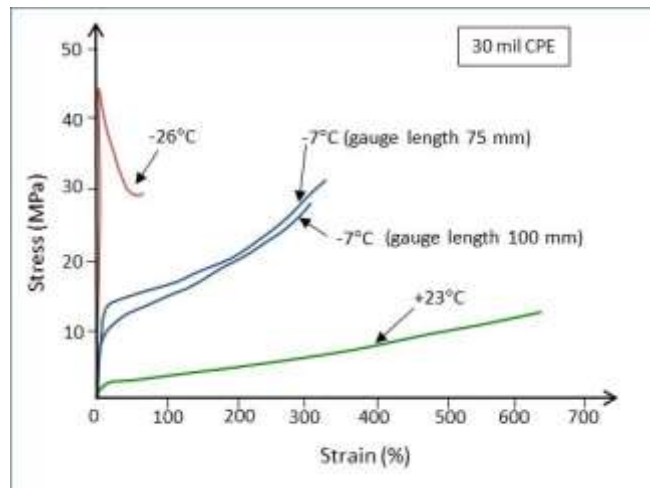
The stimulus for writing the white paper is the myriad questions that regularly come to GSI as to the potential negative effects on the tensile strength of geomembranes and their seams under cold temperature and cyclic freeze-thaw field conditions. As will be seen, the primary source for the information to be presented herein is a joint U.S. EPA/U.S. BuRec study conducted by Alice Comer and Grace Hsuan in 1996. Other companion technical information will also be presented.

Cold Temperature Behavior of Geomembranes

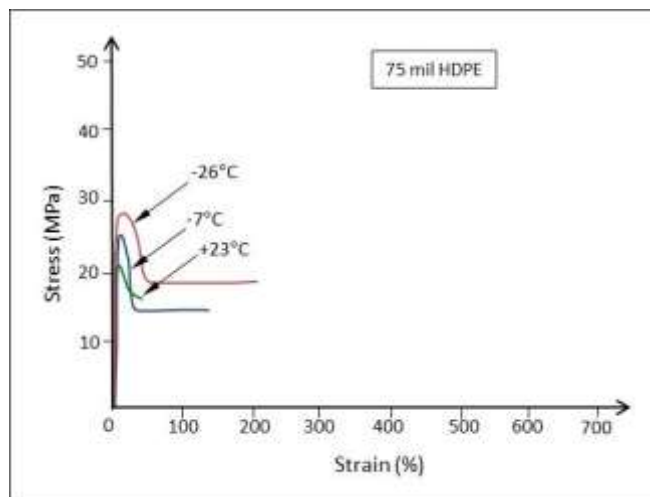
A report by Thornton and Blackall (1976) appears to be the first in describing Canadian experiences with geomembranes in cold regions. Subsequently, Rollin, et al. (1984) conducted a laboratory study on 21 types of geomembranes at temperatures down to -35°C . They found increasing tensile strength with decreasing temperature. Richards, et al. (1985) did similar studies which also resulted in an increase in strength and a decrease in elongation with decreasing temperatures. They evaluated PVC, CPE and HDPE geomembranes and presented the stress-versus-strain curves at $+23^{\circ}\text{C}$, -7°C and -26°C temperatures; see Figures 1a, 1b, and



(a) Tensile test results for PVC geomembranes



(b) Tensile test results for CPE geomembranes



(c) Tensile test results for HDPE geomembranes

Figure 1 – Stress-versus-strain behavior of three geomembrane types under progressively colder testing environments, Richards, et al. (1985)

1c. Here one can readily observe how the sets of curves transition from relatively ductile behavior at +23°C, to relatively brittle behavior at -26°C, with the intermediate behavior at -7°C. There are a few outliers, but the trends are undeniable. This general behavior was confirmed by Peggs, et al. (1990) and Giroud, et al. (1993), the latter working with both smooth and textured HDPE geomembranes.

While this type of thermal behavior is of interest, such information for a specific type of geomembrane must be obtained by performing or commissioning individual tests so as to obtain actual design information. Such individual testing is required due to the uniqueness of each polymer type and its specific formulation. Additives such as plasticizers, fillers, antioxidants, carbon black, colorants, etc., can influence the results to varying degrees. Even the resins themselves have behavioral differences at different temperatures. For example, the glass transition temperature of propylene is -7°C, below which the polymer is glassy and above which it is characterized as rubbery. In such a case the tensile properties are greatly influenced, as well as the material's creep and stress relaxation behavior.

There are other aspects of cold temperatures on geomembranes that go beyond the scope of this white paper. In particular are cases of impact shattering failures in cold climates and installation concerns such as frozen subgrade, bridging, snow and ice removal and worker discomfort, Burns, et al. (1990).

Freeze-Thaw Cycling of Geomembrane Sheets and Seams

Budiman (1994) reported on both cold temperature behavior but also appears to be the first to include freeze-thaw cycling for up to 150 repetitions. He focused entirely on HDPE sheet (of different thicknesses) but not on seams. There was no degradation observed during his tests but he suggested that more cycles would be appropriate. At approximately the same time a much

larger freeze-thaw study was ongoing. The final report by Comer and Hsuan was released by the U.S. Bureau of Reclamation in 1996. Related papers leading up to this final report are Hsuan, et al. (1993), Comer, et al. (1995), and Hsuan, et al. (1997). Their combined study involved 19 different geomembrane sheet materials and 31 different seam types. Furthermore, seven different resin types were evaluated. The resin types were the following:

- polyvinyl chloride (PVC)
- linear low density polyethylene (LLDPE)
- high density polyethylene (HDPE)
- flexible polypropylene (fPP)
- chlorosulfonated polyethylene (CSPE)
- fully crosslinked elastomeric alloy (FCEA)

All except FCEA are currently available, however, changes in additives and formulations have occurred and will likely to do so in the future. The entire study was conducted in four discrete parts although the fourth part was focused on induced tensile stress and stress relaxation and is not the specific purpose of this white paper. See Table 1 for the relevant three parts of their study.

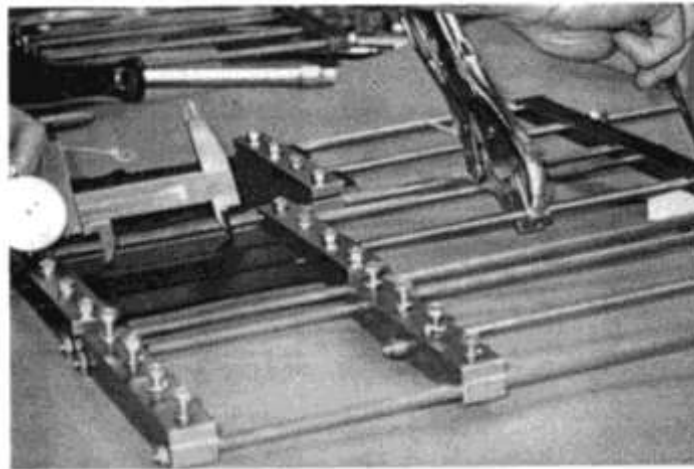
Table 1 – Experimental Design of Different Parts of Comer and Hsuan (1996) Study

Part	Cyclic Temperature Range	Maximum Cycles	Incubation Condition	Tensile Test Temperature
I	+20°C to -20°C	200	relaxed	+20°C
II	+20°C to -20°C	200	relaxed	-20°C
III	+30°C to -20°C	500	constrained	+20°C

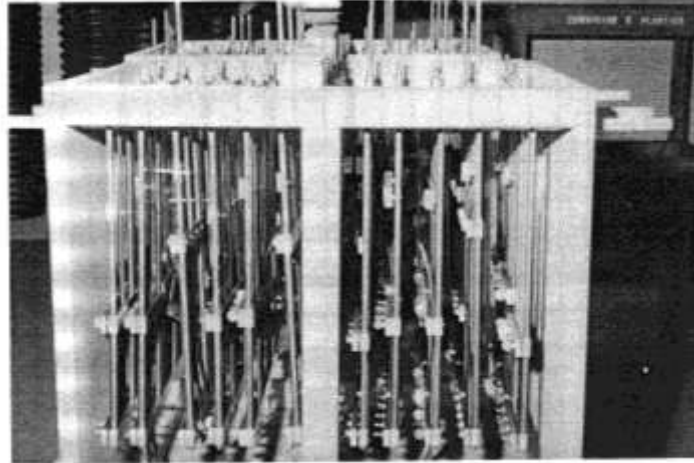
Part I consisted of 19 sheet materials and 27 seams. They underwent freeze-thaw cycles at +20°C for 8 hours and then -20°C for 16 hours. Tensile tests were then conducted at +20°C after 1, 5, 10, 20 50, 100 and 200 cycles.

Part II consisted of 6 sheet materials and 13 seams. They also underwent freeze-thaw cycling at $+20^{\circ}\text{C}$ for 8 hours and then -20°C for 16 hours. Different in this regard was that tensile tests were then conducted at -20°C after 1, 5, 10, 20, 50, 100 and 200 cycles. The -20°C tests were conducted in an environmental chamber (both specimens and their grips) cooled by liquid nitrogen and set at -20°C temperature.

Part III consisted of the same set of 19 sheet materials and 27 seams as in Part I but were now tensioned at a constant strain during the freeze-thaw cycling. The rack used for the tensioning is shown in Figure 2a and the assembly within the environmental chamber is shown in Figure 2b. After the targeted number of freeze-thaw cycles at $+20^{\circ}\text{C}$ for 8 hours and -20°C for 16 hours, specimens were removed and tested at $+20^{\circ}\text{C}$ after 1, 10, 50, 100, 200 and 500 cycles.



(a) Method of applying tensile load to test specimens in Part III tests



(b) Geomembrane racks in holding frame used in Part III series

Figure 2 – Method used for tensioning samples during incubation; Comer and Hsuan (1996)

Rather than showing the graphic results of the above freeze-thaw cycling study (it is available in full in the Comer and Hsuan report by the Bureau of Reclamation and the related papers by these authors) only the concluding comments will be reproduced here. They follow verbatim from the report.

Part I – Results on 200 Freeze-Thaw Cycles Tested at +20°C

- Tensile tests on geomembrane sheets: “The results show no change in either the peak strength or peak elongation of any of the tested materials”.
- Shear tests on the geomembrane seams: “The results show no change in shear strength of any of the tested seam materials”.
- Peel tests on the geomembrane seams: “The results show no change in peel strength of any of the tested seam materials.”

Part II – Results on 200 Freeze-Thaw Cycles Tested at -20°C

- Tensile tests on geomembrane sheets: “The results show no change in either the peak strength or peak elongation of any of the tested materials”.
- Shear tests on the geomembrane seams: “The results show no change in shear strength of any of the tested seam materials”.
- Peel tests on the geomembrane seams: “The results show no change in peel strength of any of the tested seam materials.”

Part III – Results on 500 Freeze-Thaw Cycles Tested at +20°C in a Constrained Condition

- Tensile tests on geomembrane sheets: “The results show no change in either the peak strength or peak elongation of any of the tested materials”.
- Shear tests on the geomembrane seams: “The results show no change in shear strength of any of the tested seam materials”.
- Peel tests on the geomembrane seams: “The results show no change in peel strength of any of the tested seam materials.”

Conclusion and Recommendations

This two-part white paper focused initially on the cold temperature tensile behavior of the stress- versus-strain curves of several different types of geomembranes. As expected, the colder the temperature the more brittle, hence less ductile, were the response curves. Geomembranes made from PVC, CPE and HDPE were illustrated in this regard. The recommendation reached for this part of the white paper is that if a formulation-specific geomembrane under site-specific conditions is to be evaluated for its stress-versus-strain response, actual tests must be commissioned accordingly. The literature can only give general trends in this regard.

The second (and more important) part of this white paper focused entirely on freeze-thaw behavior of geomembranes and their different seam types. The U.S. Bureau of Reclamation report is extremely revealing in this regard. *The conclusion that the authors reached is that there is simply “no change” in tensile behavior of geomembrane sheets or their seams after freeze-thaw cycling.* It is felt that this conclusion in the context of their study is so impressive that it has essentially “closed the door” to further research on this specific topic. The essential question often raised in this regard, i.e., “will freeze-thaw conditions affect geomembrane sheets or their seam behavior,” is answered with a resounding “NO”.

References

- Budiman, J. (1994), “Effects of Temperature on Physical Behavior of Geomembranes,” Proc. 5th Intl. Conf. on Geosynthetics, Singapore, SEAC-IGS Publication, pp. 1093-1100.
- Burns, D. E. and Pierce, S. V. (1990), “Technical Note on Cold Weather Installation of HDPE,” Jour. Geotextiles and Geomembranes, Vol. 9, Nos. 4-6, pp. 457-459.
- Comer, A. I. and Hsuan, Y. G. (1996), “Freeze-Thaw Cycling and Cold Temperature Effects on Geomembrane Sheets and Seams,” U. S. Bureau of Reclamation Report R-96-03, March, 136 pgs.
- Comer, A. I., Sculli, M. L. and Hsuan, Y. G. (1995), “Effects of Freeze-Thaw Cycling on Geomembrane Sheets and Their Seams,” Proc. of Geosynthetics '95, Nashville, TN, pp. 853-866.
- Giroud, J. P., Soderman, K. L. and Monroe, M. (1993), “Mechanical Design of Geomembrane Applications,” Proc. of Geosynthetics '93, Vancouver, Canada, pp. 1455-1468.
- Hsuan, Y. G., Sculli, M. L. and Comer, A. I. (1997), “Effects of Freeze-Thaw Cycling on Geomembranes Sheets and Their Seams – Part II Cold Temperature Tensile Behavior and

Thermal Induced Cyclic Stress,” Geosynthetics '97 Conference Proceedings, Long Beach, CA, published by IFAI, pp. 201-216.

Hsuan, Y. G., Sculli, M. L. and Koerner, R. M. (1993), “Effects of Freeze-Thaw Cycling on Geomembranes and Their Seams,” Proc. GRI-7 Conference on Geosynthetic Liner Systems: Innovations, Concerns and Designs, IFAI, Rosewell, IN, pp. 209-224.

Koerner, R. M. (2012), Designing With Geosynthetics, 6th Edition, Xlibris Publ. Co., 914 pgs.

Lord, Jr., A.E., Soong, T. Y. and Koerner, R. M. (1995), “Relaxation Behavior of Thermally-Induced Stress in HDPE Geomembranes,” Geosynthetics International, Vol. 2, No. 3, pp. 626-634.

Peggs, I. D., Carlson, D. S. and Peggs, S. J. (1990), “Understanding and Preventing ‘Shattering’ Failures of Polyethylene Geomembranes,” Geotextiles, Geomembranes and Related Products, Rotterdam, Balkema.

Richards, E. A., Scott, J. D. and Chalaturnyk (1985), “Cold Temperature Properties of Geomembranes,” Proc. 2nd Conf. on Geotextiles and Geomembranes, Canadian Geotechnical Society, Edmonton, Alberta, pp. 121-132.

Rollin, A. L., Lafleur, J., Marcotte, M., Dascal, O. and Akber, Z. (1984), “Selection Criteria for the Use of Geomembranes in Dams and Dykes in Northern Climate,” Proc. of the Intl. Conf. on Geomembranes, Denver, CO, pp. 493-499.

Thornton, D. E. and Blackall, P. (1976), “Field Evaluation of Plastic Film Liners for Petroleum Storage Areas in the Mackenzie Delta,” Canadian Environmental Protection Service, Economic and Technical Review Report EPA-3-76-13.

CHEMICAL COMPATIBILITY OF POLY-FLEX LINERS

Chemical compatibility or resistance as applied to geomembranes is a relative term. Actually compatibility would mean that one material will dissolve in the other such as alcohol in water or grease in gasoline. An example of incompatibility would be oil and water. In liners it is undesirable to have the chemicals dissolve in the liner hence the term compatibility is the reverse of what is normally meant in the chemical industry. In the strictest sense and from a laboratory prospective, chemical compatibility, as the term applies to this industry, would imply that the chemical has no effect on the liner. On the other hand, from an engineering prospective, chemical compatibility means that a liner will survive the exposure to a given chemical even though the chemical could have some effect on the performance of the liner, but not enough to cause failure. Therefore, one must understand and define chemical compatibility for a specific project.

Generally polyethylene will be effected by chemicals in one of three ways.

1. No effect—This means that the chemical in question and the polyethylene do not interact. The polyethylene does not gain (lose) weight, swell, and the physical properties are not significantly altered.
2. Oxidizes (cross linking)—Chemicals classed as oxidizing agents will cause the polyethylene molecules to cross link and cause irreversible changes to the physical properties of the liner. Basically it makes the liner brittle.
3. Plasticizes—Chemicals in this classification are soluble in the polyethylene structure. They do not change the structure of the polyethylene itself but will act as a plasticizer. In doing so, the liner will experience weight gain of 3-15%, may swell by up to 10%, and will have measurable changes in physical properties (i.e. the tensile strength at yield may decrease by up to 20%). Even under these conditions the liner will maintain its integrity and will not be breached by liquids, provided the liner has not been subjected to any stress. These effects are reversible once the chemicals are removed and the liner has time to dry out.

Aside from the effect that chemicals have on a liner is the issue of vapor permeation through the liner. Vapor permeation is molecular diffusion of chemicals through the liner. Vapor transmission for a given chemical is dependent primarily on liner type, contact time, chemical solubility, temperature, thickness, and concentration gradient, but not on hydraulic head or pressure. Transmission through the liner can occur in as little as 1-2 days. Normally, a small amount of chemical is transmitted. Generally HDPE has the lowest permeation rate of the liners that are commercially available.

As stated above chemical compatibility is a relative term. For example, the use of HDPE as a primary containment of chlorinated hydrocarbons at a concentration of 100% may not be recommended, but it may be acceptable at 0.1% concentration for a limited time period or may be acceptable for secondary containment. Factors that go into assessment of chemical compatibility are type of chemical(s), concentration, temperature and the type of application. No hard and fast rules are available to make decisions on chemical compatibility. Even the EPA 9090 test is just a method to generate data so that an opinion on chemical compatibility can be more reliably reached.

A simplified table on chemical resistance is provided to act as a screening process for chemical containment applications.

CHEMICAL RESISTANCE INFORMATION

CHEMICAL CLASS	CHEMICAL EFFECT	PRIMARY CONTAINMENT (LONG TERM CONTACT)		SECONDARY CONTAINMENT (SHORT TERM CONTACT)	
		HDPE	LLDPE	HDPE	LLDPE
CARBOXYLIC ACID	1				
- Unsubstituted (e.g. Acetic acid)		B	C	A	C
- Substituted (e.g. Lactic acid)		A	B	A	A
- Aromatic (e.g. Benzoic acid)		A	B	A	A
ALDEHYDES	3				
- Aliphatic (e.g. Acetaldehyde)		B	C	B	C
- Hetrocyclic (e.g. Furfural)		C	C	B	C
AMINE	3				
- Primary (e.g. Ethylamine)		B	C	B	C
- Secondary (e.g. Diethylamine)		C	C	B	C
- Aromatic (e.g. Aniline)		B	C	B	C
CYANIDES (e.g. Sodium Cyanide)	1	A	A	A	A
ESTER (e.g. Ethyl acetate)	3	B	C	B	C
ETHER (e.g. Ethyl ether)		C	C	B	C
HYDROCARBONS	3				
- Aliphatic (e.g. Hexane)		C	C	B	C
- Aromatic (e.g. Benzene)		C	C	B	C
- Mixed (e.g. Crude oil)		C	C	B	C
HALOGENATED HYDROCARBONS	3				
- Aliphatic (e.g. Dichloroethane) +A4		C	C	B	C
- Aromatic (e.g. Chlorobenzene)		C	C	B	C
ALCOHOLS	1				
- Aliphatic (e.g. Ethyl alcohol)		A	A	A	A
- Aromatic (e.g. Phenol)		A	C	A	B
INORGANIC ACID					
- Non-Oxidizers (e.g. Hydrochloric acid)	1	A	A	A	A
- Oxidizers (e.g. Nitric Acid)	2	C	C	B	C
INORGANIC BASES (e.g. Sodium hydroxide)	1	A	A	A	A
SALTS (e.g. Calcium chloride)	1	A	A	A	A
METALS (e.g. Cadmium)	1	A	A	A	A
KETONES (e.g. Methyl ethyl ketone)	3	C	C	B	C
OXIDIZERS (e.g. Hydrogen Peroxide)	2	C	C	C	C

Chemical effect (see discussion on Chemical Resistance)

1. No Effect--Most chemicals of this class have no or minor effect.
2. Oxidizer--Chemicals of this class will cause irreversible degradaton.

3. Plasticizer--Chemicals of this class will cause a reversible change in physical properties.

Chart Rating

- A. Most chemicals of this class have little or no effect on the liner.
Recommended regardless of concentration or temperature (below 150° F).
- B. Chemicals of this class will effect the liner to various degrees.
Recommendations are based on the specific chemical, concentration and temperature.
Consult with Poly-Flex, Inc.
- C. Chemicals of this class at high concentrations will have significant effect on the physical properties of the liner.
Generally not recommended but may be acceptable at low concentrations and with special design considerations.
Consult with Poly-Flex, Inc.

This data is provided for informational purposes only and is not intended as a warranty or guarantee. Poly-Flex, Inc. assumes no responsibility in connection with the use of this data. Consult with Poly-Flex, Inc. for specific chemical resistance information and liner selection.

Poly-Flex, Inc. • 2000 W. Marshall Dr. • Grand Prairie, TX 75051 U.S.A. • 888-765-9359
© Poly-Flex, Inc. • All Rights Reserved

CHEMICAL COMPATIBILITY OF POLY-FLEX LINERS

Chemical compatibility or resistance, as applied to geomembranes, is a relative term. Actual compatibility would mean that one material dissolves in the other such as alcohol in water or grease in gasoline. An example of incompatibility would be oil and water. In liners it is undesirable to have the chemicals dissolve in the liner, hence the term compatibility is the reverse of what is normally meant in the chemical industry. In the strictest sense and from a laboratory perspective, chemical compatibility, as the term applies to this industry, would imply that the chemical has no effect on the liner. On the other hand, from an engineering perspective, chemical compatibility means that a liner survives the exposure to a given chemical even though the chemical could have some effect on the performance of the liner, but not enough to cause failure. Therefore, one must understand and define chemical compatibility for a specific project.

Generally polyethylene is effected by chemicals in one of three ways.

1. No effect—This means that the chemical in question and the polyethylene do not interact. The polyethylene does not gain (lose) weight or swell, and the physical properties are not significantly altered.
2. Oxidizes (cross linking)—Chemicals classed as oxidizing agents cause the polyethylene molecules to cross link and cause irreversible changes to the physical properties of the liner. Basically they make the liner brittle.
3. Plasticizes—Chemicals in this classification are soluble in the polyethylene structure. They do not change the structure of the polyethylene itself but act as a plasticizer. In doing so, the liner experiences weight gain of 3-15%, may swell by up to 10%, and has measurable changes in physical properties (e.g. the tensile strength at yield may decrease by up to 20%). Even under these conditions the liner maintains its integrity and is not breached by liquids, provided the liner has not been subjected to any stress. These effects are reversible once the chemicals are removed and the liner has time to dry out.

Aside from the effect that chemicals have on a liner is the issue of vapor permeation through the liner. Vapor permeation is molecular diffusion of chemicals through the liner. Vapor transmission for a given chemical is dependent primarily on liner type, contact time, chemical solubility, temperature, thickness, and concentration gradient, but not on hydraulic head or pressure. Transmission through the liner can occur in as little as 1-2 days. Normally, a small amount of chemical is transmitted. Generally HDPE has the lowest permeation rate of the liners that are commercially available.

As stated above chemical compatibility is a relative term. For example, the use of HDPE as a primary containment of chlorinated hydrocarbons at a concentration of 100% may not be recommended, but it may be acceptable at 0.1% concentration for a limited time period or may be acceptable for secondary containment. Factors that go into assessment of chemical compatibility are type of chemical(s), concentration, temperature and the type of application. No hard and fast rules are available to make decisions on chemical compatibility. Even the EPA 9090 test is just a method to generate data so that an opinion on chemical compatibility can be more reliably reached.

A simplified table on chemical resistance is provided to act as a screening process for chemical containment applications.

CHEMICAL RESISTANCE INFORMATION



CHEMICAL CLASS	CHEMICAL EFFECT	PRIMARY CONTAINMENT (LONG TERM CONTACT)		SECONDARY CONTAINMENT (SHORT TERM CONTACT)	
		HDPE	LLDPE	HDPE	LLDPE
CARBOXYLIC ACID - Unsubstituted (e.g. Acetic acid) - Substituted (e.g. Lactic acid) - Aromatic (e.g. Benzoic Acid)	1	B A A	C B B	A A A	C A A
ALDEHYDES - Aliphatic (e.g. Acetaldehyde) - Hetrocyclic (e.g. Furfural)	3	B C	C C	B B	C C
AMINE - Primary (e.g. Ethylamine) - Secondary (e.g. Diethylamine) - Aromatic (e.g. Aniline)	3	B C B	C C C	B B B	C C C
CYANIDES (e.g. Sodium Cyanide)	1	A	A	A	A
ESTER (e.g. Ethyl acetate)	3	B	C	B	C
ETHER (e.g. Ethyl ether)		C	C	B	C
HYDROCARBONS - Aliphatic (e.g. Hexane) - Aromatic (e.g. Benzene) - Mixed (e.g. Crude oil)	3	C C C	C C C	B B B	C C C
HALOGENATED HYDROCARBONS - Aliphatic (e.g. Dichloroethane) +A4 - Aromatic (e.g. Chlorobenzene)	3	C C	C C	B B	C C
ALCOHOLS - Aliphatic (e.g. Ethyl alcohol) - Aromatic (e.g. Phenol)	1	A A	A C	A A	A B
INORGANIC ACID - Non-oxidizers (e.g. Hydrochloric acid) - Oxidizers (e.g. Nitric Acid)	1 2	A C	A C	A B	A C
INORGANIC BASES (e.g. Sodium hydroxide)	1	A	A	A	A
SALTS (e.g. Calcium chloride)	1	A	A	A	A
METALS (e.g. Cadmium)	1	A	A	A	A
KETONES (e.g. Methyl ethyl ketone)	3	C	C	B	C
OXIDIZERS (e.g. Hydrogen peroxide)	2	C	C	C	C

Chemical Effect (see discussion on Chemical Resistance)

1. No Effect—Most chemicals of this class have no or minor effect.
2. Oxidizer—Chemicals of this class will cause irreversible degradation.
3. Plasticizer—Chemicals of this class will cause a reversible change in physical properties.

Chart Rating

- A. Most chemicals of this class have little or no effect on the liner.
Recommended regardless of concentration or temperature (below 150° F).
- B. Chemicals of this class will affect the liner to various degrees.
Recommendations are based on the specific chemical, concentration and temperature.
Consult with Poly-Flex, Inc.
- C. Chemicals of this class at high concentrations will have significant effect on the physical properties of the liner.
Generally not recommended but may be acceptable at low concentrations and with special design considerations.
Consult with Poly-Flex, Inc.

The data in this table is provided for informational purposes only and is not intended as a warranty or guarantee. Poly-Flex, Inc. assumes no responsibility in connection with the use of this data. Consult with Poly-Flex, Inc. for specific chemical resistance information and liner selection.

Chemicals Resistance Table

Low Density and High Density Polyethylene

INTRODUCTION

The table in this document summarises the data given in a number of chemical resistance tables at present in use in various countries, derived from both practical experience and test results.

Source: ISO/TR 7472, 7474; Carlowitz: "Kunststofftabellen-3. Auflage".

The table contains an evaluation of the chemical resistance of a number of fluids judged to be either aggressive or not towards low and high density polyethylene. This evaluation is based on values obtained by immersion of low and high density polyethylene test specimens in the fluid concerned at 20 and 60°C and atmospheric pressure, followed in certain cases by the determination of tensile characteristics.

A subsequent classification will be established with respect to a restricted number of fluids deemed to be technically or commercially more important, using equipment which permits testing under pressure and the determination of the coefficient of chemical resistance for each fluid. These tests will thus furnish more complete indications on the use of low and high density polyethylene products for the transport of stated fluids, including their use under pressure.

SCOPE AND FIELD APPLICATION

This document establishes a provisional classification of the chemical resistance of low and high density polyethylene with respect to about 300 fluids. It is intended to provide general guidelines on the possible utilisation of low and high density polyethylene:

- at temperatures up to 20 and 60°C
- in the absence of internal pressure and external mechanical stress (for example flexural stresses, stresses due to thrust, rolling loads etc).

DEFINITIONS, SYMBOLS AND ABBREVIATIONS

The criteria of classification, definitions, symbols and abbreviations adopted in this document are as follows:

S = Satisfactory

The chemical resistance of low or high density polyethylene exposed to the action of a fluid is classified as "satisfactory" when the results of test are acknowledged to be satisfactory by the majority of the countries participating in the evaluation.

L = Limited

The chemical resistance of low or high density polyethylene exposed to the action of a fluid is classified as "limited" when the results of tests are acknowledged to be "limited" by the majority of the countries participating in the evaluation.

Also classified as "limited" are the resistance to the action of chemical fluids for which judgements "S" and "NS" or "L" are pronounced to an equal extent.

NS = Not satisfactory

The chemical resistance of low or high density polyethylene exposed to the action of a fluid is classified as "not satisfactory" when the results of tests are acknowledged to be "not satisfactory" by the majority of the countries participating in the evaluation.

Also classified as "not satisfactory" are materials for which judgements "L" and "NS" are pronounced to an equal extent.

Sat.sol Saturated aqueous solution, prepared at 20°C

Sol Aqueous solution at a concentration higher than 10 %, but not saturated

Dil.sol Dilute aqueous solution at a concentration equal to or lower than 10 %

Work.sol Aqueous solution having the usual concentration for industrial use

Solution concentrations reported in the text are expressed as a percentage by mass. The aqueous solutions of sparingly soluble chemicals are considered, as far as chemical action towards low or high density polyethylene is concerned, as saturated solutions.

In general, common chemical names are used in this document.

The table is made as a first guideline for user of polyethylene. If a chemical compound is not to be found or if there is an uncertainty on the chemical resistance in an application, please contact Borealis for advise and proposal on testing.

**Chemical resistance of low density and high density polyethylene,
not subjected to mechanical stress, to various fluids at 20 and 60°C**

Chemical or product	Concentration	LD °C		HD °C	
		20	60	20	60
Acetaldehyde	100 %	L	NS	S	L
Acetanilide	—			S	S
Acetic acid	10 %	S	S	S	S
Acetic acid	60 %	S	L	S	S
Acetic acid, glacial	Greater than 96 %	L	NS	S	L
Acetic anhydride	100 %	L	NS	S	L
Acetone	100 %	L	NS	L	L
Acrylnitrile	—	S	S	S	S
Acetylsilicacid	—	S	S	S	S
Adipic acid	Sat.sol	S	S	S	S
After shave	—	NS	NS	NS	NS
Aliphatic hydrocarbons	—	L	NS	L	L
Allyl acetate	—	S	L	S	L
Allyl alcohol	100 %	L	NS	—	—
Allyl alcohol	96 %	—	—	S	S
Allyl chloride	—	L	NS	L	NS
Aluminium chloride	Sat.sol	S	S	S	S
Aluminium fluoride	Sat.sol	S	S	S	S
Aluminium hydroxide	Sat.sol	S	S	S	S
Aluminium nitrate	Sat.sol	S	S	S	S
Aluminium oxychloride	Sat.sol	S	S	S	S
Al/potassium sulphate	Sat.sol	S	S	S	S
Aluminium sulphate	Sat.sol	S	S	S	S
Alums	Sol	S	S	S	S
Aminobenzoic acid	—	S	S	S	S
Ammonia, dry gas	100 %	S	S	S	S
Ammonia, liquid	100 %	L	L	S	S
Ammonia, aqueous	Dil.sol	S	S	S	S
Ammonium acetate	—	S	S	S	S
Ammonium carbonate	Sat.sol	S	S	S	S
Ammonium chloride	Sat.sol	S	S	S	S
Ammonium fluoride	Sol	S	—	S	S
Ammonium hexafluorosilicate	Sat.sol	S	S	S	S
Ammonium hydrogen carbonate	Sat.sol	S	S	S	S
Ammonium hydroxide	10 %	S	S	S	S
Ammonium hydroxide	30 %	S	S	S	S

Chemical or product	Concentration	LD °C		HD °C	
		20	60	20	60
Ammonium metaphosphate	Sat.sol	S	S	S	S
Ammonium nitrate	Sat.sol	S	S	S	S
Ammonium oxalate	Sat.sol	S	S	S	S
Ammonium phosphate	Sat.sol	S	S	S	S
Ammonium persulphate	Sat.sol	S	S	S	S
Ammonium sulphate	Sat.sol	S	S	S	S
Ammonium sulphide	Sol	S	S	S	S
Ammonium thiocyanate	Sat.sol	S	S	S	S
Amyl acetate	100 %	NS	NS	L	L
Amyl alcohol	100 %	L	L	S	L
Amyl chloride	100 %	NS	NS	-	-
Amyl phthalate	-	L	L	S	L
Aniline	100 %	NS	NS	S	L
Anilinchlorohydrate	-	L	-	-	-
Antimony (III) chloride	90 %	-	-	S	S
Antimony (III) chloride	Sat.sol	S	S	S	S
Antimony trichloride	Sol	S	S	S	S
Apple juice	Sol	-	-	S	L
Aqua regia	HCl/HNO ₃ = 3/1	NS	NS	NS	NS
Aromatic hydrocarbons	-	NS	NS	NS	NS
Arsenic acid	Sat.sol	S	S	S	S
Asorbic acid	10 %	S	S	S	S
Barium bromide	Sat.sol	S	S	S	S
Barium carbonate	Sat.sol	S	S	S	S
Barium chloride	Sat.sol	S	S	S	S
Barium hydroxide	Sat.sol	S	S	S	S
Barium sulphate	Sat.sol	S	S	S	S
Barium sulphide	Sat.sol	S	S	S	S
Beer	-	S	S	S	S
Benzaldehyde	100 %	L	NS	S	L
Benzene	100 %	NS	NS	L	L
Benzoic acid	Sat.sol	S	S	S	S
Benzoylchloride	-	S	L	S	L
Benzyl alcohol	-	S	L	S	S
Benzylsulphonic acid	10 %	S	S	S	S
Bismuth carbonate	Sat.sol	S	S	S	S
Bitumen	-	S	L	S	S
Bleach lye	10 %	S	S	S	S

Chemical or product	Concentration	LD °C		HD °C	
		20	60	20	60
Borax	Sat.sol	S	S	S	S
Boric acid	Sat.sol	S	S	S	S
Boron trifluoride	-	L	NS	L	NS
Brake fluid	-	L	NS	L	NS
Brine	-	S	S	S	S
Bromine, dry gas	100 %	NS	NS	NS	NS
Bromine, liquid	100 %	NS	NS	NS	NS
Bromoform	100 %	NS	NS	NS	NS
Butandiol	10 %	S	S	S	S
Butandiol	60 %	S	S	S	S
Butandiol	100 %	S	S	S	S
Butane, gas	100 %	-	-	S	S
Butanol	100 %	S	L	S	S
Butter	-	S	S	S	S
Butyl acetate	100 %	S	L	S	L
Butyl alcohol	100 %	S	S	S	S
Butyl chloride	-	S	-	S	-
Butylene glycol	10 %	S	S	S	S
Butylene glycol	60 %	S	S	S	S
Butylene glycol	100 %	S	S	S	S
Butyraldehyde	-	-	-	S	L
Butyric acid	100 %	L	L	S	L
Calcium arsenate	-	S	S	S	S
Calcium benzoate	-	S	S	S	S
Calcium bisulphide	-	S	S	S	S
Calcium bromate	10 %	S	S	S	S
Calcium bromide	Sat.sol	S	S	S	S
Calcium carbonate	Sat.sol	S	S	S	S
Calcium chlorate	Sat.sol	S	S	S	S
Calcium chloride	Sat.sol	S	S	S	S
Calcium chromate	40 %	S	S	S	S
Calcium cyanide	-	S	S	S	S
Calcium hydrosulphide	Sol	S	S	S	S
Calcium hydroxide	Sat.sol	S	S	S	S
Calcium hypochlorite	Sol	S	S	S	S
Calcium nitrate	Sat.sol	S	S	S	S
Calcium oxide	Sat.sol	S	S	S	S
Calcium perchlorate	1 %	S	-	S	S

Chemical or product	Concentration	LD °C		HD °C	
		20	60	20	60
Calcium permanganate	20 %	S	S	S	S
Calcium persulphate	Sol	S	S	S	S
Calcium sulphate	Sat.sol	S	S	S	S
Calcium sulphide	Dil.sol	-	-	L	L
Camphor oil	-	NS	NS	L	L
Carbon dioxide, dry gas	100 %	-	-	S	S
Carbon dioxide, wet	-	S	S	S	S
Carbon disulphide	100 %	NS	NS	L	NS
Carbon monoxide	100 %	S	S	S	S
Carbon tetrachloride	100 %	NS	NS	L	NS
Carbonic acid		S	S	S	S
Castor oil	Sol	S	S	S	S
Chlorine, water	2 % Sat.sol	L	L	S	S
Chlorine, aqueous	Sat.sol	NS	NS	L	NS
Chlorine, dry gas	100 %	NS	NS	L	NS
Chloroacetic acid	Sol	-	-	S	S
Chlorobenzene	100 %	NS	NS	NS	NS
Chloroethanol	100 %	S	S	S	S
Chloroform	100 %	NS	NS	NS	NS
Chloromethane, gas	100 %	L	-	L	-
Chlorosulphonic acid	100 %	NS	NS	NS	NS
Chloropropene	-	NS	-	L	-
Chrome alum	Sol	S	S	S	S
Chromic acid	Sat.sol	S	S	-	-
Chromic acid	20 %	-	-	S	L
Chromic acid	50 %	-	-	S	L
Chromium VI oxide	Sat.sol	S	S	S	S
Cider	-	S	S	S	S
Citric acid	Sat.sol	S	S	S	S
Citric acid	10 %	S	S	S	S
Citric acid	25 %	S	S	S	S
Coconut oil alcoholic	-	S	S	S	S
Coffee	-	S	S	S	S
Copper (II) chloride	Sat.sol	S	S	S	S
Copper cyanide	Sat.sol	S	S	S	S
Copper (II) fluoride	Sat.sol	S	S	S	S
Copper (II) fluoride	2 %	S	S	S	S
Copper (II) nitrate	Sat.sol	S	S	S	S
Copper (II) sulphate	Sat.sol	S	S	S	S

Chemical or product	Concentration	LD °C		HD °C	
		20	60	20	60
Corn oil	–	S	S	S	S
Cottonseed oil	–	S	S	S	S
Cresylic acid	Sat.sol	–	–	L	–
Crotonaldehyde	Sat.sol	L	–	–	–
Cyclanone	–	S	S	S	S
Cyclohexane	–	NS	NS	NS	NS
Cyclohexanol	Sat.sol	L	NS	–	–
Cyclohexanol	100 %	–	–	S	S
Cyclohexanone	100 %	NS	NS	S	L
Decahydronaphthalene	100 %	L	NS	S	L
Decane	–	NS	NS	L	NS
Decalin	100 %	–	–	S	L
Detergents, synthetic	–	S	S	S	S
Developers (photographic)	Work.conc	–	–	S	S
Dextrin	Sol	S	S	S	S
Dextrose	Sol	S	S	S	S
Diacetone alcohol	–	L	L	L	L
Diazo salts	–	S	S	S	S
Dibutyl amine	–	NS	NS	L	NS
Dibutyl ether	–	NS	NS	L	–
Dibutylphthalate	–	L	L	S	L
Dichlorobenzene	–	NS	NS	NS	NS
Dichloroethylene	–	NS	NS	NS	NS
Dichloropropylene	–	NS	NS	NS	NS
Diesel oil	–	S	NS	S	L
Diethyl ether	100 %	NS	NS	L	–
Diethyl ketone	–	L	NS	L	L
Diethylene glycol	–	S	S	S	S
Diglycolic acid	–	S	S	S	S
Diisobutylketone	100 %	S	L	S	L
Dimethyl amine	100 %	NS	NS	–	–
Dimethyl formamid	–	S	L	S	S
Diethyl phthalate	100 %	L	NS	S	L
Dioxan	100 %	–	–	S	S
Dipentene	–	NS	NS	NS	NS
Disodium phosphate	–	S	S	S	S
Drano, plumbing cleaner	–	S	S	S	S

Chemical or product	Concentration	LD °C		HD °C	
		20	60	20	60
Emulsions, photographic	—	S	S	S	S
Ethandiol	100 %	S	S	S	S
Ethanol	40 %	S	L	S	L
Ethanol	96 %	L	L	—	—
Ethyl acetate	100 %	L	NS	S	NS
Ethyl acrylate	100 %	NS	NS	L	NS
Ethyl alcohol	35 %	S	S	S	S
Ethyl alcohol	100 %	S	S	S	S
Ethyl benzene	—	NS	NS	NS	NS
Ethyl chloride	100 %	NS	NS	NS	NS
Ethylene chloride	100 %	NS	NS	NS	NS
Ethylene diamine	100 %	S	L	S	S
Ethyl ether	—	NS	NS	NS	NS
Ethylene glycol	100 %	S	S	S	S
Ethyl mercaptan	—	NS	NS	NS	NS
Ferric chloride	Sat.sol	S	S	S	S
Ferric nitrate	Sat.sol	S	S	S	S
Ferric sulphate	Sat.sol	S	S	S	S
Ferrous chloride	Sat.sol	S	S	S	S
Ferrous sulphate	Sat.sol	S	S	S	S
Fish solubles	Sol	S	S	S	S
Fluoboric acid	—	S	S	S	S
Fluorine gas	100 %	L	NS	NS	NS
Fluorine gas, dry	100 %	NS	NS	NS	NS
Fluorine gas, wet	100 %	NS	NS	NS	NS
Fluorosilic acid	Conc	S	L	S	L
Fluorosilic acid	40 %	S	S	S	S
Formaldehyde	40 %	S	S	S	S
Formic acid	40 %	S	S	S	S
Formic acid	98 to 100 %	S	S	S	S
Fructose	Sat.sol	S	S	S	S
Fruit pulps	Sol	S	S	S	S
Furfural	100 %	NS	NS	NS	NS
Furfuryl alcohol	100 %	L	NS	S	L
Gallic acid	Sat.sol	S	S	S	S
Gasoline, petrol	—	L	NS	L	L
Gelatine	—	S	S	S	S

Chemical or product	Concentration	LD °C		HD °C	
		20	60	20	60
Glucose	Sat.sol	S	S	S	S
Glycerine	100 %	S	S	S	S
Glycerol	100 %	S	S	S	S
Glycolic acid	30 %	S	L	-	-
Glycolic acid	Sol	-	-	S	S
n-Heptane	100 %	NS	NS	L	NS
Hexachlorobenzene	-	S	S	S	L
Hexachlorophene	-	NS	NS	L	L
Hexamethylenetriamine	40 %	S	-	S	-
Hexane	-	S	L	S	L
Hexanol, tertiary	-	S	S	S	S
Hydrobromic acid	50 %	S	S	S	S
Hydrobromic acid	Up to 100 %	S	S	S	S
Hydrochloric acid	Up to 36 %	S	S	S	S
Hydrochloric acid	Conc	S	S	S	S
Hydrochlorous acid	Conc	S	S	S	S
Hydrocyanic acid	10 %	S	S	S	S
Hydrocyanic acid	Sat.sol	S	S	S	S
Hydrofluoric acid	40 %	S	S	S	S
Hydrofluoric acid	60 %	S	L	S	L
Hydrogen	100 %	S	S	S	S
Hydrogen chloride	Dry gas	S	S	S	S
Hydrogen peroxide	30 %	S	L	S	S
Hydrogen peroxide	90 %	S	NS	S	NS
Hydrogen sulphide gas	100 %	S	S	S	S
Hydroquinone	Sat.sol	S	S	-	-
Hydroxylamine	up to 12 %	S	S	S	S
Inks	-	S	S	S	S
Iodine (in potassium sol)	-	L	NS	NS	NS
Iodine (in alcohol)	-	NS	NS	NS	NS
Iron (II) chloride	Sat.sol	S	S	S	S
Iron (II) sulphate	Sat.sol	S	S	S	S
Iron (III) chloride	Sat.sol	S	S	S	S
Iron (III) nitrate	Sol	S	S	S	S
Iron (III) sulphate	Sat.sol	S	S	S	S
Iso octane	100 %	S	NS	S	L
Iso pentane	-	NS	NS	NS	NS

Chemical or product	Concentration	LD °C		HD °C	
		20	60	20	60
Isopropanol	–	S	S	S	S
Isopropyl amine	–	NS	NS	NS	NS
Isopropyl ether	100 %	L	NS	S	NS
Kerosene	–	NS	NS	NS	NS
Lactic acid	10 %	S	S	S	S
Lactic acid	28 %	S	S	S	S
Lactic acid	up to 100 %	S	S	S	S
Latex	–	S	S	S	S
Lead acetate	Dil.sol	S	S	S	S
Lead acetate	Sat.sol	S	S	S	S
Lead arsenate	–	S	S	S	S
Lubricating oil	–	S	S	S	S
Lysol	–	NS	NS	L	NS
Magnesium carbonate	Sat.sol	S	S	S	S
Magnesium chloride	Sat.sol	S	S	S	S
Magnesium hydroxide	Sat.sol	S	S	S	S
Magnesium nitrate	Sat.sol	S	S	S	S
Magnesium sulphate	Sat.sol	S	S	S	S
Maleic acid	Sat.sol	S	S	S	S
Mercury	–	S	S	S	S
Mercury (I) nitrate	Sol	S	S	S	S
Mercury (II) chloride	Sat.sol	S	S	S	S
Mercury (II) cyanide	Sat.sol	S	S	S	S
Mercury	100 %	S	S	S	S
Methanol	100 %	S	L	S	S
Methyl alcohol	100 %	S	L	S	S
Methyl benzoic acid	Sat.sol	NS	NS	L	–
Methyl bromide	100 %	NS	NS	NS	NS
Methyl chloride	100 %	NS	NS	NS	NS
Methylcyclohexane	–	L	NS	L	NS
Methyl ethyl ketone	100 %	–	–	S	L
Methylene chloride	–	NS	NS	NS	NS
Methoxybutanol	100 %	S	L	S	L
Milk	–	S	S	S	S
Milk of Magnesia	–	S	L	S	L
Mineral oils	–	L	NS	S	L

Chemical or product	Concentration	LD °C		HD °C	
		20	60	20	60
Molasses	Work.conc	S	S	S	S
Motor oil	-	S	L	S	S
Naphtha	-	L	NS	L	NS
Naphtahalene	-	NS	NS	L	-
Nickel chloride	Sat.sol	S	S	S	S
Nickel nitrate	Sat.sol	S	S	S	S
Nickel sulphate	Sat.sol	S	S	S	-
Nicotine	Dil.sol	S	S	S	S
Nicotinic acid	Dil.sol	L	L	S	-
Nitric acid	25 %	S	S	S	S
Nitric acid	50 %	S	L	S	L
Nitric acid	70 %	S	L	S	L
Nitric acid	95 %	NS	NS	NS	NS
Nitric acid	100 %	NS	NS	NS	NS
Nitrobenzene	100 %	NS	NS	NS	NS
Nitroethane	100 %	S	NS	S	NS
Nitromethane	100 %	S	-	S	-
Nitrotoluene	-	NS	NS	NS	NS
n-Octane	-	S	S	S	S
Octyl alcohol	-	S	NS	S	NS
Oil and fats	-	L	NS	S	L
Oleic acid	100 %	L	NS	S	S
Oleum (H ₂ SO ₄ + 10 % SO ₃)	-	NS	NS	NS	NS
Oleum (H ₂ SO ₄ + 50 % SO ₃)	-	NS	NS	NS	NS
Olive oil	-	S	NS	S	NS
Orthophosphoric acid	50 %	S	S	S	S
Orthophosphoric acid	95 %	S	L	S	L
Oxalic acid	Sat.sol	S	S	S	S
Oxygen	100 %	S	-	S	L
Ozone	100 %	NS	NS	L	NS
Paraffin oil	-	S	L	S	S
n-Pentane	-	NS	NS	NS	NS
Pentane-2	-	NS	NS	NS	NS
Perchloric acid	20 %	S	S	S	S
Perchloric acid	50 %	S	L	S	L
Perchloric acid	70 %	S	NS	S	NS

Chemical or product	Concentration	LD °C		HD °C	
		20	60	20	60
Perchloroethylene	—	NS	NS	NS	NS
Phenol	Sol	L	NS	S	S
Phosphine	100 %	S	S	S	S
Phosphoric acid	up to 25 %	S	S	S	S
Phosphoric acid	25 to 50 %	S	S	S	S
Phosphoric (III) chloride	100 %	S	L	S	L
Phosphorous (II) chloride	100 %	—	—	S	L
Phosphorous pentoxide	100 %	S	S	S	S
Phosphorous trichloride	100 %	S	L	S	L
Photographic solutions	—	S	S	S	S
Phtalic acid	50 %	S	S	S	S
Picric acid	Sat.sol	S	L	S	—
Plating solutions	—	S	S	S	S
Potassium acetate	—	S	S	S	S
Potassium aluminium sulphate	Sat.sol	S	S	S	S
Potassium benzoate	—	S	S	S	S
Potassium bicarbonate	Sat.sol	S	S	S	S
Potassium borate	Sat.sol	S	S	S	S
Potassium bromate	Sat.sol	S	S	S	S
Potassium bromide	Sat.sol	S	S	S	S
Potassium carbonate	Sat.sol	S	S	S	S
Potassium chlorate	Sat.sol	S	S	S	S
Potassium chloride	Sat.sol	S	S	S	S
Potassium chromate	Sat.sol	S	S	S	S
Potassium cyanide	Sol	S	S	S	S
Potassium dichromate	Sat.sol	S	S	S	S
Potassium fluoride	Sat.sol	S	S	S	S
Potassium hexacyanoferrate (III)	Sat.sol	S	S	S	S
Potassium hexacyanoferrate (II)	Sat.sol	S	S	S	S
Potassium hexafluorosilicate	Sat.sol	S	S	S	S
Potassium hydrogen carbonate	Sat.sol	S	S	S	S
Potassium hydrogen sulphate	Sat.sol	S	S	S	S
Potassium hydrogen sulphide	Sol	—	—	S	S
Potassium hydroxide	10 %	S	S	S	S
Potassium hydroxide	Sol	S	S	S	S
Potassium hypochlorite	Sol	S	L	S	L
Potassium iodate	10 %	S	S	S	S
Potassium iodide	Sat.sol	S	S	S	S
Potassium nitrate	Sat.sol	S	S	S	S

Chemical or product	Concentration	LD °C		HD °C	
		20	60	20	60
Potassium orthophosphate	Sat.sol	S	S	S	S
Potassium oxalate	Sat.sol	S	S	S	S
Potassium perchlorate	Sat.sol	S	S	S	S
Potassium permanganate	20 %	S	S	S	S
Potassium persulphate	Sat.sol	S	S	S	S
Potassium phosphate	Sat.sol	S	S	S	S
Potassium sulphate	Sat.sol	S	S	S	S
Potassium sulphide	Sol	S	S	S	S
Potassium sulphite	Sat.sol	S	S	-	-
Potassium thiocyanate	Sat.sol	S	S	S	S
Potassium thiosulphate	Sat.sol	S	S	S	S
Propargul alcohol	-	S	S	S	S
n-Propyl alcohol	-	S	S	S	S
Propionic acid	50 %	-	-	S	S
Propionic acid	100 %	-	-	S	L
Propylene dichloride	100 %	NS	NS	NS	NS
Propylene glycol	-	S	S	S	S
Pyridine	100 %	-	-	S	L
Quinol (hydroquinone)	Sat.sol	S	S	S	S
Resorcinol	Sat.sol	S	S	S	S
Salicylic acid	Sat.sol	S	S	S	S
Sea water	-	S	S	S	S
Selenic acid	-	S	S	S	S
Silicon oil	-	S	S	S	S
Silver acetate	Sat.sol	S	S	S	S
Silver cyanide	Sat.sol	S	S	S	S
Silver nitrate	Sat.sol	S	S	-	-
Soap solution	100 %	S	S	S	S
Sodium acetate	Sat.sol	S	S	-	-
Sodium antimonate	Sat.sol	S	S	S	S
Sodium arsenite	Sat.sol	S	S	S	S
Sodium benzoate	Sat.sol	S	S	S	S
Sodium bicarbonate	Sat.sol	S	S	S	S
Sodium bisulphate	Sat.sol	S	S	S	S
Sodium bisulphite	Sat.sol	S	S	S	S
Sodium borate	-	S	S	S	S
Sodium bromide	Sat.sol	S	S	S	S
Sodium carbonate	Sat.sol	S	S	S	S

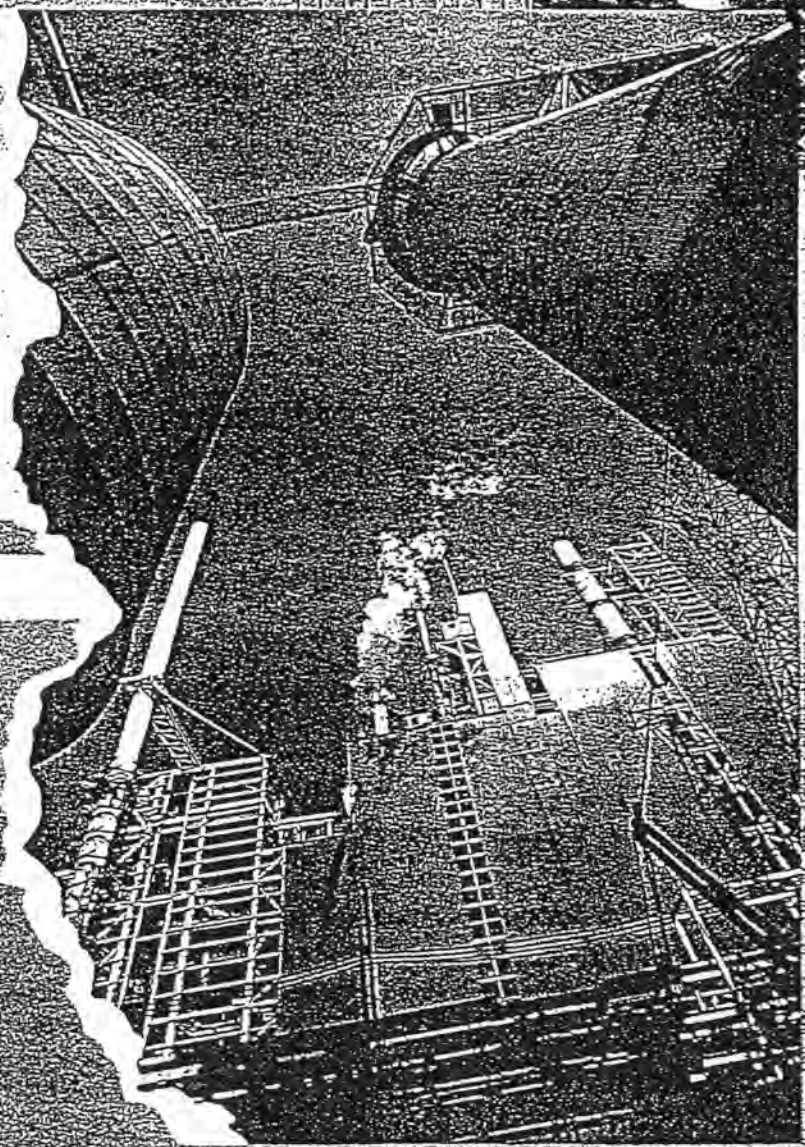
Chemical or product	Concentration	LD °C		HD °C	
		20	60	20	60
Sodium chlorate	Sat.sol	S	S	S	S
Sodium chloride	Sat.sol	S	S	S	S
Sodium chlorite	Sat.sol	L	-	-	-
Sodium cyanide	Sat.sol	S	S	S	S
Sodium dichromate	Sat.sol	S	S	S	S
Sodium fluoride	Sat.sol	S	S	S	S
Sodium hexacyanoferrate (III)	Sat.sol	-	-	S	S
Sodium hexacyanoferrate (II)	Sat.sol	-	-	S	S
Sodium hexafluorosilicate	Sat.sol	S	S	S	S
Sodium hydrogen carbonate	Sat.sol	S	S	S	S
Sodium hydrogen sulphate	Sat.sol	S	S	S	S
Sodium hydrogen sulphite	Sol	S	S	S	S
Sodium hydroxide	40 %	S	S	S	S
Sodium hydroxide	Sol	-	-	S	S
Sodium hypochloride	-	L	NS	S	S
Sodium hypochlorite	15 %	-	-	S	S
	available Cl	-	-	S	S
Sodium iodate	10 %	S	S	S	S
Sodium iodide	Sat.sol	S	S	S	S
Sodium nitrate	Sat.sol	S	S	S	S
Sodium nitrite	Sat.sol	S	S	S	S
Sodium orthophosphate	Sat.sol	S	S	S	S
Sodium oxalate	Sat.sol	S	S	S	S
Sodium phosphate	Sat.sol	S	S	S	S
Sodium silicate	Sol	S	S	S	S
Sodium sulphate	Sat.sol	S	S	S	S
Sodium sulphide	Sat.sol	S	S	S	S
Sodium sulphite	Sat.sol	S	S	S	S
Sodium thiocyanate	Sat.sol	S	S	S	S
Stannic chloride	Sat.sol	S	S	S	S
Stannous chloride	Sat.sol	S	S	S	S
Starch solution	Sat.sol	S	S	S	S
Stearic acid	Sat.sol	S	L	S	-
Styrene	Sol	L	NS	L	NS
Sulphur dioxide, dry	100 %	S	S	S	S
Sulphur trioxide	100 %	NS	NS	NS	NS
Sulphur acid	10 to 50 %	S	S	S	S
Sulphuric acid	10 %	S	S	S	S
Sulphuric acid	50 %	S	S	S	S

Chemical or product	Concentration	LD °C		HD °C	
		20	60	20	60
Sulphuric acid	70 %	S	L	S	L
Sulphuric acid	80 %	S	NS	S	NS
Sulphuric acid	98 %	L	NS	S	NS
Sulphuric acid	Fuming	NS	NS	NS	NS
Sulphurous acid	30 %	S	S	S	S
Sulphurous acid	Sol	S	S	S	S
Tallow	-	S	L	S	L
Tannic acid	Sol	S	S	S	S
Tartaric acid	Sat.sol	S	S	S	S
Tartaric acid	Sol	-	-	S	S
Tetrachloroethylene	100 %	NS	NS	NS	NS
Tetrachloromethane	100 %	NS	NS	L	NS
Tetradecane	-	NS	NS	NS	NS
Tetrahydrofuran	-	NS	NS	NS	NS
Tetrahydronaphthalene	100 %	L	NS	S	L
Thionyl chloride	100 %	NS	NS	NS	NS
Tin (II) chloride	Sat.sol	S	S	S	S
Tin (IV) chloride	Sol	S	S	S	S
Tin (IV) chloride	Sat.sol	-	-	S	S
Titanium tetrachloride	Sat.sol	NS	NS	NS	NS
Toluene	100 %	NS	NS	L	NS
Tribromomethane	-	NS	NS	NS	NS
Trichloroacetaldehyde	-	S	-	S	-
Trichlorobenzene	-	NS	NS	-	-
Trichloroethylene	100 %	NS	NS	NS	NS
Triethanolamine	100 %	S	-	S	-
Triethanolamine	Sol	-	-	S	L
Triethylene glycol	-	S	S	S	S
Trisodium phosphate	Sat.sol	S	S	-	-
Turpentine	-	NS	NS	NS	NS
Urea	up to 30 %	S	S	S	S
Urea	Sol	S	S	S	S
Urine	-	S	S	S	S
Vanilla extract	-	S	S	S	S
Vaseline	-	S	L	S	S
Vegetables oils	-	S	L	S	S
Vinegar	-	S	S	S	S
Water	-	S	S	S	S
Wetting agents	-	S	S	S	S
Wines and spirits	-	S	S	S	S
Chemical or product	Concentration	LD °C		HD °C	
		20	60	20	60

Xylene	100 %	NS	NS	L	NS
Yeast	Sol	S	S	S	S
Zinc bromide	Sat.sol	S	S	S	S
Zinc carbonate	Sat.sol	-	-	S	S
Zinc chloride	Sat.sol	S	S	S	S
Zinc oxide	Sat.sol	S	S	S	S
Zinc stearate	-	S	S	S	S
Zinc sulphate	Sat.sol	S	S	S	S
o-Zylene		NS	NS	NS	NS
p-Zylene	-	NS	NS	NS	NS

CONTAINMENT SOLUTIONS FOR INDUSTRIAL WASTE

Dike raising
Sludge caps
Sludge ponds
Secondary
containment
Landfill linings
Landfill caps
Floating covers



NOC

HIGH DENSITY POLYETHYLENE (HDPE) GEOMEMBRANE

Over the past five years, the geomembrane industry has experienced numerous changes. Factors such as the increased concern for the environment; new products in the marketplace; and the push for tighter governmental control over the environment have all played a significant role in revolutionizing the geosynthetic industry.

Today, the most widely used geomembrane in the waste management industry is High Density Polyethylene (HDPE). HDPE offers superior performance by maintaining the highest standards of durability.

FEATURES AND BENEFITS

National Seal Company's HDPE geomembrane is manufactured on a computer controlled, flat sheet extruder using virgin, first quality, high molecular weight polyethylene. This process guarantees a material thickness of $\pm 5\%$ from target, the most stringent quality control available in the industry. NSC also guarantees the minimum average thickness of our liner will be greater than or equal to the nominal thickness. HDPE is available in 40 (1.0mm), 50 (1.25mm), 60 (1.5mm), 80 (2.0mm), and 100 (2.5mm) mil thicknesses.

★ Chemical Resistance - Often the chemical resistance of the liner is the most critical aspect of the design process. HDPE is the most chemically resistant of all geomembranes. Typical landfill leachates pose no threat to a liner made of HDPE.

Low Permeability - The low permeability of HDPE provides assurance that groundwater will not penetrate the liner; rainwater will not infiltrate a cap; and methane gas will not migrate away from the gas venting system.

Ultraviolet Resistance - HDPE has excellent resistance to ultraviolet degradation. NSC adds carbon black which provides UV protection. Plasticizers are never used in NSC's geomembranes so there is never a concern about volatilization of the plasticizer which can be caused by UV exposure.

APPLICATIONS:

Landfill (primary and secondary containment)	Retention ponds for mining applications
Landfill caps	Wastewater treatment facilities
Lagoon liners	Potable water reservoirs
Pond liners	Tank linings
Floating covers	Canal linings
Secondary containment for above ground storage tanks	Heap leach pads

HDPE GEOMEMBRANE PHYSICAL PROPERTIES

60 mil

The properties on this page are not part of NSC's Manufacturing Quality Control program and are not included on the material certifications. Seam testing is the responsibility of the installer and/or CQA personnel.

PROPERTIES	METHOD	UNITS	MINIMUM ¹	TYPICAL
Multi-Axial Tensile Elongation	GRI, GM-4	percent	20.0	28.0
Critical Cone Height	GRI, GM-3, NSC mod.	cm	1.0	1.5
Wide Width Tensile	ASTM D 4885			
Stress at Yield		psi	2000	2110
Strain at Yield		%	15.0	20.0
Brittleness Temp. by Impact ²	ASTM D 746	°C	-75	<-90
Coef. of Linear Thermal Exp. ²	ASTM D 696	°C ⁻¹	1.5 x 10 ⁻⁴	1.2 x 10 ⁻⁴
ESCR, Bent Strip	ASTM D 1693	hours	1500	>10,000
Hydrostatic Resistance	ASTM D 751	psi	450	510
Modulus of Elasticity	ASTM D 638	psi	80,000	135,000
Ozone Resistance	ASTM D 1149, 168 hrs	P/F	P	P
Permeability ²	ASTM E 96	cm/sec · Pa	2.3x10 ⁻¹⁴	8.1 x 10 ⁻¹⁵
Puncture Resistance	FTMS 101, method 2065	ppi	1300	1700
		lbs	78	105
Soil Burial Resistance ²	ASTM D 3083, NSF mod.	% change	10	0
Tensile Impact	ASTM D 1822	ft lbs/in ²	250	420
Volatile Loss ²	ASTM D 1203, A	percent	0.10	0.06
Water Absorption ²	ASTM D 570, 23°C	percent	0.10	0.04
Water Vapor Transmission ²	ASTM E 96	g/day · m ²	0.024	0.009

SEAM PROPERTIES	METHOD	UNITS	MINIMUM ¹	TYPICAL
Shear Strength	ASTM D 4437, NSF mod.	psi	2000	2700
		ppi	120	166
Peel Strength (hot wedge fusion)	ASTM D 4437, NSF mod.	psi	1500	1870
		ppi	90	115
Peel Strength (fillet extrusion)	ASTM D 4437, NSF mod.	psi	1300	1590
		ppi	78	98

STANDARD ROLL DIMENSIONS

Length	1110 feet	Area	16,650 ft ²
Width	15 feet	Weight	5,000 lbs

This information contained herein has been compiled by National Seal Company and is, to the best of our knowledge, true and accurate. All suggestions and recommendations are offered without guarantee. Final determination of suitability for use based on any information provided, is the sole responsibility of the user. There is no implied or expressed warranty of merchantability or fitness of the product for the contemplated use.

NSC reserves the right to update the information contained herein in accordance with technological advances in the material properties.

6H-0893

NSC

NATIONAL SEAL COMPANY

245 Corporate Blvd. • Suite 300

Aurora, IL 60504

(708) 898-1161 • (800) 323-3820

Fax: (708) 898-3461



HDPE GEOMEMBRANE QUALITY CONTROL SPECIFICATIONS

60 mil

National Seal Company's High Density Polyethylene (HDPE) Geomembranes are produced from virgin, first quality, high molecular weight resins and are manufactured specifically for containment in hydraulic structures. NSC HDPE geomembranes have been formulated to be chemically resistant, free of leachable additives and resistant to ultraviolet degradation.

The following properties are tested as a part of NSC's quality control program. Certified test results for properties on this page are available upon request. Refer to NSC's Quality Control Manual for exact test methods and frequencies.

All properties meet or exceed NSF Standard Number 54.

RESIN PROPERTIES	METHOD	UNITS	MINIMUM ¹	TYPICAL
Melt Flow Index ²	ASTM D 1238	g/10 min	0.50	0.25
Oxidative Induction Time	ASTM D 3895, Al pan, 200°C, 1 atm O ₂	minutes	100	120

SHEET PROPERTIES	METHOD	UNITS	MINIMUM ¹	TYPICAL
Thickness	ASTM D 751, NSF mod.			
Average		mils	60.0	61.5
Individual		mils	57.0	59.7
Density	ASTM D 1505	g/cm ³	0.940	0.948
Carbon Black Content	ASTM D 1603	percent	2.0-3.0	2.35
Carbon Black Dispersion	ASTM D 3015, NSF mod.	rating	A1, A2, B1	A1
Tensile Properties	ASTM D 638			
Stress at Yield		psi	2200	2550
		ppi	132	157
Stress at Break		psi	3800	4850
		ppi	228	298
Strain at Yield	1.3" gage length (NSF)	percent	13.0	16.9
Strain at Break	2.0" gage or extensometer	percent	700	890
	2.5" gage length (NSF)	percent	560	710
Dimensional Stability ²	ASTM D 1204, NSF mod.	percent	1.5	0.4
Tear Resistance	ASTM D 1004	ppi	750	860
		lbs	45	53
Puncture Resistance	ASTM D 4833	ppi	1800	2130
		lbs	108	131
Constant Load ESCR, Single Point	GRI, GM-5a	hours	200	>400

¹ This value represents the minimum acceptable test value for a roll as tested according to NSC's Manufacturing Quality Control Manual. Individual test specimen values are not addressed in this specification except thickness.

² Indicates Maximum Value



NATIONAL SEAL COMPANY
1245 Corporate Blvd. • Suite 300
Aurora, IL 60504
(708) 898-1161 • (800) 323-3820
Fax: (708) 898-3461

How long will my liner last?

| What is the remaining service life of my HDPE geomembrane?

By Ian D. Peggs, P.E., P.Eng., Ph.D.

Introduction

In his keynote lecture at the GeoAmericas-2008 conference last March, Dr. Robert Koerner (et al., 2008) of the Geosynthetic Institute (GSI) reported the ongoing Geosynthetic Research Institute (GRI) work to make the first real stab at assessing the service lives of high-density polyethylene (HDPE), linear low-density polyethylene (LLDPE), reinforced PE, ethylene propylene diene terpolymer (EPDM), and flexible polypropylene (fPP) exposed geomembranes.

The selected environment simulated that of Texas, USA, in sunny ambient temperatures between ~7°C (45°F) and 35°C (95°F). Of course, an exposed black HDPE geomembrane in the sun will achieve much higher temperatures, probably in excess of 80°C (176°F).

I do not know what the temperature would be at 150-300mm above the liner (for those still specifying this parameter), but it is quite immaterial. The only temperature of concern is the actual geomembrane temperature.

The lifetimes are shown in **Table 1**, but it must be recognized that these data are for specific manufactured products with specific formulations. The “greater than” notation indicates that laboratory exposures (incubations) are still on-going, not

that some samples have failed after the indicated time period. The PE-R-1 material is a thin LLDPE, so it might be expected to be the first to reach the defined end of life; the half-life—the time to loss of 50% of uniaxial tensile properties.

It is interesting to note that HDPE-1 and LLDPE-1 are proceeding apace, but it would be expected that the LLDPE-1 would reach its half-life earlier than HDPE-1. However, this does not automatically follow. With adequate additive formulations, perhaps LLDPE could be left exposed and demonstrate more weathering resistance than some HDPEs. This demonstrates the fact that all PEs, whether HD or LLD, are not identical—they can have different long-term performances dependent on the PE resin used and the formulation of the stabilizer package. However, such differences are not evident in the conventional mechanical properties such as tensile strength/elongation, puncture and tear resistances, and so on.

The two fPPs are performing well. However, there had also been an fPP-1, one of the first PP geomembranes that did not perform well. This was due to a totally inappropriate stabilizer formulation. That particular product lasted 1.5 years in service. In

Final Inspection continued on page 44

Type	Specification	Predicted Lifetime in Texas, USA
HDPE-1	GRI-GM13	>28 years (Incubation ongoing)
LLDPEE-1	GRI-GM17	>28 years (Incubation ongoing)
EPDM-1	GRI-GM21	>20 years (Incubation ongoing)
PE-R-1	GRI-GM22	≈17 years (reached halflife)
fPP-2	GRI-GM18 (temp. susp.)	>27 years (Incubation ongoing)
fPP-3	GRI-GM18 (temp. susp.)	>17 years (Incubation ongoing)

Table 1 | Estimated exposed geomembrane lifetimes

| Ian Peggs is president of I-CORP International Inc. and is a member of *Geosynthetics* magazine's Editorial Advisory Committee.

Final Inspection continued from page 56

the QUV weatherometer, it lasted 1,800 light hours at 70°C (158°F). Therefore, the lab/field correlation is that 1,000 QUV light hours is equivalent to a 0.83yr service life under those specific environmental conditions.

At another location in Texas, Korrner/GRI found 1,000hr of QUV exposure was equivalent to 1.1 year actual field exposure. Consequently, for Texas exposures GRI is using a correlation of 1000hr QUV exposure as equivalent to 1yr of in-service exposure. Clearly, the correlation would be different in less sunny and colder environments.

The failed fPP-1 liner was replaced with a correctly stabilized fPP that, subsequently, performed well.

So how can we evaluate the condition of our exposed liners in a simple and practical manner to ensure they will continue to provide adequate service lifetimes and to get sufficient warning of impending expiration?

For each installation, a baseline needs to be established, and changes from that baseline need to be monitored.

A liner lifetime evaluation program

Rather than be taken by surprise when a liner fails or simply expires, it should be possible to monitor the condition of the liner to obtain a few years of notice for impending expiration. One can then plan for a timely replacement without the potential for accidental environmen-

values that generally significantly exceed the specification.

A final option for the baseline would be to use the values at the time of the first liner assessment.

The first liner condition assessment would consist of a site visit during which a general visual examination would be done together with a mechanical probing of the edges of welds. A visual examination would include the black/gray shades of different panels that might indicate low carbon contents.

A closer examination should be done using a loupe (small magnifier) on suspect areas such as wrinkle peaks, the tops and edges of multiple extrusion weld beads, and the apex-down creases of round die-manufactured sheet.

The last detail is significant because the combination of oxidizing surface and exposed surface tension when the liner contracts at low temperatures and the crease is pulled flat can be one of the first locations to crack. The apex-up creases do not fail at the same time because the oxidized exposed surface is under compression (or less tension) when the crease is flattened out.

Appropriate samples for detailed laboratory testing will be removed.

It may be appropriate to do a water lance electrical integrity survey on the exposed sideslopes, but this would only be effective on single liners, and on double liners with a composite primary liner, a conductive geomembrane, or a geocomposite with a conductive geotextile on top.

A sampling and testing regime

A liner lifetime evaluation program should be simple, meaningful, and cost-effective.

While it will initially require expert polymer materials science/engineering input to analyze the test data and to define the critical parameters, it should ultimately be possible to use an expert system to automatically make predictions using the input test data.

Small samples will be taken from deep in the anchor trench and from appropriate

... it should be possible to monitor the condition of the liner to obtain a few years of notice for impending expiration.

While estimated correlations might be made for other locations using historical weather station sunshine and temperature data, there is no question that the best remaining lifetime assessments will be obtained using samples removed from the field installation of interest.

A lifetime in excess of 28yr, demonstrated for a recently-made HDPE geomembrane, is comparable to the present actual service periods of as long as 30-35yr. However, actual lifetimes of as low as ~15yr have also been experienced.

Do service lifetimes now exceeding 30yr mean that we might expect to see another round of stress cracking failures as exposed liners finally oxidize sufficiently on the surface to initiate stress cracking?

This would be frustrating after resolving the early 1980s problems with stress cracking failures at welds and stone protrusions when the liners contracted at low temperatures, but it is the way end-of-life will become apparent. And will that be soon or in another 5-20 years? It would be useful to know.

tal damage and undesirable publicity. A program of periodic liner-condition assessment is proposed.

For baseline data, it would be useful to have some archive material to test, but that is not usually available. Manufacturers often discard retained samples after about 5 years. Perhaps facility owners should be encouraged to keep retained samples at room temperature and out of sunlight. The next best thing is to use material from the anchor trench or elsewhere that has not experienced extremes in temperature and that has not been exposed to UV radiation or to expansion/contraction stresses.

Less satisfactory options are to use the original NSF 54 specifications, the manufacturer's specifications, or the GRI-GM13 specifications at the appropriate time of liner manufacturing. The concern with using these specifications is that while aged material may meet them, there is no indication of whether the measured values have significantly decreased from the actual as-manufactured

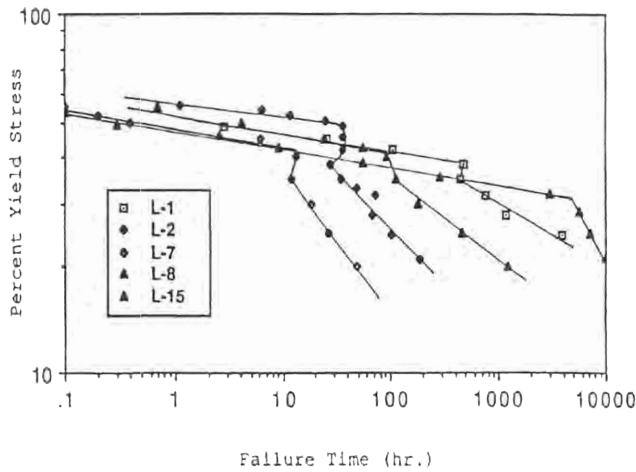


Figure 1 | Standard stress rupture curves for five HDPE geomembranes (Hsuan, et al. 1992)

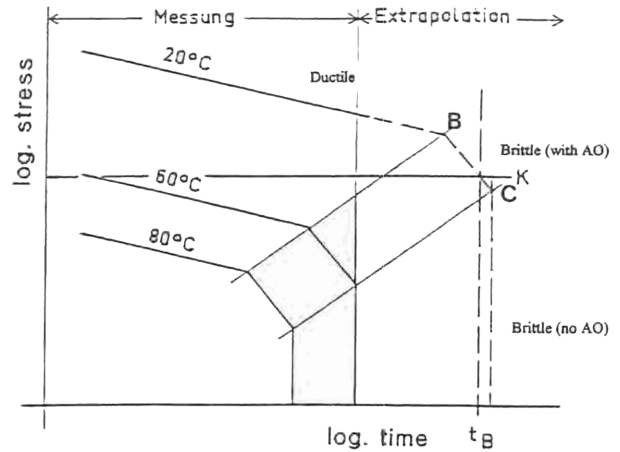


Figure 2 | Stress rupture curves showing third stage (Brittle no AO) oxidized limit. (Gaubé, et al. 1985)

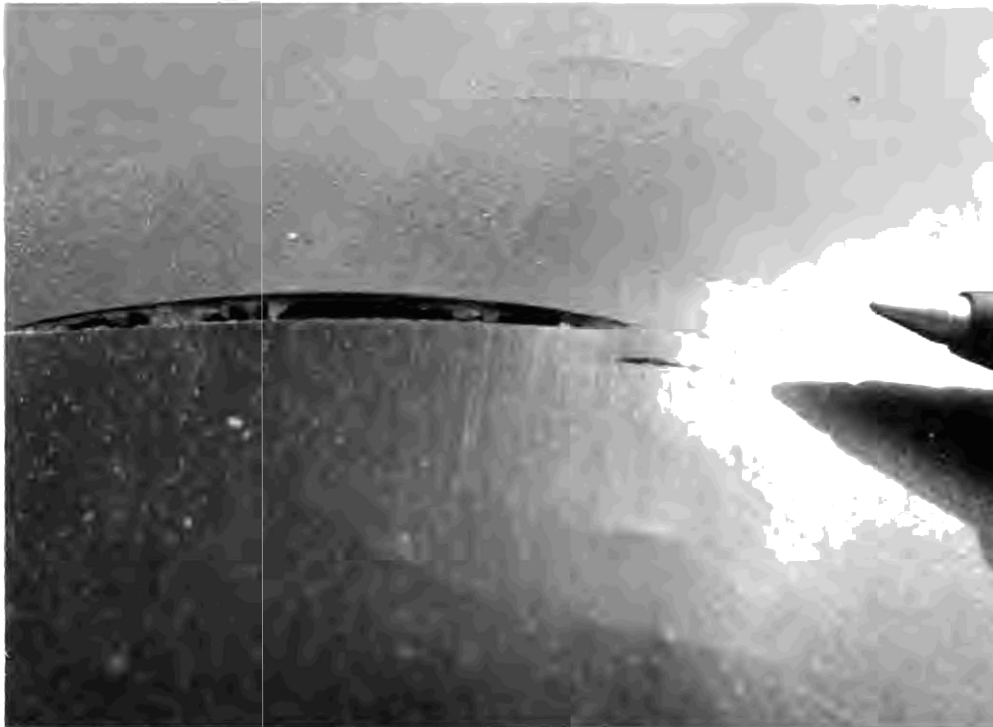


Figure 3 | Stress crack initiated by extruder die line at stone protrusion

The exposed samples will be tested as follows:

- Carbon content (ASTM D1603)
- Carbon dispersion (ASTM D5596)
- Single-point SCR on molded plaque (ASTM D5397)
- Light microscopy of exposed surface, through-thickness cross sections, and thin microsections (~15 μm thick) as necessary
- HP-OIT on 0.5-mm-thick exposed surface layers from basic sheet and from sheet at edge of extruded weld bead (ASTM D5885), preferably at a double-weld bead
- FTIR-ATR on exposed surface to determine CI
- Oven aging/HP-OIT on 0.5mm surface layer (GRI-GM13)
- UV resistance/HP-OIT on 0.5 mm surface layer (GRI-GM13)

Carbon content is done to ensure adequate basic UV protection. Carbon dispersion is done to ensure uniform surface UV protection and to evaluate agglomerates that might act as initiation sites for stress cracking.

HP-OIT is used to assess the remaining amount of stabilizer additives, both in the liner panels and in the sheet adjacent to an extrusion weld. Most stress cracking is observed at the edges of extrusion

exposed locations. Potential sites for future sample removal by the facility owner for future testing will be identified and marked by the expert during the first site visit.

The baseline sample(s) will be tested as follows:

- Single-point stress cracking resistance (SCR) on a molded plaque by ASTM D5397

- High-pressure oxidative induction time (HP-OIT) by ASTM D5885
- Fourier transform infrared spectroscopy (FTIR-ATR) on upper surface to determine carbonyl index (CI) on nonarchive samples only
- Oven aging/HP-OIT (GRI-GM13)
- UV resistance/HP-OIT (GRI-GM13)

weld beads in the lower sheet, so it is important to monitor this location.

While standard OIT (ASTM D3895 at 200°C) better assesses the relevant stabilizers effective at processing (melting) and welding temperatures, the relevant changes in effective stabilizer content during continued service, including in the weld zone, will be provided by measurement of HP-OIT. There will be no future high temperature transient where knowledge of S-OIT will be useful. It is expected that the liner adjacent to the weld bead will be more deficient in stabilizer than the panel itself. Therefore, S-OIT is not considered in this program.

Note that HP-OIT is measured on a thin surface layer because the surface layer may be oxidized while the body of the geomembrane may not. If material

from the full thickness of the geomembrane is used it could show a significant value of OIT, implying that there is still stabilizer present and that oxidation is far from occurring. However, the surface layer could be fully oxidized with stress cracks already initiated and propagating. A crack will then propagate more easily through unoxidized material than would initiation and propagation occur in unoxidized material.

The fact that the HP-OIT meets a certain specification value in the as-manufactured condition provides no guarantee that thermo- and photo-oxidation protection will be provided for a long time. Stabilizers might be consumed quickly or slowly while providing protection. They may also be consumed quickly to begin with, then more slowly, or vice versa.

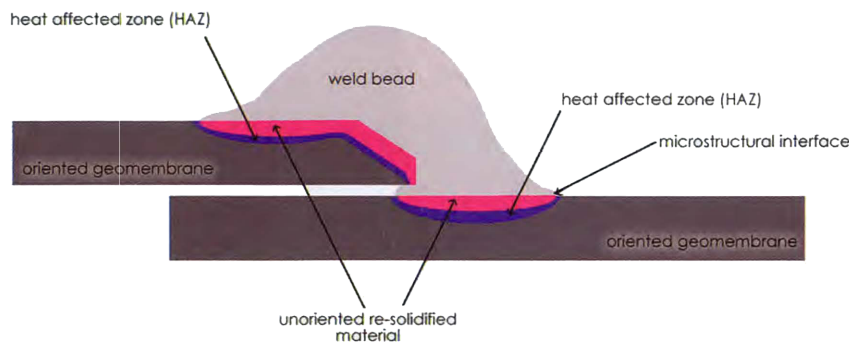


Figure 4 | Schematic of microstructure at extrusion weld

Hence, the need for continuing oven (thermal) aging and UV resistance tests. These two parameters, assessed by measuring retained HP- OIT, are critical to the assessment of remaining service life.

Oven (thermal) aging and UV resistance tests performed in this program will provide an extremely valuable data base that relates laboratory testing to in-service performance and that will further aid in more accurately projecting in-service performance from laboratory testing results.

Special considerations

Because we do not know, by OIT measurements alone, whether the surface layer is or is not oxidized (unless OIT is zero), and since we do not yet know at what level of OIT loss there might be an oxidized surface layer (the database has not yet been generated), FTIR directly on the surface of the geomembrane is performed using the attenuated total reflectance (ATR) technique to deny or confirm the presence of oxidation products (carbonyl groups).

Following the practice of Broutman, et al. (1989) and Duvall (2002) on HDPE pipes, if the ratio of the carbonyl peak at wave number 1760 cm^{-1} and the C-H stretching (PE) peak at wave number 1410 cm^{-1} is more than 0.10, there is a sufficiently oxidized surface layer that

stress cracking might be initiated. For those familiar with the two slope stress rupture curve (Figure 1) where the brittle stress cracking region is the steeper segment below the knee, there is a third vertical part of the curve (Figure 2) where the material is fully oxidized and fracture occurs at the slightest stress. This is what will happen at the end of service life. But first note the times to initiation of stress cracking (the knees in the curves) in Figure 1—they range from $\sim 10/\text{hr}$ to

$\sim 5,000/\text{hr}$ —clearly confirming that all HDPEs are not the same. Some are far more durable than others.

At the end of service life, at some level of OIT, there will be a critically oxidized surface layer that when stressed, such as at low temperatures by an upwards protruding stone, or by flexing due to wind uplift, will initiate a stress crack on the surface that will propagate downward through the geomembrane, as shown by the crack in Figure 3.

This crack, initiated at a stress concentrating surface die mark, occurred when the liner contracted at low temperatures, and tightened over an upwardly protruding stone. The straight morphology of the crack, and the ductile break at the bottom surface as the stress in the remaining ligament rose above the knee in the stress rupture curve, are typical of a stress crack. Note the shorter stress cracks initiated along other nearby die marks.

Stress cracks are preferentially initiated along the edges of welds because the adjacent geomembrane has been more depleted of stabilizers during the high temperature welding process. Thus, under further oxidizing service conditions, it will become the first location to

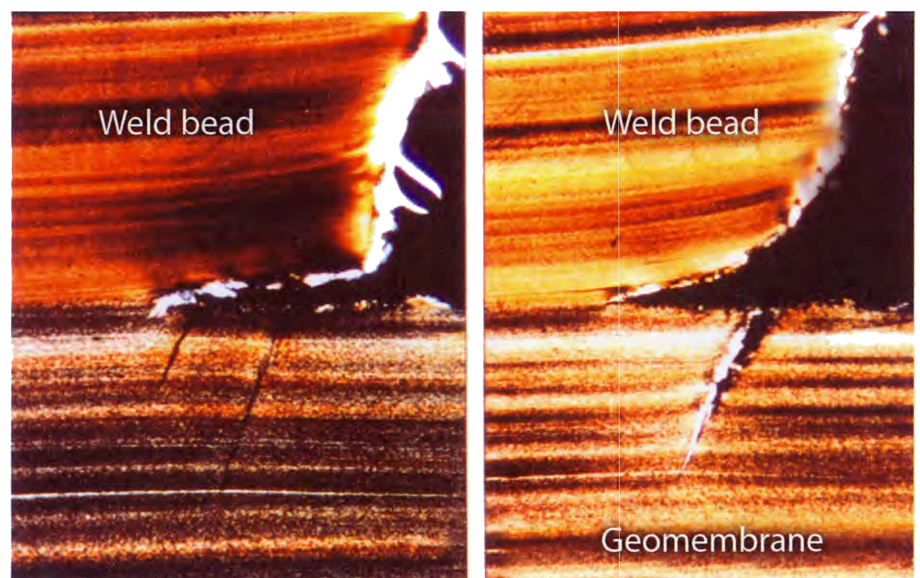


Figure 5 | Typical off-normal angle of precursor crazes (left) and stress crack (right) at edge of extrusion weld.

Type	Specification	Predicted Lifetime in Texas, USA
Side wall exposed	54	5
Side wall concrete side	81	71
Lower launder exposed	16	3
Lower launder concrete side	145	1

Table 2 | S-OIT values on solution and concrete liner surfaces (Peggs, 2008).

be oxidized to the critical level at which stress cracks will be initiated under any applied stress. In addition, the geometrical notches at grinding gouges and at the edges of the bead increase local stresses to critical levels for SC to occur.

I also believe that an internal microstructural flaw exists between the originally oriented geomembrane structure and the pool of more isotropic melted and resolidified material at the edge of the weld zone, as shown schematically in **Figure 4**. Most stress cracks occur at an off-normal angle at the edge of the weld bead that may be related to the angle of this molten-pool to oriented-structure interface (**Figure 5**). It is also known that stress increases the extraction of stabilizers from polyolefin materials.

With all of these agencies acting synergistically, it is not surprising that stress cracking often first occurs adjacent to extrusion welds.

Looking ahead

With the first field assessment test results available to us, and the extent of changes from the baseline sample known, removal of a second set of samples by the facility owner (at locations previously identified and marked by the initial surveyor), will be planned for a future time, probably in 2 or 3 years.

Why 2 or 3 years? In an extreme chemical environment, extensive reductions in

S-OIT of studded HDPE concrete protection liners in mine solvent extraction facilities using kerosene/aromatic hydrocarbon/sulfuric acid process solutions at 55°C (131°F) have been observed on the solution and concrete sides of the liner (**Table 2**) within 1 year (Peggs 2008). But it is unlikely that such rapid decreases will be observed in air-exposed material.

With this second set of field samples, and with three sets of data points, practically reliable extrapolations of remaining lifetime can start to be made.

It is expected that a few years of notice for impending failures will be possible.

The key point to note in making these condition assessments is that, while all HDPE geomembranes have very similar conventional index properties, they can have widely variable photo-oxidation, thermal-oxidation, and stress-cracking resistances. Therefore, some HDPEs are more durable than others.

Thus, while one HDPE geomembrane manufactured in 1990 failed after 15 years in 2005, another HDPE geomembrane made in 1990 from a different HDPE resin (or more correctly a medium-density polyethylene [MDPE] resin), and with a better stabilizer additive package, could still have a remaining lifetime of 5, 20, or 30 years.

So, keep a close eye on those exposed liners and we'll learn a great deal more about liner performance and get notice of

the end of service lifetime. And if owners can retain some archive material from new installations, so much the better.

References

- Broutman L.J., Duvall, D.E., So, P.K. (1989). "Fractographic Study of a Polyethylene Sewer Pipe Failure." SPE Antec, pp 1599-1602.
- Duvall, D.E. (2002). "Analyses of Large Diameter Polyethylene Piping Failures." Proceedings of the Society of Plastics Engineers, 60th Annual Technical Conference.
- Gaube, E., Gebler, H., Müller, W., and Gondro, C. (1985). "Creep Rupture Strength and Aging of HDPE Pipes 30 Years Experience in Testing of Pipes." *Kunststoffe* 74 7, pp 412-415.
- Koerner, R.M., Hsuan, Y.G., Koerner, G. (2008). "Freshwater and Geosynthetics: A Perfect Marriage." Keynote Lecture at GeoAmericas 2008, IFAI, Roseville, Minn., USA.
- Hsuan, Y.G., Koerner, R.M., Lord, A.E., Jr., (1992). "The Notched Constant Tensile Load (NCTL) Test to Evaluate Stress Cracking Resistance." 6th GRI Seminar, MQC/MQA and CQC/CQA of Geosynthetics, Folsom, Pa., USA, pp 244-256.
- Peggs, I.D., (2008). "The Performance of Concrete Protection liners in Mine SX/EW Mixers and Settlers: The Need for Chemical Resistance Testing." Proceedings of GeoAmericas 2008, IFAI, Roseville, Minn., USA. 